December 2016 M.Sc. in Civil Engineering HINDREEN MOHAMMED NAZIF JABBAR

UNIVERSITY OF GAZIANTEP
GRADUATE SCHOOL OF
NATURAL & APPLIED SCIENCES

DAM BREAK ANALYSIS OF AN EXISTING DAM BY INTEGRATED HYDROLOGIC MODELING AND GENE-EXPRESSION PROGRAMMING

M. SC. THESIS
IN
CIVIL ENGINEERING

BY
HINDREEN MOHAMMED NAZIF JABBAR
DECEMBER 2016

DAM BREAK ANALYSIS OF AN EXISTING DAM BY INTEGRATED HYDROLOGIC MODELING AND GENE-EXPRESSION PROGRAMMING

M.Sc. Thesis

In

Civil Engineering

University of Gaziantep

Supervisor

Supervisor: Assoc.Prof.Dr. Aytaç Güven

BY

HINDREEN MOHAMMED NAZIF JABBAR

DECEMBER 2016

REPUBLIC OF TURKEY
UNIVERSITY OF GAZİANTEP
GRADUATE SCHOOL OF NATURAL & APPLIED SCIENCES
CIVIL ENGINEERING DEPARTMENT

Name of the thesis: Dam break analysis of an existing dam by integrated hydrologic modeling and gene-expression programming
Name of the student: Hindreen Mohammed Nazif Jabbar
Exam date: 26/December/2016
Approval of the Graduate School of Natural and Applied Sciences

Prof. Dr. A. Necmeddin Yazıcı
Director

I certify that this thesis satisfies all the requirements as a thesis for the degree of Master of Science.

Prof. Dr. Abdulkadir Çevik
Head of Department

This is to certify that we have read this thesis and that in our consensus/majority opinion it is fully adequate, in scope and quality, as a thesis for the degree of Master of Science.

Assoc. Prof. Dr. Aytaç Güven
Supervisor

Examining Committee Members	Signature
Prof. Dr. Mustafa Günal	.....
Assoc. Prof. Dr. Aytaç Güven	.....
Dr. Ali Aytek	.....

I hereby declare that all information in this document has been obtained and presented in accordance with academic rules and proper conduct. I also declare that, as required by these rules and conduct, I have fully cited and referenced all material and results that are not original to this work.

Hindreen Jabbar

ABSTRACT

Dam Break Analysis of an Existing Dam By Integrated Hydrologic Modeling and Gene-Expression Programming

Mohammed, Hindreen

M.Sc. Thesis in Civil Engineering

Supervisor: Assoc.Prof.Dr. Aytaç Güven

December 2016, 143 Pages

Dams can be considered the most dangerous structures in civil engineering because of the devastation that occurs as impounded reservoir water escapes through the breach of a failed dam and rushes downstream, beside of losing billions of dollars in infrastructure and property damages. Application of GIS techniques from satellite data in integration with hydrological modeling for mapping of flood inundated areas can play a momentous role in minimizing the risk.

For this purpose, the numerical dam break model for analyzing of Dukan Dam is performed under various scenarios. Dukan Dam is located on the Lesser Zab River near the city of Sulaymaniyah in Iraq. The objective of these analyses is to investigate adverse effects of dam break failure on the regions downstream of the dam. The numerical model used in the simulations is SMPDBK model of WMS software, which is developed by the National Weather Service (NWS) in the United States. The analysis results show that most adversely effected regions are those that are closest to the dam location. The results of these simulations can be efficiently used to prepare emergency action plans in case of possible failures. In addition, Gene Expression Programming (GEP) is used in this research as an evolutionary symbolic regression technique for obtaining formulas that predict flood characteristics that can be used in future without using any type of numerical dam break models and without using a lot of information, effort and time.

Keyword: Dam break analysis, GIS, Gene-Expression Programming, Flood simulation, Watershed modeling system.

ÖZ

Entegre Hidrolojik Modelleme ve Gen-Ekspresyon Programlama Kullanarak Mevcut Bir Barajın Yıkılma Analizi

Mohammed, Hindreen

Yüksek Lisans Tezi, İnşaat Mühendisliği

Danışman: Doç. Dr. Aytaç Güven

Aralık 2016, 143 Sayfa

Barajlar, biriken rezervuar suyunun yıkılan baraj yarığından sızmasıyla mansapa hücum etmesinden kaynaklanan tahribattan dolayı en tehlikeli inşaat mühendisliği yapıları olarak kabul edilebilir. Uydu verilerine Coğrafi Bilgi Sistemelri (CBS) tekniklerinin uygulanması ve taşkın altında kalan alanların hidrolojik modelleme ile haritalandırılması bu riski azaltmada önemli bir rol oynayabilir.

Bu amaçla, Dukan Barajı'nın farklı senaryolar altında baraj yıkılması analizi gerçekleştirilmiştir. Dukan Barajı, Irak'ta Süleymaniye ilinde ve Aşağı Zap Nehri üzerindedir. Bu analizlerin amacı bafaj yıkılmasının barajın mansabında bulunan alanlara olan kötü etkisinin araştırılmasıdır. Simülasyonlarda kullanılan sayısal model, Birleşik Amerika Devletleri Ulusal Durumu Servisi tarafından geliştirilen Watershed Modeling System yazılımında mevcut olan Basitleştirilmiş Baraj Yıkılması Analizi (BBYA) modelidir. Analiz sonuçları, en kötü etkinin baraja en yakın olan bölgelerde meydana geldiğini göstermektedir.Bu simülasyonların sonuçları olası baraj yıkılması için hazırlanacak acil önlem planlarında etkin olarak kullanılabilir. Ayrıca bu çalışmada, gelecekte herhangi bir tipik sayısal baraj yıkılması modeli kullanmadan yada birçok bilgi, çaba ve zaman harcamadan taşkın karakteristiklerini tahmin eden denklemler elde etme amacıyla sembolik regresyon tekniği olan Gen-Ekspresyon Programlama (GEP) tekniği kullanılmıştır.

Anahtar kelimeler: Baraj yıkılma analizi, CBS, Gen-Ekspresyon Programlama, Taşkın simülasyonu, Havza modelleme sistemi

To My Family

ACKNOWLEDGEMENTS

I would like to express my gratitude and honest respect to my supervisor, Assoc. Prof. Dr. Aytaç Güven for his contributions during this thesis, invaluable helps and constructive suggestions.

Special thanks to Mr. Anas M. Al-Juboori Assistant professor at the University of Mosul for his endless information and important comments about my thesis. although I would like to congratulate him for his excellent thesis with Dr. Aytaç about Hydropower Plant Site Assessment by Integrated Hydrological Modeling, Gene Expression Programming, and Visual Basic Programming which is published in Water Resources Management for the European Water Resources Association (EWRA).

A lot of thanks to Ms. Mina H. Abdulla holder of MA degree in English Literature and Culture at Brunel University London for her contribution in proofreading of my thesis.

Finally, I would like to express my particular thanks to my family for their continuous support and encouragement.

TABLE OF CONTENTS

LIST OF FIGURES

LIST OF TABLES

CHAPTER 1

1. INTRODUCTION

1.1. General

Dam is a universally argued subject starting from its advantages (p. petchprayoon, 2001). Historical Indications showed that some of the earth masonry dams around 4000 years B.C were constructed at Jawa in Jordan (Kerisel, 1985). Ever since the earliest dams were built, there have been dam failures (Costa, 1985). The flood which results in the breach of the dam is quite larger than any other previous floods that originated from the runoff of rainfall and/or snowmelts, and its consequences are often catastrophic if human development exists downstream of the dam (Fread 1981). To reduce the effect of the dam break, the flood wave should be transferred downstream to the location where the effect of failure will no longer have passive consequences (Atallah, 2002).

History has adequately documented close relation of dams with the fall and rise of civilizations; large dams had been constructed continuously on the rivers around the world for irrigation, water supply, hydro-electric power generation, recreation, navigation, and other objectives, such as floods control during seasonal climatic changes, but then serious plan and analysis should be taken into account for larger risk assessment which is potential catastrophic flood that will produce from dam failure (Singh, 2013). The destruction that takes place as saved reservoir water releases during the breach locations of a broken dam and rushes downstream is deadly and fast (Wetmore and Fread, 1983). This is beside the loss of millions of dollars in infrastructure development and private property damages (Cook and Merwade, 2009). From this perspective, dams can be considered the most unsafe structures in civil engineering (Martins, 2000). In spite of very wide improvement in the field of dam construction, dam failures are continuous. A recent example is the failure of (Bento Rodrigues dam) in Brazil in 2015 that killed 19 people, and left 600 people homeless.

Therefore, during the design of any dam, the scenario of dam failure must be considered as a major part of the project even before dam construction. Likewise, it also must be used as a guide for a future project that will be located and constructed at downstream of the dam (Wikipedia, 2016).

However, in the absence of sufficient information or alarm time, the death toll caused by the flood would be 19 times more (Costa and John E., 1985). Therefore, application of GIS methods incorporated with hydrological modeling for the mapping of the flood inundated areas can play a fundamental role in further reducing the hazard and likely losses (Lodhi and Agrawal, 2012).

Researchers have been developed many methodologies and techniques (physical models, mathematical models, and CFD models) to predict the flood wave resulted by a dam failure. At first, they attempted to solve dam break problems by using an analytical solution made by Ritter (1892). Several investigators have developed a 1D mathematical model to analyze dam break problems (Hicks et al. 1997; Sanders 2001; Macchione et al. 2004). Two-dimensional mathematical models were developed in the last decades for simulating a flood due to dam failure (Akanbi et al. 1988; Zhao et al. 1996; Sarma 1999; Zoppou et al. 2000).

Depending on the type of dam and reasons of failure, dams can fail either suddenly or gradually. The causes of dam breach can be natural or deliberate. Natural breaches may occur as a result of natural distortion of the structure, extraordinary natural events like earthquakes, extreme rainfalls and floods, differential settlement, piping, rockslides, seepage, wave action, overtopping, etc. deliberate causes include poor construction, bombing, faulty design, sabotage, improper reservoir operation, animal burrowing, improper location, etc. (Singh, 2013). As reported by US Committee on Large Dams in cooperation with the American Society of Civil Engineering (ASCFJUSCOLD, 1975) and the International Commission on large Dams (ICOLD, 1973), about 38% of dam breaches are resulted from overtopping of the dam due to wrong and inappropriate design capacity of the spillway against large quantity of inflows to the reservoir from intense precipitation runoff. Also around 33% of dam failures were resulted by piping or seepage. While around 23% of the breaches are correlated with base problems and the remaining 6% are due to other reasons. One of the biggest dam breaks in the history happened in 1889 was the failure of the

Johnstown dam in Pennsylvania. The dam breakdown killed an estimated 2,209 people and caused 17 millions dollars of damage (Gibson 2006). Also, the failure of the Banqiao Reservoir Dam and other dams in Henan Province, China in 1975 caused more losses than any other dam failure in history. The disaster killed around 171,000 people, and left 11 million people without home (Osnos and Evan, 2011). As a result of the risks posed to people, there is an increasing interest in dam safety management (Cheng et al., 2011).

In the present, global warming and climate change have caused an observed changes in the hydrological data; therefore, forecasters need recalculated scenarios in many situations (Tofiq and Guven, 2014). The European Union in 2007, built a new flood guidance requiring all member countries to reproduce risk assessments flood inundation maps for their regions by 2015 (EXSCIMAP, 2007). Therefore, a lot of European countries now have created flood maps via insurance industries and nongovernmental organizations (Moel et al., 2009). Depending upon statistics; in U.S, more than one dam fails per year at an average rate of dam breaches (Ellingwood et al., 1993). According to National Flood Insurance Program (NFIP) in U.S, the Federal Emergency Management Agency (FEMA) produces and updates flood maps that match to return period flow of 100-year. FEMA has created almost 100,000 flood maps for 150,000 mi^2 of floodplain areas that covers 19,200 regions (NFIP, 2002).

In this study, the simplified dam break model (SMPDBK) is used to simulate the flood wave due to a hypothetical dam failure. Version 8.3 of Watershed Modeling System (WMS) is used for mapping the flood. Gene Expression Programming (GEP) is used to improve a symbolic regression model to predict flood characteristics (flood discharge, flood level and flood time) based on the SMPDBK model outputs.

1.2. Scope of the Thesis

The purpose of this study is to route the flood in Lesser Zab River locating at downstream of Dukan Dam as a consequence of a possible breach, characterizing the inundation area focusing on Dukan and TaqTaq town. The maximum depth covering the town and the discharge that will enter to Tigris River which is located at the end

of Lesser Zab River, are predicted by making maps describing these drowned areas along the Lesser Zab River; showing the travel time of flood wave on each significant point along the river stream. A model named simplified dam break (SMPDBK) of (WMS) software version 8.3 would be utilized for this analysis. SMPDBK is used due to its flexibility, and it permits for the analysis achievement of the breach, happening over a finite period of time. Geographic Information System (GIS) capabilities are used to obtain digital elevation model from satellite information.

The fundamental equations used by the model are the Saint Venant equations which are the momentum and continuity equations based on conservation of mass of unsteady flow. Such investigation work could be helpful in performing the evacuation procedures and risks assessment that should be put into account by the government in the state if there is a possibility of dam failure to reduce the risks that may affect the life and the properties at downstream of the dam.

1.3. Layout of the Thesis

This thesis is composed of six chapters. The contents of the thesis chapters are summarized below:

Chapter Two: This chapter includes literature review about dam break.

Chapter Three: This chapter contains information about case study (Dukan Dam).

Chapter Four: This chapter contains methodology of the research.

Chapter Five: This chapter contains results and discussion.

Chapter Six: This chapter includes conclusions and recommendations.

CHAPTER 2

2. LITERATURE REVIEW

2.1. General

Dams provide so many improvements to our community, but floods producing from the breach of formed barriers, have further created some of the most destructive catastrophes of the last two decades. When dams break, property destruction is inevitable. However the death tolls can fluctuate drastically with the range of the drowning areas, the amount of alarm time obtainable, and the number of the residents at danger (Wahl 1998). Costa (1985) tells that 60% of 11,100 deaths related with every dam failure around the world has happened in these three breaches: Vaiont Dam in Italy which was concrete arch type, in 1963 killed almost 2,600 people; Machhu II Dam in India which was embankment type, in 1974 killed around 2,000 people; Johnstown Dam in Pennsylvania which was embankment type, in 1889 killed 2,200 people. The reasons for these dam failures were overtopping, and the short or no warning times for evacuations at downstream.

The various dam breaches that happened in the 1970's including: Kelly Barnes Dam in Georgia in 1977; Sandy Run Dam and Laurel Run Dam in Pennsylvania in 1977; Teton Dam in U.S in 1976 and Buffalo Creek dam in U.S in 1972, led up to extensive revisions of Reclamation's dam security plans. Numerous investigations suggested that emergency preparation planning with drowning maps be asserted. The Federal Guidelines for Dam Security Assessment, set in 25/6/1979, declared that drowning maps should be provided (Wahl 1998).

Individual incidents are showing the essential need for improving systems for evaluating dam failure effects. Evacuation and Warning time can significantly affect the loss of life from a dam break. During setting up hazard classifications, right

Evaluation of the warning time and providing accurate emergency action plans are essential. Evacuation alert time is equal to the initial failure time plus failure creation time plus flood travel time from a body of the dam to a populated place (Wahl 1998). Historical breaches analysis investigated by the U.S. Reclamation's Bureau shows that the death tolls can change from 50% of the people at danger when the alert time is less than 15 minutes, to 0.02% of the people at risk when the warning time is more than 90 minutes (Brown and Graham, 1988). Latest activity by McClelland and DeKay (1991) gives similar sensibility to alarm period. Costa (1985) published that "when there is short, or no alarm time the average number of deaths are 19 times greater for each dam breach at downstream.

Results analysis of the possible dam failure has been classified into (Wahl 1998):

1. Routing of the outflow discharge from the breached dam within the downstream channel, applying a model like SMPDBK model.
2. Forecast of disasters and loss of life due to the flood wave and produce inundation maps for a future project.

Three common methods can be classified for dam break analysis. The first one is to compare results to the same analyzed or broken case studies and the second one is to use predictor equations based on various case studies investigations. These are the two simplest approaches. The third method is the use of a physical dam failure routing model that applies laws of sediment transportation and hydraulics to route the failure flow. This process is complex but gives the possibility for additional detailed results, like a forecast of failure initial time and forecast of standard break dimensions (Wahl 1998).

According to (Fread, 1988), the NWS BREACH physical model is the commonly used one. All these three methods have weaknesses. Compare results analysis suffers from a lack of accurate and extensive case study details on different kinds of dams. Predictor equations suffer from similar problems, and regression associations depended on the available data have considerable uncertainty. Physically based models suffer from a weak agreement of the components of failure improvement and an incapability to model those high energy erosion methods and the mechanisms that constrain dam failure.

Table 2.1 shows which types of mode failure can hit which type of dams

Table 2.1. Mode of failures on different types of dams (Atallah, 2002)

failures Mode	Embankment	Gravity	Buttress	Arch	Multiple Arch
Sliding	✓	✓	✓		
Cracking	✓	✓	✓	✓	✓
Overturning		✓		✓	
Maintenance	✓	✓	✓	✓	✓
Overtopping	✓	✓	✓	✓	✓
Internal erosion	✓	✓	✓	✓	✓
Rapid drawdown	✓				
Piping	✓	✓	✓	✓	✓

2.2. Historical Dam Breaks

A report was provided via Graham in the U.S (Graham, 2001), entitled "Human and Financial Implications of Dam Failure ", concentrating on 13 dam breaches in the U.S. The report involved an argumentation of dam features, dam breach evacuation time, the reasons for dam breaches, in addition to the lives lost and financial costs and damages. Detailing some of the dam failure accidents in Graham's research can be seen in this section.

2.2.1. TETON DAM

Dam properties:

Type: earthfill dam

Height of the dam: 93 m

Volume of the Reservoir: 308.3×10^6 m^3

Purpose: irrigation

The dam broke: at 11:57 a.m, 5/6/1976.

Breach reason: Piping in the foundation.

Location: Idaho, United States.

Specifications about propagation of warning: Police, television, telephone, radio, neighbor word of mouth.

Summary of flooding resulted from dam breach: 400 to 500 km^2 flooded, above 3,700 homes damaged.

The disasters involved: 11 death tolls (one suicide committed, one accidental gunshot, three heart failure and six from sinking) with about 800 injuries and 25,000 souls at danger. Complete destruction was about 400$ million.

2.2.2. BUFFALO CREEK COAL WASTE DAM

Dam properties:

Type: Coal waste

Height of the dam: 14 m

Volume of the Reservoir: $50x10^4$ m^3

Purpose: dispose of coal waste and Improve water quality.

The dam broke: about 8 a.m., February 26, 1972.

Breach reason: falling of the dam face.

Location: Logan County, West Virginia.

Specifications about propagation of warning: The official of dam security on the dam, rejected two security guards who had been asked to help evacuation at about 6:30 a.m.

Summary of flooding resulted from dam breach: Destroyed above 1,000 houses, along 24 km at downstream valley by the velocity of 8 kmph.

The disasters involved: 125 death tolls, 4,000 people lost their houses and property loss of 50$ million.

2.2.3. KELLY-BARNES DAM

Dam properties:

Type: Earthfill dam

Height of the dam: 12 m

Volume of the Reservoir: $77.7x10^4$ m^3 at time of dam break

The dam broke: at 1:20 a.m., 11/6/1977.

Breach reason: downstream slope failure due to heavy rain.

Location: Stephens County, Georgia.

Specifications about propagation of warning: A lot of people were not informed. It was a horrible situation for evacuation due to dark and problematic climatic conditions.

Summary of flooding resulted from dam breach: In the populated floodplain, the depth of flood reached to 3 m.

The disasters involved: 39 deaths along 3 km of the downstream. 13 houses and two university structures were destroyed. And the property losses were 2.8$ million.

2.2.4. SOUTH FORK DAM

Dam properties:

Type: Earthfill

Height of the dam: 22 m

Volume of the Reservoir: $14.18x10^6$ m^3

Purpose: For water supplying to the canal system.

The dam broke: at 3:10 p.m., 31/5/1889.

Breach reason: Overtopping.

Location: Pennsylvania, U.S.

Specifications about propagation of warning: Weak Warning.

Summary of flooding resulted from dam breach: About 1 hour after failure, 3 m of floodwater reached Johnstown, 22 km downstream of the dam.

The disasters involved: 2,209 death tolls and 20,000 people at inundation risk along 22.5 km downstream of the dam.

2.2.5. AUSTIN DAM

Dam properties:

Type: Concrete gravity

Height of the dam: 15 m

Volume of the Reservoir: $105x10^4$ m^3

The dam broke: at 2:00 p.m., 30/9/1911.

Breach reason: Foundation Weakness.

Location: Potter County, Pennsylvania, U.S.

Specifications about propagation of warning: The false whistle signals had been received from the employees while repairing telephone line. The two false alarms caused, many populations to think that the sound of warning of dam breach was the third wrong alert.

Summary of flooding resulted from dam breach: The water reached to Austin town, 2.5 km at downstream of the dam in 30 minutes.

The disasters involved: 78 death tolls, at 3 km downstream of the dam.

2.3. Historical Modeling of Dam Break

The National Weather Service (NWS) improved DAMBRK model, in 1977 to analyze the dam failure manner and simulate flood wave to describe drowning maps toward downstream of the dam. Several regression relations obtained from 1977 to 1990s for estimating maximum outflow and failure parameters from broken embankment dams. Mathematical regression investigations like Froehlich (1995), Gillette and Dewey (1993), Gillette and Von Thun (1990), USBR (1988), Monopolies and MacDonald (1984) obtained dam failure parameters by utilizing empirical methods. More advanced modeling process used for predicting hazards that produced from dam breach were two types of breach models: parametric and physical (FEMA, 2013).

Parametric methods control erosion and flow, and Physical models depend on physical rules. But those kinds of models are tough for dam failure evaluation because of the large amount of data required for preparing breach erosion. NWS BREACH (1985) is the most serious model utilized physical laws to predict the failure properties and the outflow discharge flowing from the broken earthen dam. This model was formed by combining the conservation of mass in the reservoir inflow plus spillway outflow plus breach outflow inside the sediment transportation capacity of the uniform-unsteady flow during an erosion gapped channel (Wahl, 2004; Fread, 2001).

Parametric models are also known as empirical models depending on previously determined input data for evaluation of the break results in the regression equations. Those models depended on detailed investigation data for evaluation of failure time, and final breach dimensions, which can then be used to analyze the simulated data. Some of the one-dimensional Parametric models for dam breach analysis involve NWS DAMBRK (1988) plus its replacement NWS Flood Dynamic Wave (FLDWAV) Model (1998), HEC- HMS, HEC-RAS, and HEC-1 (Wahl, 1997 and 2004; State of Colorado Department of Natural Resources, 2010).

HEC-HMS and HEC-1 are watershed modeling system software able of producing a dam breach hydrograph from the breach parameters by entering the predefined input data like (time of failure, breach height, breach width, etc.) into the model. FLDWAV and NWS DAMBRK are unsteady models, in addition to HEC-RAS

model which can simulate both unsteady and steady-state flow. These models are based on the fluid dynamics of St. Venant equations which produce a breach hydrograph and simulate the flood wave to the downstream of the breached dam. Furthermore, HEC-RAS and HEC-HMS are regularly renewed by the U.S. Army Corps of Engineers USACE to insert new abilities. HEC-RAS can interface with GIS for the production of flood maps using previously defined downstream locations of the dam connected with water surface elevation and storage in the reservoir, maximum breach flow and failure time of the breach (FEMA, 2013).

According to Wahl (2004), simplified techniques for evaluating maximum break discharge as a function were produced utilizing regression equations from analyses of different historical dam failures by Froehlich (1995), Evans (1986), Costa (1985), Snorrason and Singh (1984), Monopolis and MacDonald (1984), Hagen (1982), Soil Conservation Service (SCS) at (1981), Kirkpatrick (1977).

In 1983 the NWS developed a simplified model for forecasting downstream flood wave performed by dam breach. This method recognized as Simplified Dam Break (SMPDBK), model use the empirical equation for the prediction of the breach geometry of dam. It is a simple form of NWS DAMBRK. This program is qualified for providing the data required to estimate inundated distances resulting from the dam breach while considerably decreasing data, time, and expertise needed to operate a simulation of the most complex NWS DAMBRK. SMPDBK is able of forecasting relevant data to determine flooded zones resulting from a dam breach (Wetmore and Fread, 1983).

In 2012, Federal Emergency Management Agency (FEMA) produced toolset for GeoDamBREACH, depended on the SMPDBK model. Modern improvements in the dam break modeling have been focused on the field of two-dimensional hydraulic analysis for flood wave simulating and erosion methods, depending on the physical concept. 2D models like MIKE software by DHI (2005) and FLO-2D by FLO-2D group (2013), beside GIS combination are now common, providing more complicated analysis. Two-dimensional model strengths are highlighted in alluvial fan flooding where cannot be accurately modeled for overland flow in a one-dimensional model (Wahl, 2010and 2009; Wahl et al., 2008). Investigators are concentrating on producing a different production of physically based hydraulic

simulating models to predict the erosion principles correlated with dam breach; knowing certain manners rightly will aid higher accurate measurements of downstream dam break flood mapping areas. Nowadays models depend on the parametric input types of the broken case, and the model routes flow into the breach as it expands at the defined scale (Wahl, et al., 2008).

According to the information provided by FEMA (2013), Agricultural Research Service (ARS) had researched for the Simplified Breach Analysis (SIMBA) model; SIMBA was generated to estimate and approve the resulting from a complicated erosive effect during overtopping, correlated with an embankment break. Throughout a cooperative work between Natural Resources Conservation Services (NRCS) and ARS, the erosion mechanism inside SIMBA has been integrated into Windows Dam Analysis Modules (WinDAM B). WinDAM B continues WinDAM A to include the erosion and possible break of a uniform embankment dam to produce a failure in any slope at dam body (Visser, et al., 2013).

According to the ARS, the future of dam breach modeling will proceed to develop with the combination of modeling downstream effects with more accurate inundation mapping using GIS principles (FEMA, 2013).

2.4. Software Applications on Dam Break

According to Bernedo (2011), the dam break flood wave investigation is a traditional problem of open canal flow and has theoretical importance to engineers of hydraulic for more than a century. Mathematical models have been developed to meet this need. Instructions development of dam breach is still in the operation of various developments, with renewed extended versions of the models being published periodically.

The two modeling responsibilities of calculating the reservoir storage-outflow hydrograph and simulating the hydrograph during the downstream channel can be analyzed separately but must be unified to consider backwater consequences on tailwater positions. A model must involve some mechanism for interpreting the flow of water from the broken dam body. There are several dams break flood wave analysis models available that are typically used in the engineering industry with

different capabilities and different levels of modeling complexity. For example, some models simulate both the dam break and the flood wave routing, while others may do one or the other. Some models produce the complete output hydrograph, while others may only output the estimated peak flow rate. Some models can simulate two- or three-dimensional flow while some only consider one-dimensional flow. Finally, while most models are capable of modeling Newtonian flow (clear fluids or low concentrations of suspended solids), only some are able to simulate non-Newtonian flow (such as high concentration viscous flow). The user must choose a model required to perform the simulation based on the specific problem to be modeled and the input information available. Figure 2.1 shows a summary of some of the available dam break and flood wave routing models broken down by their capability to model Newtonian or non- Newtonian fluid flows (models with non-Newtonian flow simulation capabilities can also simulate Newtonian fluid flow).

Non-Newtonian flow models: (water and sediment) which the absolute viscosity changes with the rate of deformation.

Newtonian flow models: (water) which has a constant viscosity with the rate of deformation.

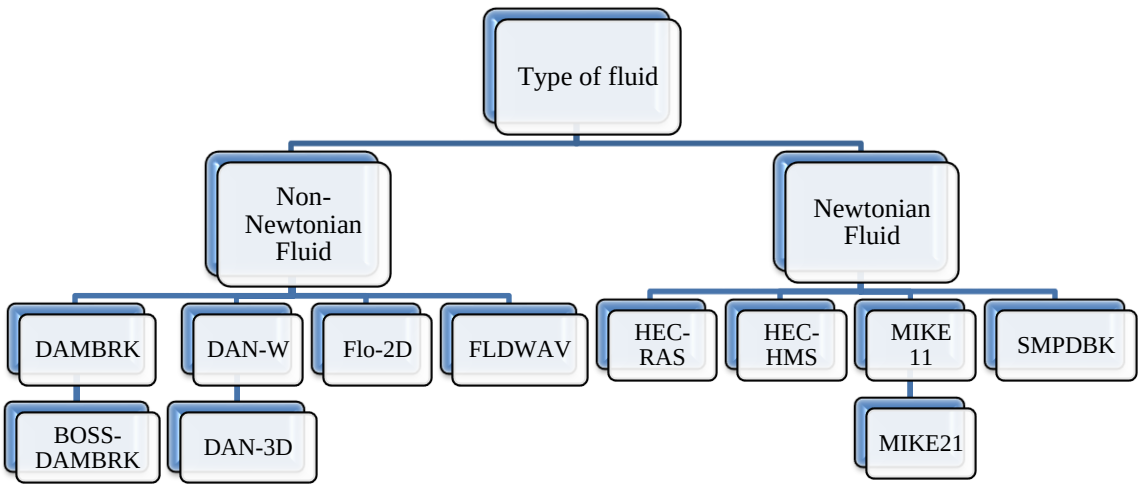

Figure 2.1. Dams break models for Newtonian vs. Non- Newtonian fluids

The equations used in hydraulic modeling software often assumes that the fluid being modeled is Newtonian in order to allow for an analytical solution to a given fluid mechanics problem. In a Newtonian fluid, the shearing stress (τ) is linearly related to the shearing strain rate (Δx/h) and the relationship between (τ) and (Δl/h) is proportional to the fluid viscosity (μ) as shown in shearing stress Equation:

$\tau = \mu * (\Delta x/h)$ (shearing stress Equation)

In a non-Newtonian fluid, the shearing stress is not linearly related to the shearing strain rate as shown in Figure 2.2.

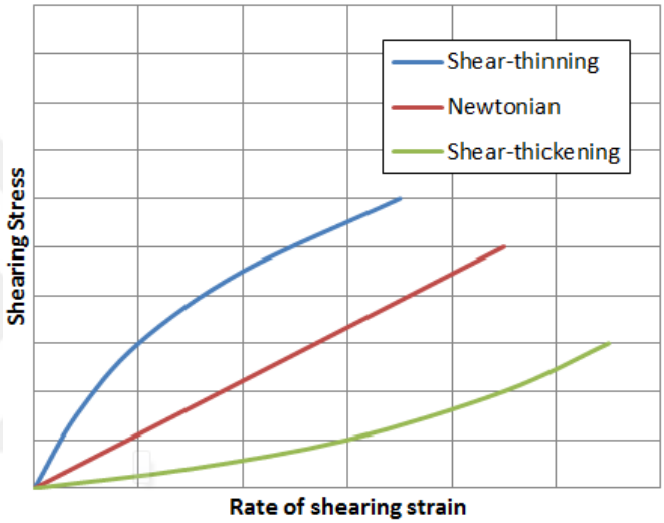

Figure 2.2. Nonlinear relationship between shearing stress and shearing strain rate in non-Newtonian fluids (adapted from Munson et al. 2009)

2.5. Available Models/Software

Most of these models use the break characteristics of the simulated failure as input. These break characteristics can be predicted in three ways: (1) comparing the dam failure to past similar failures, (2) using specific equations based on past dam failures to find a new break width and development time, and (3) using a model that simulates the break characteristic parameters. Fourie (2011) makes an overview of software-implementing models typically used for dam break. Each of the models presented has advantages and disadvantages based on the specific case to be modeled and the available input information. The purpose of this overview is not to

recommend one model over another but to give a summary of the capabilities, complexities, and limitations of the available models for dam break analysis. Further information about these software packages can be obtained from their vendors.

DAMBRK was produced by the National Weather Service (NWS) (Fread 1984). It predicts the dam break wave formation and downstream progression. The model consists of three functional components:

(1) Description of the dam failure mode, including the temporal and geometric description of the break.
(2) Calculation of the outflow hydrograph into the break.
(3) Simulating of the outflow hydrograph during a downstream of the natural canal.

In computing the peak outflow and the outflow hydrograph from the break, the program utilizes user inputs describing the geometric and temporal patterns of the reservoir and the break. Selection of these parameters before a break forms or in the absence of observations can introduce some uncertainty in the prediction. However, it allows the user to study the sensitivity of the parameters and simulate different possible scenarios. After computing the outflow hydrograph, the program uses a dynamic wave method to route the flood wave in the downstream channel or valley. BOSS DAMBRK is an improved version of the NWS DAMBRK model. While commonly used to simulate Newtonian (clear water) flows, DAMBRK and BOSS DAMBRK can also simulate routing of non-Newtonian fluids, by specifying rheology of the fluid such as its unit weight, dynamic viscosity, initial shear strength, and a stress rate of strain (Browne, 2011).

FLO-2D was created by James S. O'Brien for the Federal Emergency Management Agency in 1989, and it is discussed by O'Brien et al. (1993). The model predicts flood hazards, mudflows, and debris flows over alluvial fans using three different systems. A uniform grid is used to describe the floodplain topography so that the model can simulate interactive flood or mudflow routing between the channel, street, and floodplain flow. Both clear water and sediment flow flooding conditions are modeled using a quadratic rheological model. The overall model is based on a grid system. Each sector in the grid is given a location, an elevation, a roughness factor,

and flow reduction factors by the user. Once these values are placed in the grid, flow is routed through it. Discharge is predicted using an estimated depth of flow for each sector which is then computed and summed across all four boundaries of the flood plain. When FLO-2D models mudflow takes into account the sediment volume for each sector of the grid, the sediment continuity remains intact. The model is limited by its inability to simulate abrupt changes in the flow profile like shock waves or hydraulic jumps and degradation. The model assumes that flow during the time step is steady, with hydrostatic pressure distributions, fairly uniform cross-section shape and roughness, and single input values for each grid sector. The accuracy of the prediction is governed by the grid density (Breitkreutz, 2011).

DAN3D is a model used to predict the run-out analysis of extremely high-velocity Landslides, including rock and debris avalanches. It is developed by Scott McDougall as a Ph.D. thesis in 2006 (McDougall 2006). The model is an extension of DAN, one-dimensional software that relies on a meshless, Lagrangian model that takes into account variability in the flow path. It allows the use of non-Newtonian flow. DAN3D is based on a two-dimensional Lagrangian solution of unsteady flow over three-dimensional surfaces. Like DAN, it has the ability to interpolate so that the entire surface can be modeled, and in this case, the environment is smoothed in three dimensions. The model solves depth-averaged equations for an equivalent flow which results from simple rheological relationships that are acquired through back calculations of real landslide analysis.

DAN3D has the following key features:

(1) Simulation of flow over complex three-dimensional terrain without the need to input predictive flow path or outcomes,
(2) Prediction of internal stresses resulting from three-dimensional deformation of material with internal shear stresses taking into account strain, anisotropic, and non-hydrostatic conditions,
(3) Prediction of the transfer of mass and momentum by taking into account entrainment of path material.

The overall output of the model is a prediction of the impacted area from a rapid slide event. The model is limited based on the resolution of the floodplain. It has been reported that DAN3D did well in back-calculating case studies because all data were known, and the results were calibrated to assist the model (Fourie, 2011).

FLDWAV is a computer model developed by the NWS to model flows through a single stream or network of streams (Fread and Lewis 1988, Fread 1993, Fread 2000). The FLDWAV program is an upgrade of DAMBRK. The purpose of DAMBRK is to determine the affected area from a dam break by analyzing the flow. FLDWAV was designed to analyze large flood events from more than just dam breaks by using a realtime forecasting predictive model.

This model has five main capabilities:

(1) To model single or multiple channel flow for straight or meandering channels.
(2) For modeling free surface flows in supercritical, subcritical, and combined flow regimes as well as pipe flow under pressure.
(3) To model clear water fluids and mud/debris fluid flows.
(4) To model off-channel flow areas that may take flow storage during high flows.
(5) To model timedependent dam breaks or control structures along with flow over and through multiple control structures.

The system depends on the 1D solution to the St. Venant equations for unsteady flow. It also allows the user to model one-dimensional unsteady non-Newtonian fluids (Kunkel, 2011b).

SMPDBK, which was produced by the National Weather Service (NWS) in 1983, is a simplified version of the original model (DAMBRK) by using unsteady one-dimensional flow routing of the St. Venant equations. This model is a very useful tool since it does not require much input information, it is easy and fast to use, and it returns results on the conservatively high side for large dams. Caution must be exercised in applying the model in cases where the dam impounds a small reservoir (under about 500,000 cubic meters).

In these situations, the peak flow values have been reported to be much smaller than those obtained by the normal DAMBRK model. The SMPDBK model assumes the initial break to being rectangular and constant, and peak flow time that is equal to the break development time (Browne, 2011).

HEC-RAS allows for the modeling of a dam break failure though it does not model non- Newtonian fluids. This model enables unsteady one-dimensional flow routing using all of the St. Venant equations and is often used to compute and display downstream impacts resulting from hypothetical dam failures. Given input parameters like maximum breach geometry and breach time, HEC-RAS can generate the dam breach hydrograph then simulate the resultant flood wave and downstream consequences.

HEC-RAS has been used for many flood damage analysis and dam safety studies. Routing simulations require the following from the broken model to work in HEC-RAS: location, failure mode, shape and progression, formation time, trigger condition and weir and pipe flow coefficients. HEC-RAS also provides a time-growth template for breaks (Browne, 2011) and (Breitkreutz, 2011).

MIKE21 is an extension of the Danish Hydraulic Institute (DHI) MIKE flood modeling system and has been improved to be able to model flood wave propagation from theoretical dam break scenarios. The goal of the model improvement is to increase the power of the model by allowing it to handle high Froude numbers so it can accurately model wave propagation over initially dry beds. The improvements also allow the software to perform supercritical flows, broad-crested weir flows, and hydraulic jumps in addition to dam break models. The MIKE21 model is a two-dimensional flood propagation software (another DHI product, MIKE11, is one-dimensional flood propagation software).

The software is based on numerical solutions to depth-averaged equations that describe the conservation of mass and momentum in two dimensions. Caution is recommended in simulations with steeply rising flood depths. Likewise, HEC-RAS and SMPDBK, MIKE21 (and MIKE11) can only analyze Newtonian flows. However, a mud transport (MT) module would seem to be appropriate for modeling high concentration sediment-laden flows. The MT module is utilized in a variety of

situations where the dispersion, erosion, and deposition of cohesive sediments are of importance (Hegedus, 2011) and (Soderstrom and Isaksson, 2011).

2.6. Comparison of dam break models

Bozkuş et al. (1998) analyzed three numerical breach simulations of the similar dam applying the numerical models NWS DAMBRK and NWS SMPDBK and the physical laboratory measurements. Comparisons of the evaluated and measured outcomes showed that two numerical models simulate the peak flood elevations with reasonable efficiency.

In usual, the DAMBRK model was satisfied for pre-emergency dam-break analysis since it needs detailed input data for a particular analysis, professional expertise to utilize it as well as consuming for a time. Otherwise, the SMPDBK model was better suited for real-time forecasts of the performance of dam-break flood waves in the cases where a dam failure is imminent, and there is not enough time for an extensive dam failure investigation.

Input and output data for Bozkuş and Kasap research are shown below:

Inputs:

Type of dam: concrete gravity dam.

Elevation of the reservoir when breaching occurs: (900.00 m)

Elevation of the final bottom breach: (884.20 m)

Storage volume of the reservoir: (867,000 m^3)

Surface area of the reservoir: (305,000 m^2)

Final formation of the breach width: (110 m)

Breach formation time: 1.3 min.

Outputs:

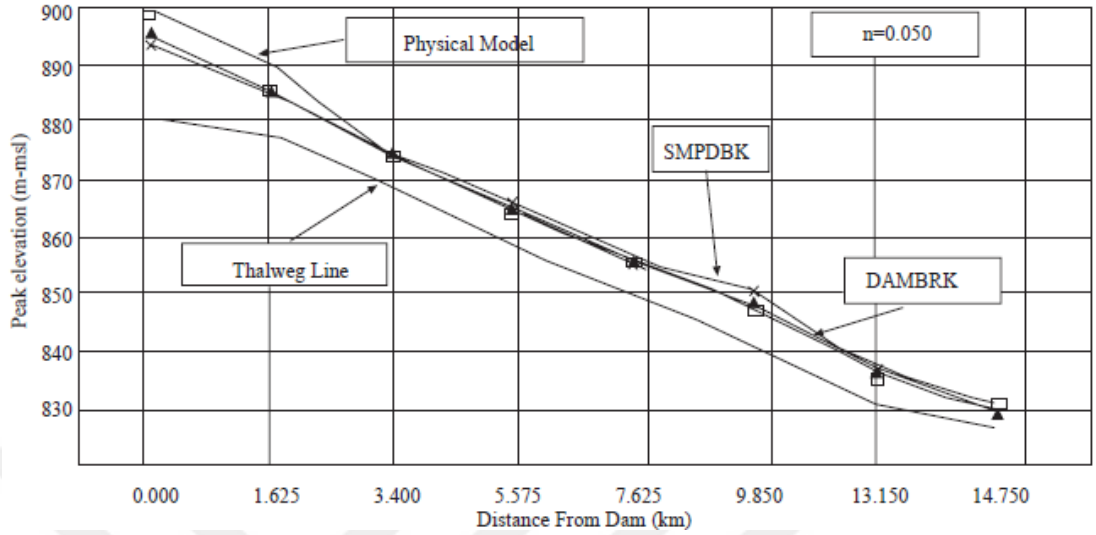

Figure 2.3. Peak water surface elevation vs. distance downstream for R.E. =900m

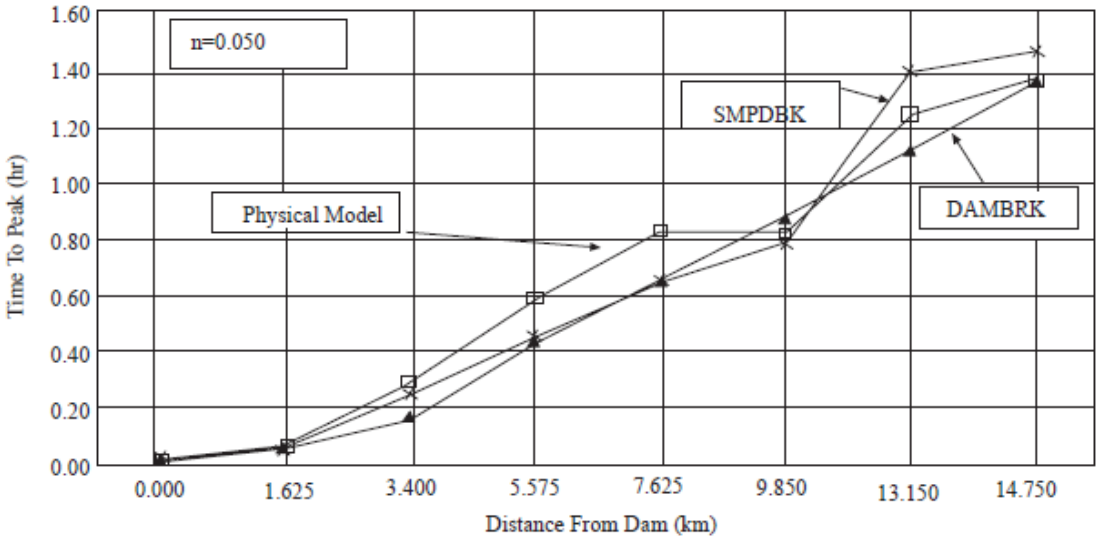

Figure 2.4. Peak occurrence time vs. Distance downstream for R.E. =900m

Wurbs (1987) explained and analyzed the models available and suggested the use of SMPDBK or DAMBRK based on the type of work, resources, and availability of input data.

Also, Thompson andWestphal (1987) compared SMPDBK and DAMBRK and supported the use of DAMBRK for more detailed analysis and use SMPDBK as a screening tool.

Lewis and Paquier (1999) analyzed and compared the results of Westphal and Thompson (1987) and National WeatherService (NWS) that predicted dam break of 6 dams in the Missouri State for (41 points) as shown in figure 2.5:

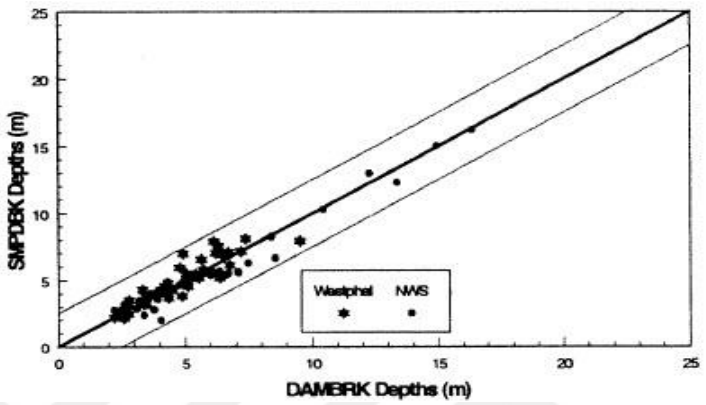

Figure 2.5. Depth comparison of DAMBRK model vs. SMPDBK model using NWS and Westphal data

According to Lewis and Paquier (1999), the SMPDBK model can be applied with courage to model dam failure analysis on the type of dams specified by the author.

Fread et al. (1991) suggests that the recent complete version of SMPDBK model includes various improvements, including the application of Manning equation to calculate the depth for a known discharge, providing cross sections to have both inactive (dead storage) widths and active flow widths. And the advantage of the energy slope rather than the channel bottom slope when calculating the maximum depth to consider the dynamic effect.

The SMPDBK model which computes the outflow hydrograph during the dam, the water surface elevation, and the peak discharge along the simulated reach, has been powerfully used for various dam investigations in the U.S and a lot of different countries for over 15 years (Fread, 1993).

It wasn't established to manage severe conditions like backwater effect, break of non-rectangular shapes, and cascades reservoirs which dynamic simulating is necessary (Fread, 1993).

Fread (1993) believes that when SMPDBK model used within the confines of its limitations, it's a very useful tool for analyzing the type of dam investigations specified by the author.

Hu and Walton (2008), Zhou et al. (2005), Gee and Brunner (2005) and Moreda et al. (2009) made comparisons between NWS FLDWAV and HEC-RAS. One of the common conclusions of these works is that FLDWAV is a more stable model that produces faster results. On the other side, HEC-RAS has better graphic output.

2.7. Gene Expression Programming (GEP)

GEP is an expansion to the genetic programming (GP) that was developed by Ferreira (2001a). Ferreira (2006, 2001a), GP was practiced in the range of hydrologic planning vastly in this decade. The fundamental difference separating GP and GEP is the description of the computer application. GEP is a symbolic regression algorithm to construct an objective function that matches a set of data. GEP is applying a genetic, development algorithm and symbolic regression to conform the data to optimum mathematical function. The program of GEP is encoded as linear strings of fixed length (genomes or chromosomes) and then candid as nonlinear groups of various sizes and shapes.

The characters for the case studies solution are produced automatically in GEP by coding the term as a tree composition with function and terminal. A convenience function is adopted to decide the formed candidates, and a qualification evaluation series is concerned to the higher achievement candidates and then reestablishment till gained an excellent generation. The GEP coding is very imaginative; the relation between the symbols of the function and the genomes is expressed regarding expression trees (ETs).

Investigations have proved that GEP is 100 to 60,000 times quicker than the traditional genetic algorithms. The genetic (ETs) are made of two segments (head and tail). The head introduces constants and variables that are used in ETs to encode a clear expression of mathematical function and the tail involves terminal symbols only.

2.8. GEP Applications in Water Resources Engineering

The application of GEP is broadly utilized in hydrologic engineering particularly in the last decade. Aytek, et al. (2014), applied GEP for the forecast of Van Lake data of the monthly water elevation, in Turkey. Seckin and Guven (2012), used linear genetic programming (LGP) of GEP and logistic regression were applied keeping in mind the end goal to determine peak flood discharges for 543 ungauged positions over Turkey. Guven and Kisi (2011) and Kisi and Guven (2010) used LGP in suspended sediment yield evaluation. Tofiq and Guven (2014) utilized LGP for forecasting the peak monthly discharges from statistical downscaling and to assess the influences of the climate change and global warming on preparing for the flood discharge by regarding various situations.

Traore and Guven (2013) utilized GEP for modeling reference evapotranspiration in "West Africa in Burkina Faso" applying simulating weather data from the tropical seasonal dry zones. And also one of the best GEP applications in water resources engineering was done by Al-Juboori, and Guven (2016). They employed GEP to produce a symbolic regression to forecast a curve of flow duration at any position inside the watershed of Hurman River, one of the main tributaries of Ceyhan river in Turkey; depended on the outputs of the runoff model in watershed modeling system software.

GEP was applied to present relations for evaluation of width (ws), location (ls) and maximum scour depth (ds) at the downstream of the flip bucket spillway (Guven and Azamathulla, 2012). GEP was practiced for evaluation of downstream scour depth of stilling basin into a trapezoidal canal. The achievement of GEP strategy was analyzed with different modeling systems like multiple linear regression (MLR) and artificial neural networks (ANNs). The analysis pointed that GEP provides more scientific results than the MLR and ANN models (Moussa, 2013).

Azamathulla et al. (2011) used GEP for developing a stage-discharge (S-Q) relationship for the Pahang River. The sequences determined that GEP as a helpful tool could be applied for determining of daily discharge data in flood situations. Guven and Aytek (2009) used GEP method in two stations of Schuylkill River in U.S. The realization of GEP suggestion was compared with more traditional methods, multiple linear regression (MLR) and stage rating curve (SRC) methods.

The sequences displayed that GEP gives more accurate results than MLR and SRC models. GEP model was applied for analyzing the transportation total load in three rivers which are Kurau, Langat, and Muda (Zakaria et al., 2010).

Azamathulla and Jarrett (2013) was applied GEP model for evaluation of the manning's coefficient roughness for high gradient rivers by using field measurements data. Also, Azamathulla et al. (2012) used GEP model for evaluating the coefficient of discharge side sluice gates for conditions of free flow. Azamathulla and Karbasi (2015) produced unique equations based on GEP to define the properties of hydraulic jump over a tough bed and analyzed it with existing equations and other software computing systems like Support Vector Regression (SVR) and Artificial Neural Network (ANN). The consequences were given that the empirical equations had more computational errors than the SVR, ANN, and GEP models, and also Azamathulla and Karbasi had discussed that the derived equations from GEP are more applicable.

Also, GEP was favorably practiced in a broad variety of topics in planning water resources engineering (Zorn and Shameldin 2015; Wang et al. 2013; Kisi et al. 2012; Guven 2009).

CHAPTER 3

3. Case Study

The case study is Dukan Dam formed upon Lesser Zab River; one of the Tigris River tributaries in Iraq. Dukan Dam is a concrete arch dam with a multi-purpose dam. The geographic coordinates for the Dukan dam are (35°57′15″North 44°57′10″East). Figure 3.1 shows the case study.

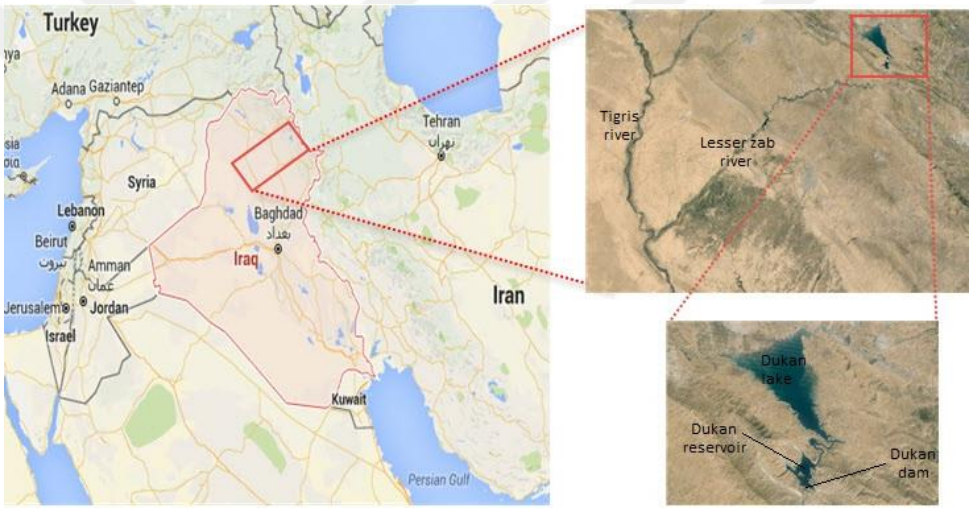

Figure 3.1. Iraq map and study area

3.1. Lesser Zab River

The Lesser Zab River springs in the Zagros Mountains of Iran at the height of 3000 m above sea level. 400 Km is the entire length of the Lesser Zab river and with the significant slope in Iranian sections among the origin springs and the beginning of the traditional border with Iraq. The total area of the basin is 22250 Km2 which is defined 5000 Km2 in the Iranian areas, and the additional parts of area 17250 Km2 in Iraqi territories which is evaluated as 74% of the total area of the basin.

Several tributaries feed the Lesser Zab River which are Sewail River and Joga soor river. And also these tributaries have branches, like Sewail River branches are Shalar and Qislaja and Joga soor river branches is Mawakan. This two tributaries Jaga soor and Sewail flowing to Qala jolan river and drain to Lesser Zab river near the Iran-Iraqi boundary. Due to a high number of branches on Lesser Zab river, and to control the streaming water to get an improvement in drought seasons at southern regions of Iraq. This dam was built. The annual average quantity of water coming to the Dukan Lake from the Lesser Zab River is 5.82 billion m^3 (TALAB, 2011).

3.2. Dukan Dam

Dukan Dam is located on the Lesser Zab River approximately 295km north of Baghdad and 65km southeast of Sulaimaniyah city. The annual average precipitation on Dukan dam watershed is 665.17 mm, and the average annual discharge that released from the dukan dam is 6.19 billion cubic meter. Evaporation reaches to 41% of the complete annual evaporation during the summer which is the highest level; the amount of missed water by evaporation from Dukan reservoir is around 0.4 billion m3 in the season.The minimum elevation for electric power generation is adapted to be 480 meters, and the normal water elevation is 511 meters and the recommended water height in the reservoir is about 495.5 meters above sea level. The crest length of the dam is 345 m and has a height of 116.5 m. Dukan dam and its reservoir are shown in figure below (SMEC, 2006):

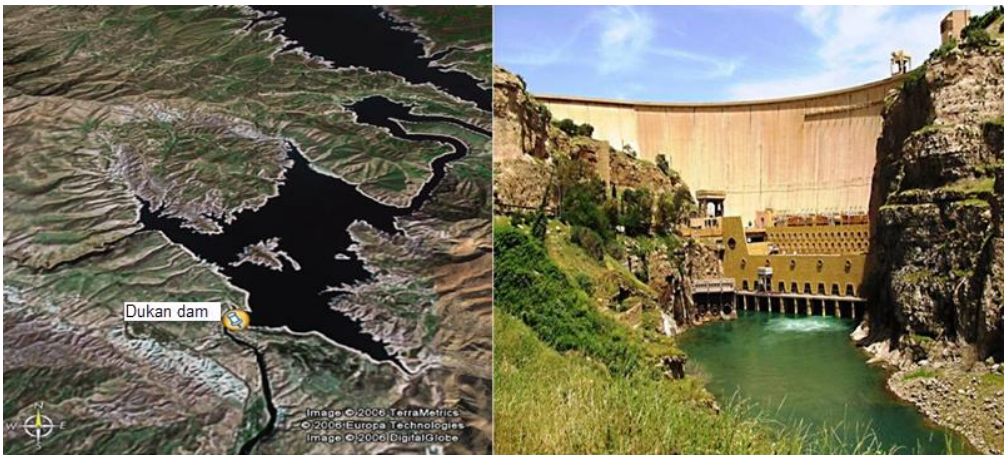

Figure 3.2. Dukan dam and its reservoir

Table 3.1 shows the characteristics of the Dukan dam (SMEC, 2006).

Table 3.1. Pertinent Data for Dukan Dam

	Details	**Value**	
HYDROLOGY	Catchment Area	11,690 km²	
	Mean Annual Catchment Precipitation	850 mm	
	Designed Peak Outflow	4,180 m³/s	
	Design Inflow	13,300 m³/s	
	Maximum Recorded Inflow	4,698 m³/s	
	Maximum Recorded Outflow	2,260 m³/s	
DAM	Dam Type	Cylindrical Arch	
	Maximum Height	116.5 m	
	Crest Level	El. 516 m A.S.L.	
	Width	At Crest 6.2 m At Base ▪ Including Foundation Socle 65.0 m ▪ Without Foundation Socle 34.3 m	
	Crest Length	Total 345 m ▪ Left Gravity Abutment 41 m ▪ Arch 240 m ▪ Right Gravity Abutment 64 m	
	Concrete Volume	Total 370,000 m³ ▪ Arch 325,000 m³ ▪ Gravity Abutments 45,000 m³	
	Cylinder Radius of Upstream Face	120.0 m	
	Excavation Volume	160,000 m³	
SPILLWAY	Type	Gated Service Spillway	Emergency Spillway
	Gate Size of the Spillway	Three gates of 10m x 6.8m	40.26m diameter bellmouth ('Morning Glory')
	Crest Level at Ogee	El. 496.50 m ASL	El. 511.00 MASL
	Discharge Capacity at El 515.1m ASL	2,450 m³/s	1,860 m³/s
	Top of Closed Gate	El. 506.50 m ASL	-
	Internal Diameter inside the Tunnel	11.00 m	10.20 m
	Internal Diameter of Shaft	-	12.50 m
	Outlet Details	Free Outlet approximately 50m above river gorge	Steel lined, reduced diameter 9.90m, inclined 47° downstream and 30° upwards for free discharge to river gorge

Table 3.1. Continued

	Details	Value
IRRIGATION OUTLETS	Irrigation Supply Tunnels	2 No. through right abutment rock ▪ Upstream part internal diameter 4.85 m ▪ Downstream part internal diameter 2.29 m
	Diameter value of Butterfly Guard Valve	2.5 m
	Diameter value of Howell Bunger Valves	2.5 m
	Maximum Discharge	2 x 110 m³/s
POWER STATION	Type	Surface Power Station at Dam Toe
	Numberand type of Turbine	5 No. Vertical Francis Turbines
	Rated Head	95 m
	Steel Penstocks diameter	5 x 3.65 m
	Rated Discharge	5 x 110 m³/s
	Rated Output	5 x 80 MW

The hazard category of Dukan Dam has been considered as 'Extreme' and accordingly, the dam should have enough dry freeboard to protect the dam from being overtopped by a flood. History shows that the flood water can increase the level of water in the dam and threaten the downstream of the dam (SMEC, 2006).

Table 3.2. Summary of previously recorded reservoir level in Dukan dam

Parameter	Maximum Recorded Values
Max. Reservoir Level m	512.26
Date	04/05/1988
Min. Reservoir Level m	430.95
Date	25/12/1960
Notes: The dam crest elevation is 516m ASL	

Storage and surface area at each level in the reservoir are described in figure 3.3:

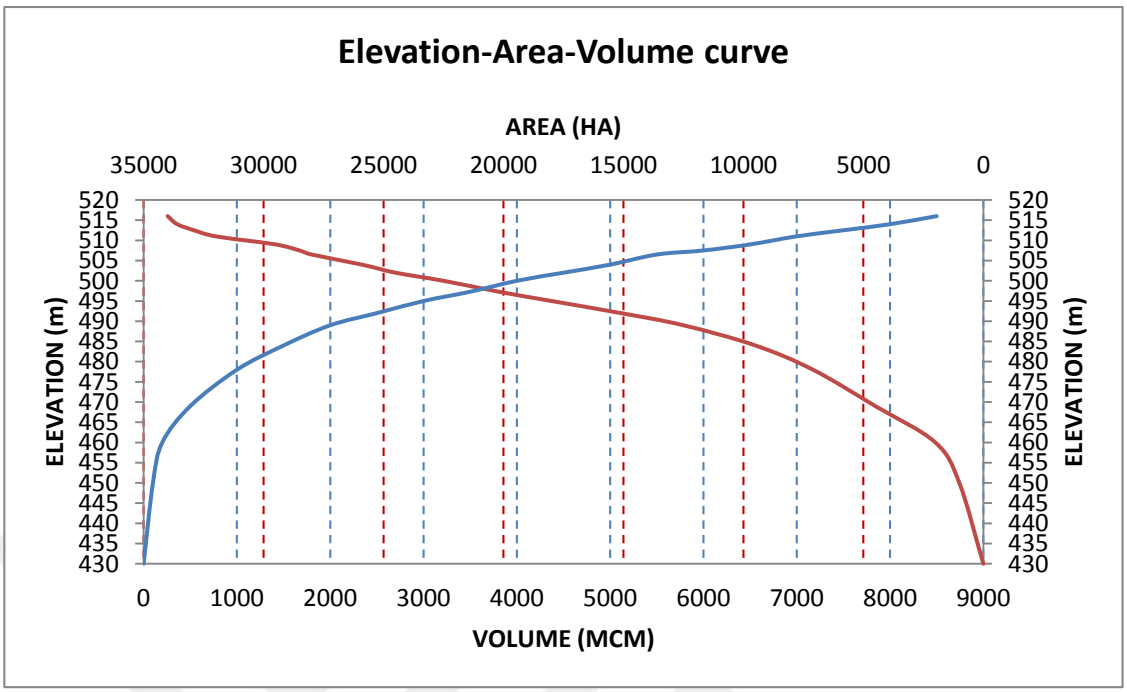

Figure 3.3. Dukan dam Elevation-Area-Volume curves (TALAB, 2011)

Also in the figure below dam cross-section with its common elevations are shown:

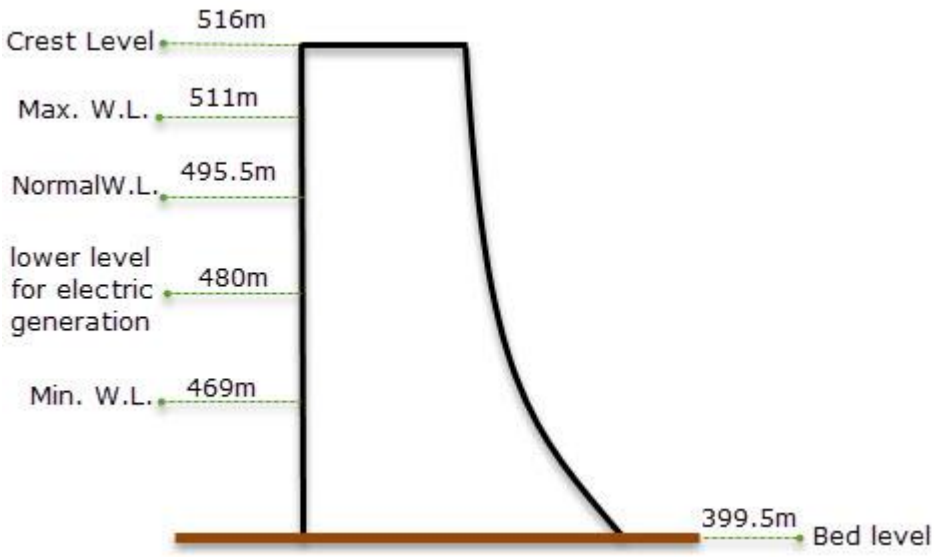

Figure 3.4. Dukan Dam cross-section

3.3. Dukan Dam problems

3.3.1. Bellmouth Spillway and Tunnel

The reservoir level at inspection day was about elevation 488m. The main leakage is characterized as three closely orifices on the west side of the Spillway. General seepage can be spotted around the remainder of the construction joint at (elevation 479m – arrow 1). Addition seepage was spotted at the next construction joint at the base of the pre-cast blocks (elevation 488m – arrow 2) on the east side of the bellmouth. The quantity of leakage from the main points of ingress appeared to be in order of 5 l/min, which could correlate with the level of the reservoir as shown in figure below:

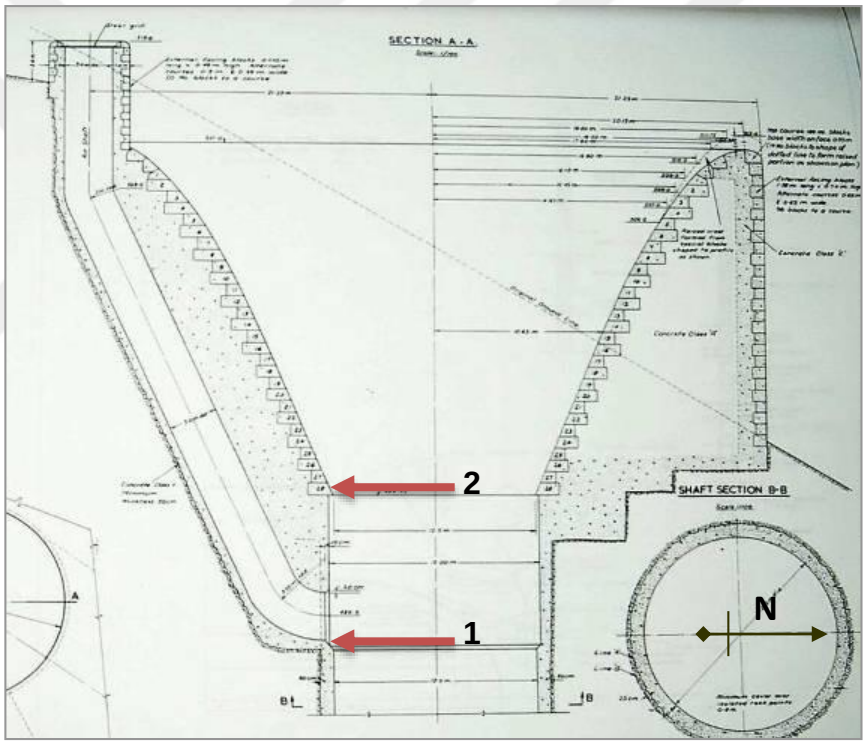

Figure 3.5. Leakage positions in Bellmouth spillway

The leakage should be treated immediately in order to stop the further decay of the bellmouth shaft lining and a good solution may be to inject a radial pattern of grout around the construction joints (elevations 479m and 488m). This may need to be carried out during a period when the reservoir is drawn down, preferably below 480m (SMEC, 2006).

3.3.2. Right Bank Grouting Gallery

An investigation was accomplished for the Right Bank Grouting Gallery when reservoir water level was at elevation 501.34m. The galleries elevation is approximately 450m. It has seepage flows which were collected and conveyed out to the river; downstream of the Dukan dam. It is evaluated that approximately 25 l/min was flowing through the V-notch weir (SMEC, 2006).

3.3.3. Left Bank Grouting Gallery

An investigation of the Right Bank Grouting Gallery was carried out when reservoir water was at elevation 501.34m. The height of the galleries is approximately 434m above sea level.The last section of the gallery is still unlined in the higher elevation; Dam Directorate staff report that large leakage flow from this unlined section is spotted at high reservoir elevation. At the time of the inspection, a flow of around 2 l/min was observed from the crown of the gallery (SMEC, 2006).

Figure 3.6. Leakage in the Unlined Section of the Left Bank Grouting Gallery

3.3.4. Left Abutment of dam

Left Abutment expands in a northeastern direction to the left bank of the reservoir at elevation 480.5m; considerable leakage can be observed with an inflow of 5 l/sec. An effort has been made to control this leakage by the installation of a pipe to catch the leakage and direct the water to the appropriate drain. However, at high reservoir pool levels, the inflow exceeds the capacity of the pipe and overflows (SMEC, 2006).

CHAPTER 4

4. METHODOLOGY

4.1. General

In this study, GIS data is downloaded as Digital Elevation Model (DEM) by using the ability of Global Mapper software, which can provide worldwide coverage of filled data by NASA Shuttle Radar Topography Mission (SRTM), 1 Arc-Second Global (30 meters) resolution. Then GIS data is imported to Watershed modeling system (WMS) software to create a Simplified Dam Break (SMPDBK) model. WMS software has capabilities of utilizing Geographic Information System (GIS) as Triangulated Irregular Network (TIN) and Digital Elevation Model (DEM) to compute the flow direction and flow accumulations for defining river center line, assign manning's roughness values as area properties and extracting cross-sections across the river. Then SMPDBK model was activated in WMS software to define the Dukan dam properties as a case study of this research. Then several scenarios were run for a dam break and affected areas by the flood were analyzed.

The output data of SMPDBK is used in DTREG software, which is one of the most successful applications of statistical analysis in developing a model for representing and explaining the relations between data items (variables). Gene Expression Programming (GEP) model in DTREG software, which is symbolic regression algorithm, is used to form a mathematical function that fits a set of data to predict water surface elevation, discharge, and travel time of the flood during a hypothetical dam break event for each significant place through the downstream river of Dukan Dam.

4.2. Watershed Modeling System (WMS) Software

WMS developed at Brigham Young University, is a complete environment graphical modeling for all aspect of the hydrological, watershed and hydraulics. WMS includes powerful tools for calculations of the basin delineation geometric parameter, computations of GIS overlay covering rainfall depth, curve numbers (CN), roughness coefficients, etc., and extraction of the cross-section from terrain data. WMS gives an interface for a set of hydraulic and hydrologic models in a GIS-based processing of frame work. Models packaged within the system include HEC-1, TR-20, TR- 55, National Flood Frequency Model (NFF), Modified Rational Method Model (MODRAT), Rational Method and HSPF as hydrologic modeling components. HEC-RAS, Simplified Dam-Break Model (SMPDBK) and CE QUAL W2 provide hydraulic modeling capabilities. Gridded Surface Subsurface Hydraulic Analysis (GSSHA), a runoff and infiltration model from the Engineering Research Development Center (ERDC), and the U.S. Army Corps of Engineers (USACE), is also included for 2-D integrated hydrology modeling with groundwater interactions. Additional calculations include the use of the rational method to compute peak flows primarily for small rural watersheds (WMS, 2008).

4.3. SMPDBK Model

Fread et al. (1991) the National Weather Service (NWS) in 1983, evolved a system for estimating the flood along downstream of the broken dam. This system identified as the Simplified Dam Break (SMPDBK) Model, gives the information required for delineating areas threatened by floodwaters of the dam-break.The SMPDBK model can predict maximum flood discharges, maximum travel times, and maximum flood elevations, of the dam-break at picked downstream points. SMPDBK model's capability for producing results efficiently makes it a valuable tool for forecasting in a dam failure. The SMPDBK model is also useful when the utility of different flood simulating models is restrained by insufficient resources.

SMPDBK model is able to provide approximate calculations of the flood's effect just after inserting the elevation of the water surface in the reservoir for the first two cross sections of the downstream river; identified from topographic maps or on-site

inspection. If, however, the user has access to further information (i.e., both the reservoir storage volume and reservoir surface area ; evaluations of the final depth and width of the breach; the time needed for breach development; the Manning roughness coefficient; the spillway, turbine, and/or overtopping flow; the elevation of flood connected with a selective waterway cross section where flooding becomes a trouble; up to 50 channel cross sections along the downstream) the model will use this data to improve the efficiency of the prediction.

For providing flood forecast of the dam-break, the SMPDBK model firstly determines the maximum outflow at the dam; this calculation has depended on the size of the reservoir, the breach size, and the time of breach formation.The channel properties and computed flood wave are utilized in integration with peak-flow routing curves to define how the maximum discharge toward the downstream will be attenuated. Depended on this strategy, the model calculates the maximum discharges toward the downstream of the valley for every defined cross sections. Then the model calculates the depth transferred by the maximum discharge depended on the slope, roughness, and geometry of the channel along the downstream cross sections. SMPDBK model also calculates the time expected for the maximum flow to access any prediction location (cross-section). Therefore it supplies the user with a time framework for fortification and evacuation depending on the preparation plan.

4.3.1. Model development

Fread et al. (1991) the SMPDBK model keeps the essential deterministic elements of the numerical DAMBRK model throughout reducing the requirement for extensive computer equipment. The model achieves this by approaching the channel at downstream as a prism, covering the impacts of the dead storage (off-channel) at any suitable place. It is associating with the maximum discharges, travel times and the elevations of the maximum water surface, ignoring the influences of backwater from downstream buildings. It uses dimensionless peak-flow simulating curves that were generated from the NWS DAMBRK model of Saint Venant equations of unsteady flow which are the momentum and continuity equations which in-turn is based on momentum equations and conservation of mass.

4.3.2. SMPDBK Descriptions

Breach description

Fread et al. (1991) suggest that SMPDBK model permits for the study of partial breaches happening over a finite period of time. While the model assumes final breach elevation is the bottom elevation of first cross section (tailwater) and a rectangular shape for breach formation in the dam body.

A single equation utilizes in the SMPDBK model (Eqn. 4.1) for determining the maximum breach outflow (Qb max.), and the values of five variables are needed as the input data to this equation. Which are:

1) The reservoir surface area (A_s).
2) Head on the breach (H) which is the difference between water surface elevation of the reservoir when breaching begins and bottom elevation of the final breach.
3) The time required for the breaking formation (T_f).
4) Non-breach outflow during failure time (Q_o).
5) The final width of the breach (B_r).

Channel description

Fread et al. (1991) mentions that the first cross-section of the river channel just at downstream of the dam body to any simulating location is estimated as a prismatic channel. All cross sections in any simulating point are taken from topographical projections (GIS data), to represent width irregularities of the valley, and significant variations in the river bed slope. This prismatic representation along the downstream of the river is needed to predict the magnitude of maximum discharge attenuation precisely.

4.3.3. SMPDBK Flow Chart

SMPDBK is easy to use, but the underlying algorithms are not so simple (Reed and Halgren, 2011):

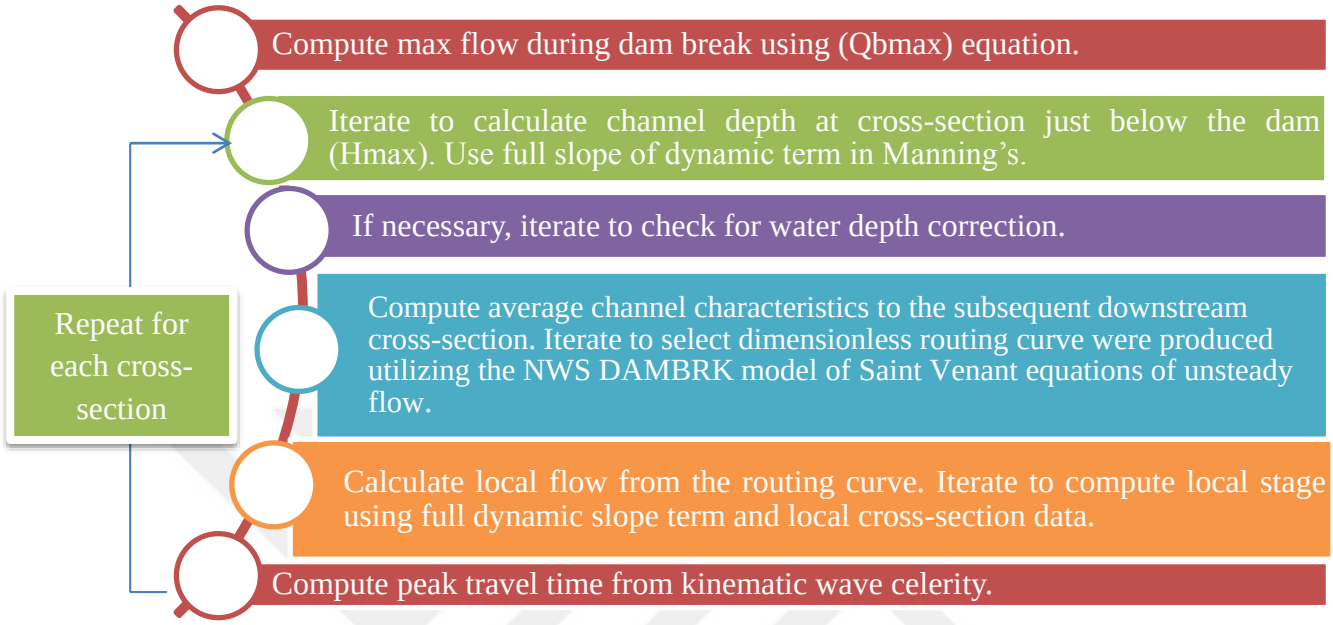

Figure 4.1. SMPDBK flow chart

4.3.4. Gene Expression Programming (GEP) Model Flow Chart

The operation starts with the random generation of a particular number of the chromosomes individuals (called the initial population). Then these chromosomes are expressed, and each fitness individual is evaluated toward the cases of the fitness set (called environmental selection). Then the individuals are chosen according to their fitness (called individuals performance in that particular environment) for reproducing with modification, leaving offspring with new features. Again in their turn, these new individuals are, subjected to the same process of the development: chromosomes expression, facing of the environmental selection, selection, and reproducing with modification. The operation is replicated for a specific number of generations or until a suitable solution has been gained (Ferreira, 2006).

The primary steps of the gene expression algorithm (GEA) are schematically expressed in Figure 4.2:

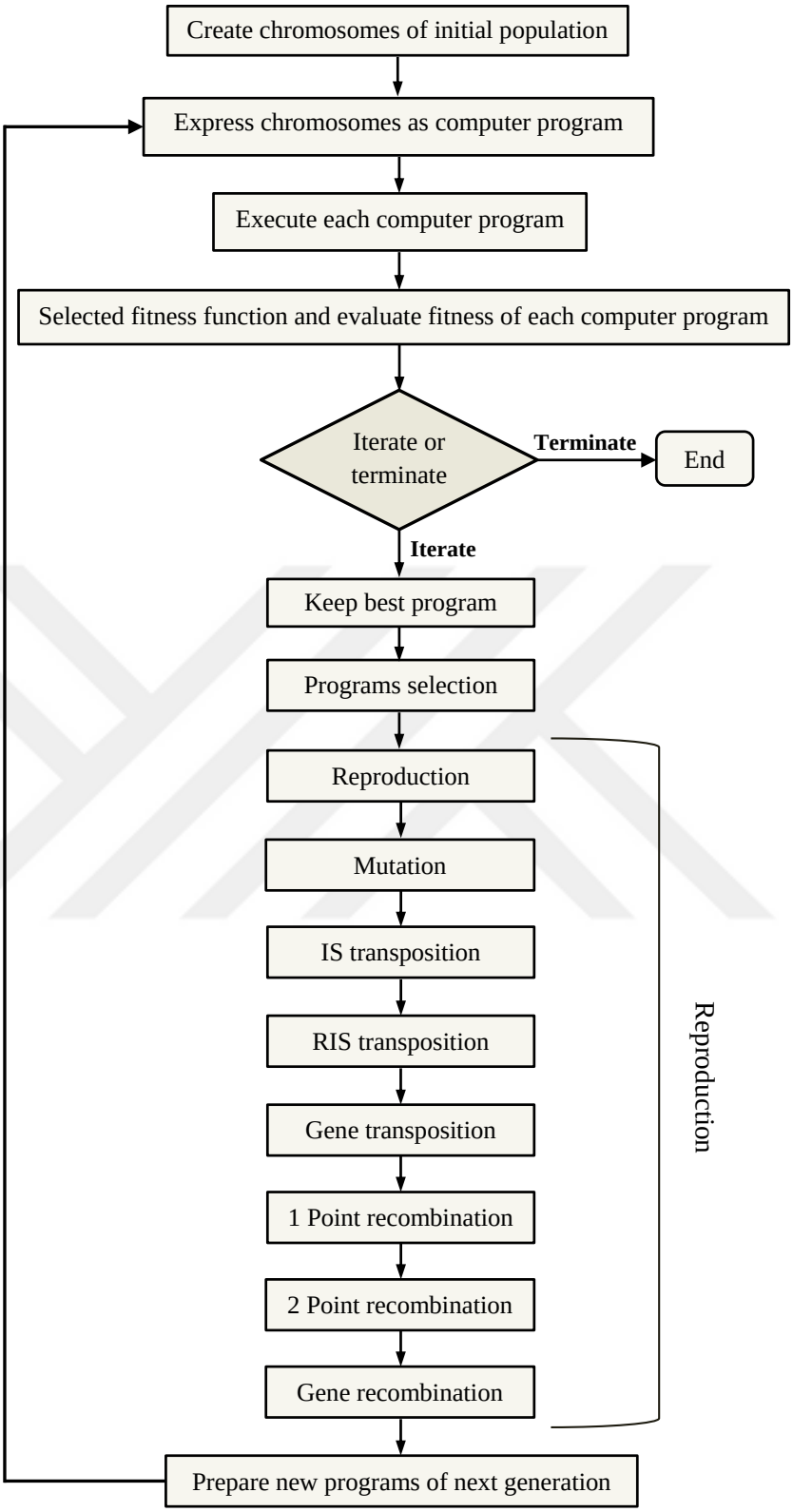

Figure 4.2. The flowchart of a gene expression programming (Ferreira, 2001)

4.4. Gene Expression Programming Operations

The genes expression tree is composed of two parts (head and tail). The head is used mainly to encode the functions and variables, and whereas the tail used to encode the variables. In GEP, the chromosomes function are exposed to modification by mutation, transposition of Insertion Sequence, root transposition, gene transposition, one-point recombination, two-point recombination, and gene recombination. The chromosomes encode expression trees which are the purpose of selection. The production of these separate entities (genome and expression tree) with prominent functions permits the algorithm to operate with high efficiency that significantly exceeds existing adaptive techniques (Ferreira, 2001b). For sure, GAs usually applied mutation and recombination; GP indicates specific recombination; and GEP involves mutation, recombination, and transposition (Ferreira, 2001a).

4.4.1. Mutation

Mutations can place wherever in the chromosome. Nevertheless, the structural organization of chromosomes must stay intact. It is the most efficient operator in GEP. In the heads, any function can change into the terminal or vice versa; in the tails, terminals (variables and constants) can only change into terminals. In this system, the fundamental set of chromosomes is controlled, and all the new individuals generated by mutation are structurally correct programs.

4.4.2. Transposition of Insertion Sequence (IS) Elements

Any position of the genome might become a transposition of IS element, being, therefore, these elements randomly selected along the chromosome. A copy of the transposon is formed and inserted at any location in the head of a gene, except the first location. The transposition operator randomly takes the length of the transposon, the start of the IS element, and the target site.

4.4.3. Root IS Transposition

All Root IS (RIS) elements begin with a function among the sequences of the heads. For this, a point is randomly chosen in the head, and the gene is shifted to the start position of the RIS element until a function is obtained. If the operator does nothing and no functions are detected; this operator randomly picks the gene to be modified in the chromosome, its length, and the start of the RIS element.

4.4.4. Gene Transposition

In gene transposition, an entire gene function in the chromosome is shifted to the beginning of the chromosome as a transposon. In opposite to the other forms of transposition, the transposon (gene) is removed from the place of origin.

4.4.5. One-Point Recombination

In one-point recombination, the chromosomes are matched and divided at the same point. The first parts of the recombination point are exchanged between the two chromosomes.

4.4.6. Two-Point Recombination

In two-point recombination, the chromosomes are matched (paired), and two points are randomly taken as crossover points. The material between the points of recombination is switched between the two chromosomes of a parent, developing two new generation chromosomes.

4.4.7. Gene Recombination

In the third type of GEP recombination, entire genes are exchanged between chromosomes of two parents forming two new generation chromosomes containing genes from both parents. The exchanged genes are randomly picked and take the same location in the parent chromosomes.

4.5. Dam Break Modeling

Digital Elevation model (1 Arc-Second DEM) resolution was used to the case study. The global projections of the case study are (Projection: UTM, Zone: 38 (42°E - 48°E) Northern Hemisphere, Datum: WGS84, Planar Units: meter, Vertical Units: meter). Figure 4.7 shows DEM of the study area.

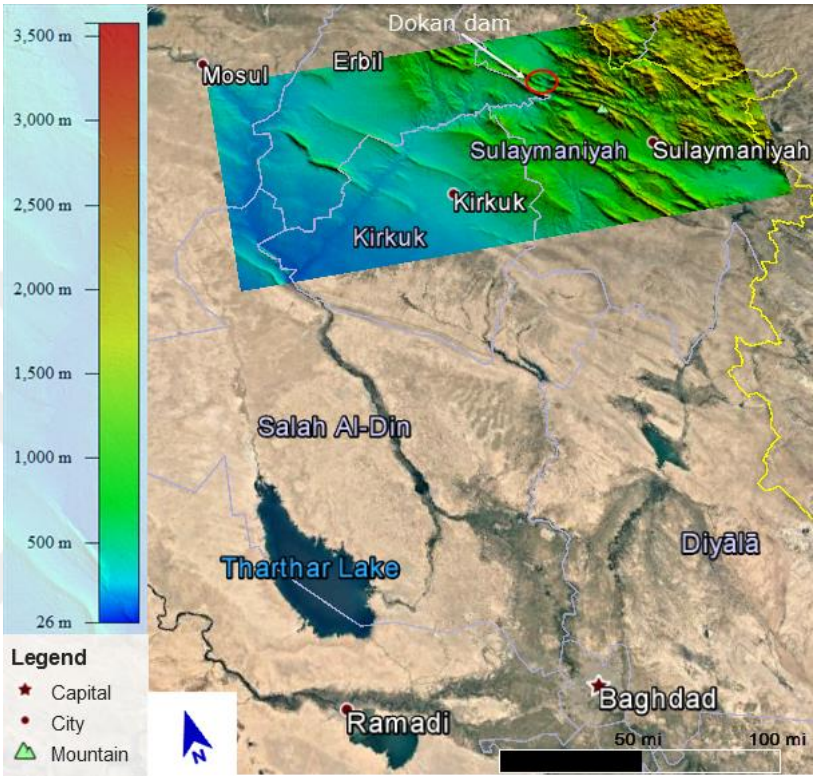

Figure 4.3. DEM of the study area and the Iraqi cities around it

Then GIS data as DEM is imported to WMS software for running TOPAZ flow for computing directions of flow and flow accumulations. The purpose of doing this is to obtain a streaming arc that represents the centerline of the River downstream of the Dukan dam. The streaming arc which is Lesser Zab River is analyzed; starting from Dukan dam to the confluence point with Tigris River.

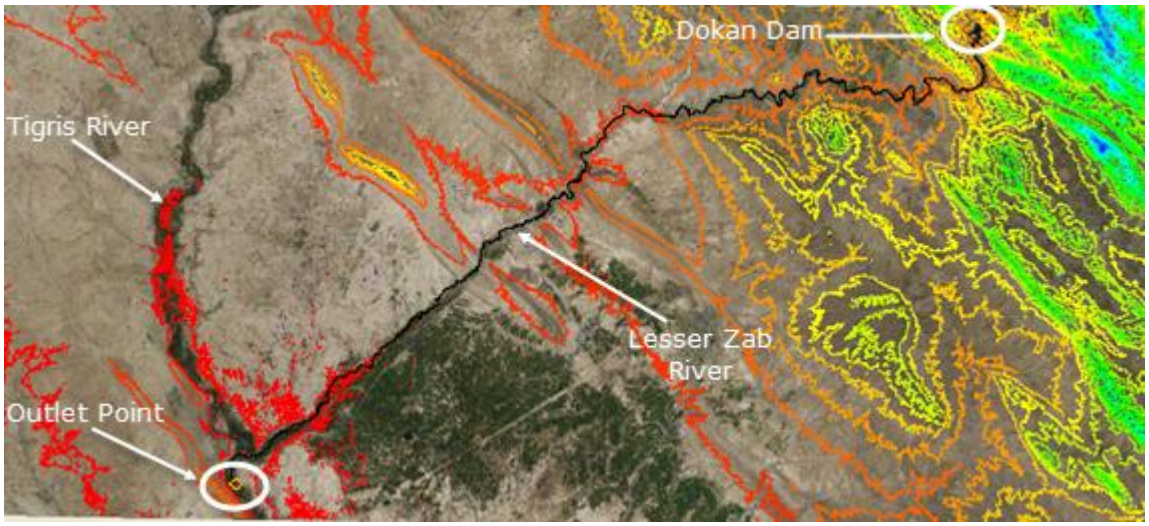

Figure 4.4. Streaming arc for Lesser Zab River

The purpose of taking the flow accumulation to the outlet point of the Lesser Zab River is to determine the discharge that will be entering the Tigris River across Lesser Zab River during Dukan dam break (God forbid).

After defining the Streaming arc as River and For preparations to extract the cross sections, DEM is Converted to Triangulated irregular network (TIN), which is a digital data structure used in a geographic information system (GIS) for the representation of a surface. Figure 4.19 shows Extracting cross sections along the Lesser Zab River.

Figure 4.5. Cross sections along Lesser Zab River

Then assign Manning's roughness values along the areas of Lesser Zab for all zones, according to the manual of WMS and Iraqi standard codes. Manning's roughness values are (0.03 for River, 0.05 for Banks, 0.08 for Towns) as shown in figure 4.21.

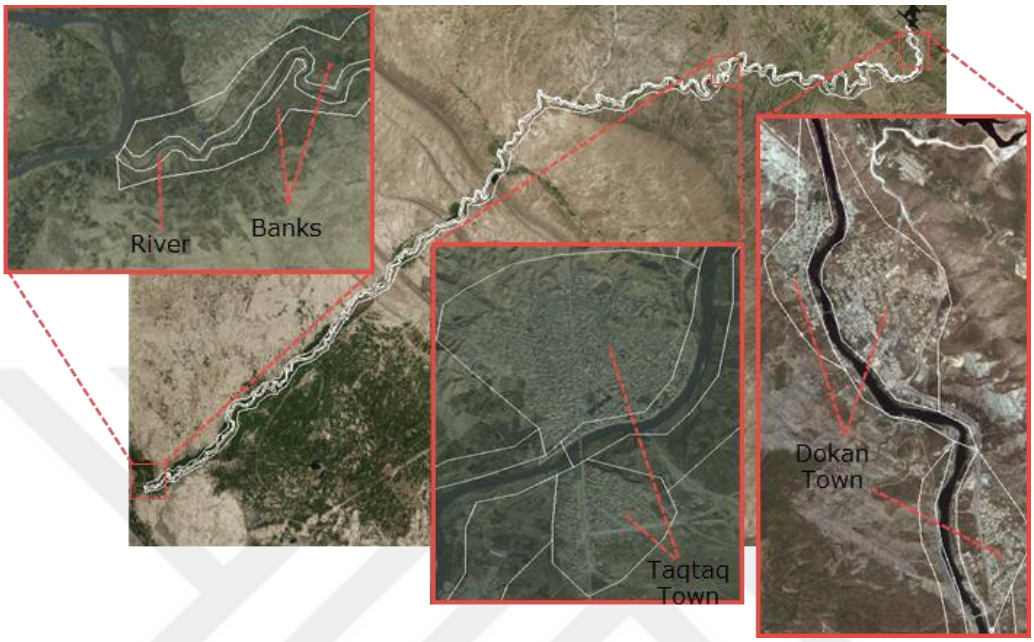

Figure 4.6. Assigning Manning's Roughness for Banks and River

4.6. Applied Dam Break Modeling

After defining (centerline, cross sections, and Area Properties), the cross sections are ready for extracting the hydraulic model by using TIN data in WMS software. Then SMPDBK model is activated. Then input data of dam are applied as steps below:

1) **Dam name:** enter name of dam, (Dukan dam for this research).
2) **River name**: enter name of the river, (Lesser zab for this research).
3) **Dam type**: There is three options (Earth, Concrete, and Arch) dam, (choose Arch dam for this research).

4) **Elevations Of water when dam breach** (ft-msl).

Table 4.1. Elevations of water in the dam when a break occurs for each scenario

Scenarios	Elev. In (M)	Elev. In (Feet)
1st	516 m	1692.91 Ft
2nd	511 m	1676.51 Ft
3rd	507 m	1663.39 Ft
4th	504 m	1653.54 Ft
5th	500 m	1640.42 Ft
6th	495 m	1624.02 Ft
7th	489 m	1604.33 Ft

5) **Elevation Of breach bottom** (ft-msl): as the default value is assumed to be the bottom elevation of tail water (first) cross section. For all scenarios is 399.5 m (1310.69558 Ft) which is equal to the bottom elevation of the first cross section.

6) **Volume of the reservoir** (ac-ft): By using (Storage-elevation) curve in Section (3.2) to find the volume of the reservoir at Dukan dam for each water elevation scenario when a breakoccurs.

Table 4.2. Volume of the reservoir when break occurs

Scenarios	Vol. (MCM)	Vol. (ac-ft)
1st	8400	6809998
2nd	7000	5674998
3rd	6000	4864284
4th	5000	4053570
5th	4000	3242856
6th	3000	2432142
7th	2000	1621428

7) **The surface area of the reservoir** (acres): By using (surface area- storage) curve in (figure 3.3) to find the surface area of the reservoir at dukan dam for each scenario when a break occurs.

Table 4.3. Surface area of the reservoir when break occurs

Scenario	A_s (ha)	A_s (acres)
1st	34000	84017.4
2nd	32000	79075.2
3rd	28500	70426.35
4th	25900	64001.49
5th	22500	55599.75
6th	18000	44479.8
7th	12600	31135.86

8) **The width of rectangular breach**: from manual equations as a default value which is equal to 0.9*Maximum width of tail water section (first cross section) for concrete arch dam (ft).

The maximum width of tail water (first) cross section =203.2 m = 666.5 ft

Br = 0.9*Maximum width of tail water section (first cross section)

Br = 0.9*666.5 = 600 ft, **Br = 600 Ft = 182.88 m** (as shown in figure 4.26)

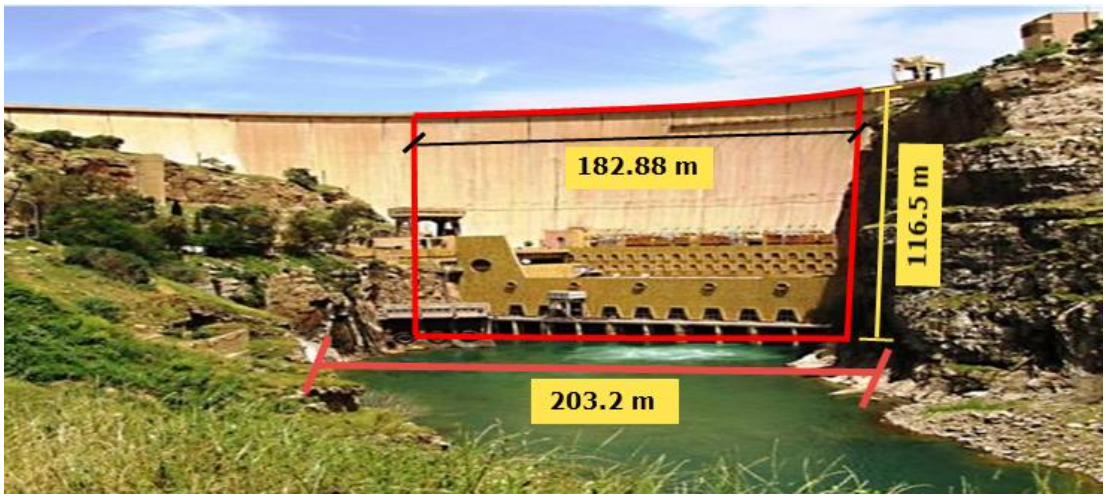

Figure 4.7. Dukan dam Break dimensions

9) **Time for breach to develop:** from manual equations as default value which is equal to H/50 for concrete arch dam (minutes).

H: The difference in (ft) between water surface elevation of the reservoir when breaching begins and bottom elevation of the final breach (h_r).

Table 4.4. Calculations of time for breach to develop

#	Water surface elevation when breach occur (Ft)	Final bottom elevation of the breach (h_r) (Ft)	Height of water (H) Ft	Time for breach to develop (H/50) (minutes)
1	1692.91	1310.69558	382.21	7.644
2	1676.51	1310.69558	365.81	7.316
3	1663.39	1310.69558	352.69	7.0538
4	1653.54	1310.69558	342.84	6.856
5	1640.42	1310.69558	329.72	6.594
6	1624.02	1310.69558	313.32	6.266
7	1604.33	1310.69558	293.63	5.872

10) **Non-breach flow (Q_o):** calculated from penstock, spillway and gated service discharges (cfs).

The outlet flow from Penstock = 550 m^3/s (work when the elevation of water in the reservoir is 480 m.a.s.l and above).

Emergency spillway (Bellmouth) Capacity = 1860 m^3/s (Crest elevation is equal to 511 m.a.s.l).

Gated service spillway Capacity = 2450 m^3/s (bottom elevation of gate is equal to 496.5 m.a.s.l).

Table 4.5. Calculations of non-breach flow (Qo)

Scenario	Elevation Of water in reservoir when dam break	Penstock flow capacity m^3/s	Bellmouth Capacitym $^3/s$	Gated service spillway Capacitym $^3/s$	Non-breach flow (Q_o) m^3/s	**Non-breach flow (Q_o) Ft^3/s**
1	516 m.a.s.l	550	1860	2450	4860	171629.4
2	511 m.a.s.l	550	1860	2450	4860	171629.4
3	507 m.a.s.l	550	-	2450	3000	105944.1
4	504 m.a.s.l	550	-	2450	3000	105944.1
5	500 m.a.s.l	550	-	2450	3000	105944.1
6	495 m.a.s.l	550	-	-	550	19423.09
7	489 m.a.s.l	550	-	-	550	19423.09

11) **Dead storage equivalent manning's N:** taken 0.5 due to the long distance of (Lesser Zab) river and due to a lot of meanders. In SMPDBK model by defining a high Manning roughness (n) in the range of 0.30 to 0.50, the inactive (dead-storage) portion of the cross sections is represented.

12) **Number of cross-section**: (50) cross-sections were taken.

13) **Distance to theprimary point of interest**: length of Lesser Zab River from Dukan dam to Tigris River.

The model is finished now, and it's ready to run the simulation. When the user is running the SMPDBK simulation, WMS is attempting to read the SMPDBK solution. Solution points which are (discharge, flood depth, flood elevation and travel time) are placed where each cross section intersects the stream centerline in the hydraulic model.

After running SMPDBK, WMS reads the solution as a 2D scattered dataset. This solution contains water surface elevation points where each cross section intersects the stream centerline. Delineating the floodplain needs additional solution points to

create a well-defined map. Interpolating solution points along the centerline, and the cross sections create additional solution points, for delineating the floodplain from these points will apply according to GIS data.

4.7. Calculation of Maximum Break Discharge ($Q_{bmax.}$) by empirical equations

The purpose from this point is to calculate the discharge that escapes from the dam when a break occurs. By using empirical equation and comparing it with the discharge of first cross-section of SMPDBK model, it will be clear whether there are any mistakes in input data of the model and the validity of the work is also checked. If the results show a large difference between Qbmax. and first (tail water) cross-sectional discharge of SMPDBK model; another software must be used instead of SMPDBK model. The empirical equation for Maximum Break Discharge calculations is:

$$\boldsymbol{Q_{bmax} = Q_o + 3.1 * B_r \left(\frac{C}{\frac{t_f}{60} + \frac{C}{\sqrt{H}}} \right)^3} \quad (4.1)$$

Where, $Q_o$is additional (no breach) outflow (cfs) at time t_f (i.e., spillway flow,turbine flow), B_r is final breach width (ft), $C = (23.4 * A_s)/B_r$, A_s is reservoir surface area (acres) at break elevation in the reservoir, t_f = H/50 for concrete arch dam, and H is the difference in (ft) between water surface elevation of the reservoir when breaching begins and bottom elevation of the final breach (h_r).

First scenario: Finding $Q_{bmax.}$ By Empirical equation

Solution:(Units ofempirical equation is in English system)

Q_o= 4860 m^3/s = 171629.4Ft^3/s (as shown in table 4.5)

Elev. of water when breach occur = 516 m = 1692.913 ft

Elev. of breach bottom (h_r) = 399.5 m = 1310.696 ft

H= 1692.913 ft - 1310.696 ft = 382.2179 ft

B_r: 0.9*Maximum width of the first (tail water) cross-section for concrete arch dam.

Br = 0.9*203.2=182.88m, Br = 182.88 m = 600 Ft (as shown in figure 4.7).

As = 34000 ha = 84017.4 acres (By using Surface area curve of the reservoir).

$$C = (23.4 * 84017.4)/600$$

C = 3276.677

t_f: Time of failure (minutes)

$$t_f = 382.2179/50$$

t_f = 7.644357 minutes

Q_{bmax}: Maximum breach outflow from the dam.

$$Q_{bmax} = Q_o + 3.1 * B_r \left(\frac{C}{\frac{t_f}{60} + \frac{C}{\sqrt{H}}} \right)^3$$

$$Q_{bmax} = 171629.4 + 3.1 * 600 \left(\frac{3276.677}{\frac{7.644357}{60} + \frac{3276.677}{\sqrt{382.2179}}} \right)^3$$

Q_{bmax} = 14038855 Ft^3/s = 397535.7 m^3/s

Note: Apply the same procedure for remaining scenarios to get the result in table 4.6:

Table 4.6. Calculations of Qbmax. by empirical equations

#	Qo (Ft^3/s)	Br (Ft)	Tf (minutes)	C	H (Ft)	Qbmax. (Ft^3/s)	**Qbmax. (m^3/s)**
1	171629.4	600	7.644	3276.677	382.2179	14038855	397535.7
2	171629.4	600	7.316	3083.931	365.8137	13155917	372533.7
3	105944.1	600	7.0538	2746.626	352.6903	12396076	351017.5
4	105944.1	600	6.856	2496.057	342.8477	11883661	336507.5
5	105944.1	600	6.594	2168.389	329.7244	11211524	317474.7
6	19423.09	600	6.266	1734.711	313.3202	10302144	291723.9
7	19423.09	600	5.872	1214.298	293.6352	9339660	264469.5

4.8. GEP Modeling

SMPDBK outputs (flood elevation, discharge and travel time) are used in GEP model for predicting flood characteristics. The format of the file must be converting to comma separated value (CSV) file, to support with GEP model as input data. The CSV file contains 6 columns and 351 rows; the first row is for the name of variables, and all other rows are variables data.

At first, Run; water elevation level in the reservoir when a break occurs and Distance of Lesser Zab River are chosen as predictor values, and the flood water level in River is chosen as a target value to predict the flood elevation equation for Lesser Zab River. At second Run; water elevation level in the reservoir when a break occurs and Distance of Lesser Zab River and the storage in the reservoir when a break occurs are chosen as predictor values, and the discharge during the Lesser Zab River is chosen as a target value to predict the Flow Equation for Lesser Zab River. At third Run; Distance of Lesser Zab River and storage in the reservoir when a break occurs, are chosen as predictor values. The travel time of the flood during River is chosen as a target value to predict the flood traveling time equation.

4.9. Application of GEP Modeling

Best settings for predicting equations of flood water level (FL), flood discharge (Q), and flood travel time (T) during the Lesser Zab River by GEP model as shown in table 3. Addition, subtraction, multiplication, and division are the arithmetic operations in the Function set to connect the mathematical structure function. Mutation rate, Inversion rate, Gene transportation rate ,One-point recombination rate, Two-point recombination rate, Gene recombination rate, IS transportation rate, and RIS transportation rate are the genetic operators. The optimum values of genetic operators that were applied on chromosomes drive optimum function for the data set (see section 4.4 for more information). Population size is the chromosomes number within the population being developed. 30 to 80 chromosomes is the best range of population size in GEP model. Genes per chromosomes are composed of one or more genes joined by a linking function. Usually, one to ten genes per chromosome work well. More complex functions require more genes. Gene head length is the

number of symbols (variables, constants, and functions) in the head section of each gene. Typically a head length in the range of two to sixteen works well. More complex functions require longer heads to allow for more variables and functions.

The fitness function is (Explained variance R^2) which is compute fitness score that ranges from 0.0 to 1.0. A fitness of 0.0 means the model fits very poorly. A fitness score of 1.0 means the model fits the data perfectly. The linking function is used to join the genes in the final function. Explained variance (R^2) for flood wave discharge equation is 98.319%, obtained in 1239training generations. Explained variance (R^2) for flood elevation wave equation is 99.469%, obtained in 773training generations. Explained variance (R^2) for flood travel time equation is 99.373%, obtained in 1741training generations.

Table 4.7. Gene expression programming model settings

	Equations title		
	Flood discharge	Flood level	Flood time
Function set	**Symbol**	**Symbol**	**Symbol**
Addition	+	+	+
Subtraction	-	-	-
Multiplication	×	×	×
Division			/
Genetic operators	**Value**	**Value**	**Value**
Mutation rate	0.037	0.047	0.047
Inversion rate	0.1	0.1	0.13
Gene transportation rate	0.1	0.1	0.1
One-point recombination rate	0.35	0.3	0.3
Two-point recombination rate	0.45	0.3	0.3
Gene recombination rate	0.1	0.1	0.1
IS transportation rate	0.1	0.1	0.1
RIS transportation rate	0.1	0.1	0.1
General	**Value**	**Value**	**Value**
Population size	60	65	50
Genes per chromosomes	6	8	6
Gene head length	10	9	8
Fitness function	R^2	R^2	R^2
Linking function	Addition	Addition	Addition

CHAPTER 5

5. RESULTS AND DISCUSSION

5.1. Cross Sections Positions

Table 5.1 shows the location of fifty cross sections, through Lesser Zab River. Cross section number two refers to the middle of Dukan town and also the location of cross section number twenty-two refers to the middle of Taqtaq town. In additional to the location of cross section number fifty which is referring to the intersection of Lesser Zab River with Tigers River. Calculating the flood characteristics between the confluence of Lesser Zab and Tigris River is a very interesting and important subject due to the beginning of another flood toward the capital Bagdad along the Tigris River. Table 5.1 is given in both Universal Transverse Mercator (UTM) and Geographic (Latitude/Longitude) system.

Table 5.1. Cross-sections positions along Lesser Zab River

Cross-sections positions				
Coordinates system			Coordinates system	
UTM DATUM: WGS84 UNIT: FEET UTM ZONE : 38 (42°E - 48°E) Northern Hemisphere			Geographic (Latitude/Longitude) DATUM: WGS84 UNIT: arc degrees	
No. of Cross sections	X (Longitude)	Y (Latitude)	X (Longitude)	Y (Latitude)
1	1628192.9030	13050865.7926	44° 57' 31.2807" E	35° 56' 44.0411" N
2	1628101.5487	13045718.0201	44° 57' 30.1960" E	35° 55' 53.1131" N
3	1633316.0989	13039891.4646	44° 58' 33.6444" E	35° 54' 55.4873" N
4	1634160.2609	13033225.5063	44° 58' 43.9285" E	35° 53' 49.5417" N
5	1629486.9462	13026545.9744	44° 57' 47.1364" E	35° 52' 43.4459" N
6	1622611.0368	13024858.0298	44° 56' 23.5643" E	35° 52' 26.7129" N
7	1617932.4983	13023980.3097	44° 55' 26.7028" E	35° 52' 17.9972" N
8	1612487.0272	13028995.8527	44° 54' 20.4538" E	35° 53' 07.5702" N
9	1606750.0066	13031754.4014	44° 53' 10.6688" E	35° 53' 34.8007" N
10	1598183.0065	13031879.7900	44° 51' 26.5062" E	35° 53' 35.9300" N

Table 5.1 continued

11	1600814.2633	13024131.8930	44° 51' 58.6269" E	35° 52' 19.3153" N
12	1592020.1529	13016080.8295	44° 50' 11.8969" E	35° 50' 59.5321" N
13	1587596.0699	13026864.2470	44° 49' 17.8978" E	35° 52' 46.1383" N
14	1579558.7323	13017961.6582	44° 47' 40.4215" E	35° 51' 17.9072" N
15	1572013.5338	13024732.6412	44° 46' 08.5345" E	35° 52' 24.7273" N
16	1560914.6656	13027491.1898	44° 43' 53.5327" E	35° 52' 51.7375" N
17	1547014.6237	13024139.8341	44° 41' 04.6902" E	35° 52' 18.1716" N
18	1544778.1825	13030988.4873	44° 40' 37.2314" E	35° 53' 25.8536" N
19	1538667.3249	13031754.4014	44° 39' 22.9043" E	35° 53' 33.2247" N
20	1529687.6965	13029931.0124	44° 37' 33.8144" E	35° 53' 14.8597" N
21	1526636.4936	13036545.2390	44° 36' 56.4039" E	35° 54' 20.1771" N
22	1518766.9291	13027045.6230	44° 35' 21.1957" E	35° 52' 45.8809" N
23	1514299.4056	13021825.7681	44° 34' 27.1650" E	35° 51' 54.0519" N
24	1506987.6373	13023918.1429	44° 32' 58.1827" E	35° 52' 14.4276" N
25	1506256.0980	13015328.4981	44° 32' 49.7745" E	35° 50' 49.4172" N
26	1497338.7996	13022670.3397	44° 31' 00.9805" E	35° 52' 01.6275" N
27	1492403.4124	13019818.4153	44° 30' 01.1732" E	35° 51' 33.1684" N
28	1484399.9344	13024356.4755	44° 28' 23.6122" E	35° 52' 17.6473" N
29	1475797.4094	13020093.2639	44° 26' 39.3471" E	35° 51' 35.0011" N
30	1467945.8354	13017101.2047	44° 25' 04.1460" E	35° 51' 04.9495" N
31	1457638.4939	13010689.1208	44° 22' 59.3894" E	35° 50' 00.8915" N
32	1450022.3844	13009059.0694	44° 21' 26.9948" E	35° 49' 44.2811" N
33	1443175.7715	13013145.6442	44° 20' 03.4859" E	35° 50' 24.2555" N
34	1437822.7223	13008306.7379	44° 18' 58.8601" E	35° 49' 36.0210" N
35	1421760.0908	13011592.3234	44° 15' 43.4421" E	35° 50' 07.3698" N
36	1401794.1110	13005493.5103	44° 11' 41.4964" E	35° 49' 05.4809" N
37	1382058.6368	12984754.9275	44° 07' 44.0369" E	35° 45' 38.6579" N
38	1375594.2892	12957852.2422	44° 06' 28.5492" E	35° 41' 11.9535" N
39	1350129.6900	12943480.8448	44° 01' 21.5166" E	35° 38' 47.3915" N
40	1326891.4160	12930340.0382	43° 56' 41.6020" E	35° 36' 35.0262" N
41	1319016.7739	12919706.8474	43° 55' 07.6296" E	35° 34' 48.9976" N
42	1310112.4209	12908545.5000	43° 53' 21.3338" E	35° 32' 57.6102" N
43	1298056.6417	12901003.7096	43° 50' 56.4783" E	35° 31' 41.6395" N
44	1285862.1620	12886301.4583	43° 48' 31.0676" E	35° 29' 14.7759" N
45	1274203.2210	12880483.2349	43° 46' 10.9388" E	35° 28' 15.8091" N
46	1263459.5856	12867535.1506	43° 44' 03.0376" E	35° 26' 06.3891" N
47	1250278.1994	12852723.7129	43° 41' 26.0980" E	35° 23' 38.1836" N
48	1233621.2197	12845470.8763	43° 38' 06.0965" E	35° 22' 24.2163" N
49	1209563.9564	12817401.1786	43° 33' 20.5187" E	35° 17' 43.2003" N
50	1174056.2470	12797563.1377	43° 26' 15.9210" E	35° 14' 21.6641" N

5.2. Scenarios Input Data

At first scenario, it is assumed that the elevation of water when a break occurs is equal to 516 m above sea level which is equal to the elevation of the crest. This is the most dangerous scenario and holds a huge devastating flood wave. So, it will be focused on this scenario for producing inundation map and defining the flooding areas. At second scenario, it is assumed that the elevation of water when a break occurs is equal to 511 m above sea level.

Non-breach flow (Qo) for both scenarios were taken as 4860m^3/s which is equal to summations of emergency spillway (Bellmouth) which is equal to 1860 m^3/s, gated service spillway which is equal to 2450 m^3/s and the outlet flow from penstock which is equal to 550 m^3/s.

Table 5.2. Input data for 1st scenario

TYPE OF DAM (IDAM)	CONCRETE ARCH
DAM BREACH ELEVATION (HDE)	516m
FINAL BREACH ELEVATION (BME)	399.5m
VOLUME OF RESERVOIR (VOL)	8400*10^6 m^3
SURFACE AREA OF RESERVOIR (SA)	34000 ha
FINAL BREACH WIDTH (BW)	182.88 m
TIME OF DAM FAILURE (TFM)	7.64 MINUTES
NON-BREACH FLOW (QO)	4860 m^3/s
DISTANCE TO PRIMARY PT OF INTEREST (DISTTN)	248.7879 Km
DEAD STORAGE EQUIV. MANN. N (CMS)	.50

Table 5.3. Input data for 2nd scenario

TYPE OF DAM (IDAM)	CONCRETE ARCH
DAM BREACH ELEVATION (HDE)	511m
FINAL BREACH ELEVATION (BME)	399.5m
VOLUME OF RESERVOIR (VOL)	7000*$10^6$$m^3$
SURFACE AREA OF RESERVOIR (SA)	32000 ha
FINAL BREACH WIDTH (BW)	182.88 m
TIME OF DAM FAILURE (TFM)	7.32 MINUTES
NON-BREACH FLOW (QO)	4860 m^3/s
DISTANCE TO PRIMARY PT OF INTEREST (DISTTN)	248.7879 Km
DEAD STORAGE EQUIV. MANN. N (CMS)	.50

The elevation of the reservoir when a break occurs is equal to 507, 504, and 500 m.a.s.l for 3rd, 4th, and 5th scenarios respectively. Non-breach flow (Qo) for these scenarios were taken as 3000 m^3/s which is equal to the summations of gated service spillway which is equal to 2450 m^3/s and the outlet flow from Penstock which is equal to 550 m^3/s. The elevations of water in 3rd, 4th, and 5th scenarios are less than 511 m which is the elevation of emergency spillway (Bellmouth), therefore 1860 m^3/s as a value of emergency spillway (Bellmouth) will be removed in the summations of Qo.

Table 5.4. Input data for 3rd scenario

TYPE OF DAM (IDAM)	CONCRETE ARCH
DAM BREACH ELEVATION (HDE)	507m
FINAL BREACH ELEVATION (BME)	399.5m
VOLUME OF RESERVOIR (VOL)	$6000*10^6$ m^3
SURFACE AREA OF RESERVOIR (SA)	28500 ha
FINAL BREACH WIDTH (BW)	182.88 m
TIME OF DAM FAILURE (TFM)	7.05 MINUTES
NON-BREACH FLOW (QO)	3000 m^3/s
DISTANCE TO PRIMARY PT OF INTEREST (DISTTN)	248.7879 Km
DEAD STORAGE EQUIV. MANN. N (CMS)	.50

Table 5.5. Input data for 4th scenario

TYPE OF DAM (IDAM)	CONCRETE ARCH
DAM BREACH ELEVATION (HDE)	504m
FINAL BREACH ELEVATION (BME)	399.5m
VOLUME OF RESERVOIR (VOL)	$5000*10^6$ m^3
SURFACE AREA OF RESERVOIR (SA)	25900 ha
FINAL BREACH WIDTH (BW)	182.88 m
TIME OF DAM FAILURE (TFM)	6.86 MINUTES
NON-BREACH FLOW (QO)	3000 m^3/s
DISTANCE TO PRIMARY PT OF INTEREST (DISTTN)	248.7879 Km
DEAD STORAGE EQUIV. MANN. N (CMS)	.50

Table 5.6. Input data for 5th scenario

TYPE OF DAM (IDAM)	CONCRETE ARCH
DAM BREACH ELEVATION (HDE)	500m
FINAL BREACH ELEVATION (BME)	399.5m
VOLUME OF RESERVOIR (VOL)	$4000*10^6 m^3$
SURFACE AREA OF RESERVOIR (SA)	22500 ha
FINAL BREACH WIDTH (BW)	182.88 m
TIME OF DAM FAILURE (TFM)	6.59 MINUTES
NON-BREACH FLOW (QO)	3000 m^3/s
DISTANCE TO PRIMARY PT OF INTEREST (DISTTN)	248.7879 Km
DEAD STORAGE EQUIV. MANN. N (CMS)	.50

The elevation of the reservoir when a break occurs is equal to 495 and 489 m.a.s.l for 6th and 7th scenarios respectively. Non-breach flow (Qo) taken to be 550 m^3/s as a value of penstock outlet discharge. Emergency spillway (Bellmouth) doesn't work under elevation 511 m.a.s.l and gated service spillway doesn't work under elevation 496.5 m.a.s.l so, both of them will be removed from the summations of Qo for 6th and 7th scenarios.

Table 5.7. Input data for 6th scenario

TYPE OF DAM (IDAM)	CONCRETE ARCH
DAM BREACH ELEVATION (HDE)	495m
FINAL BREACH ELEVATION (BME)	399.5m
VOLUME OF RESERVOIR (VOL)	$3000*10^6$ m^3
SURFACE AREA OF RESERVOIR (SA)	18000 ha
FINAL BREACH WIDTH (BW)	182.88 m
TIME OF DAM FAILURE (TFM)	6.27 MINUTES
NON-BREACH FLOW (QO)	550 m^3/s
DISTANCE TO PRIMARY PT OF INTEREST (DISTTN)	248.7879 Km
DEAD STORAGE EQUIV. MANN. N (CMS)	.50

Table 5.8. Input data for 7th scenario

TYPE OF DAM (IDAM)	CONCRETE ARCH
DAM BREACH ELEVATION (HDE)	489m
FINAL BREACH ELEVATION (BME)	399.5m
VOLUME OF RESERVOIR (VOL)	$2000*10^6$ m^3
SURFACE AREA OF RESERVOIR (SA)	12600 ha
FINAL BREACH WIDTH (BW)	182.88 m
TIME OF DAM FAILURE (TFM)	5.87 MINUTES
NON-BREACH FLOW (QO)	550 m^3/s
DISTANCE TO PRIMARY PT OF INTEREST (DISTTN)	248.7879 Km
DEAD STORAGE EQUIV. MANN. N (CMS)	.50

5.3. Comparison of First Cross Sectional Discharge of SMPDBK Model with $Q_{bmax.}$ of Empirical Equation.

It is more academic to know the validity of the work by checking the difference between Q_b max. of the empirical equation and first cross sectional discharge of SMPDBK model as shows in Table 5.9. See section 4.8 for additional information about Q_b max. calculations. Shahraki et al. (2012) published a paper in World Applied Sciences Journal by using SMPDBK model; the results showed that $Q_{bmax.}$ =17573 m^3/s and a first cross sectional discharge is equal to 13071m^3/s, as it is

noticeable that the difference is not small as compared to the size of the work. Hence, they simulate the discharge toward the downstream as an acceptable value for the research.

Table 5.9. The difference between Qbmax. and first cross sectional discharge

Scenario	$Q_{bmax.}$ **(m^3/s)**	First cross sectional discharge**(m^3/s)**
1	397535.7	398602.7
2	372533.7	373583.03
3	351017.5	353913.29
4	336507.5	339376.84
5	317474.7	320330.37
6	291723.9	297008.6
7	264469.5	269716.07

As shown in Table 5.9, the differences between Qbmax.Of Empirical Equation and first cross sectional discharge are very small, and the simulated discharges toward the downstream of the dam are accepted.

5.4. Flood Analysis

Surely the hydraulic shock produced from Dokan dam break will be stronger than any hydraulic structure in Iraq because of its large storage behind the concrete arch dam. Often the time for breach formation at concrete arch dams is ranged from 5 to 10 minutes according to the specification of the empirical equation. So releasing this amount of water toward the downstream without any warning will be deadly.

During Dokan dam break assumption, the most significant notable risk will be on Dokan town. It is 1.60934 km far from the dam's body (See Appendix B in figure B-2). According to the first scenario, the flood wave will reach to Dokan town just after 8 minutes and 24 seconds of the break. So the evacuation time is very limited, and there will be no time for any kind of warnings. The overall total population in the Dokan town is 11000. Almost 5304 (48%) of the total population is at risk. As it is noticeable a very dangerous and deadly flood wave will come toward Dokan town

with a height of 57.302 m with an elevation of 452.341 m.a.s.l in the natural river before entering the Dokan town. The left part of Dokan town as shown in Figure 5.1, will be the biggest effecting area in the town, and more than ¾ of this part will be drowning down by the flooding wave. The maximum height of water at the middle of this part will reach to 36.41 m which is 447.408 m.a.s.l. Then the flow of water will continue in the river washing all buildings and houses locating on the banks of the river. At the middle of Dokan town in the natural river, the depth of water will record 43.29 m which is 438.744 m.a.s.l as shown in Figure 5.1.

Figure 5.2 shows the lower part of the Dokan town. As it is seen from the figure, the number of victims will be less than the upper part of Dokan town because most of the constructed buildings are higher than the flood elevation. However, (¼) of all tourist areas on the banks of the river, especially on the right bank will be destroyed and washed down by the flooding water. Financial losses ranges from 930 houses and buildings including large tourist villas around the banks, the stadium of football, agricultural lands in addition to the bridge that connects both sides of the valley.

Figure 5.3 shows the inundation of Taqtaq town which is located on both banks of Lesser Zab River at coordinates system of (44° 35’ 21.1957” E, 35° 52’ 45.8809” N) along 68.413213 km far from Dokan dam. See Figure B-22 in Appendix B for cross sectional flood elevations at Taqtaq town. Taqtaq town is far enough from dam body. Therefore, there is a suitable time for evacuation and warning which is 2hr. and 8 minutes in the worst case. The overall total population of Taqtaq town is 27000. The drowning area will make 15400 (56%) of people who will face dangerous flooding wave because of its wide and low elevation with natural river in additional to financial losses which ranges from 2200 houses and government public buildings, Taqtaqs tourist park which are near the bank, and Taqtaq bridge that connects both sides of the valley.

The height of water at the middle of the Natural Rivers will reach to 29.8 m which is 354.2995 m.a.s.l. This large height of water will leave a lot of families homeless. The flood depth will reach to 22.86 m as maximum depth of water in close places to the natural river of Lesser Zab in Taqtaq town because of the lower elevation of its bed (ground) which is 331.402 m.a.s.l. For more information see scaled inundation map of Taqtaq town in Figure 5.3.

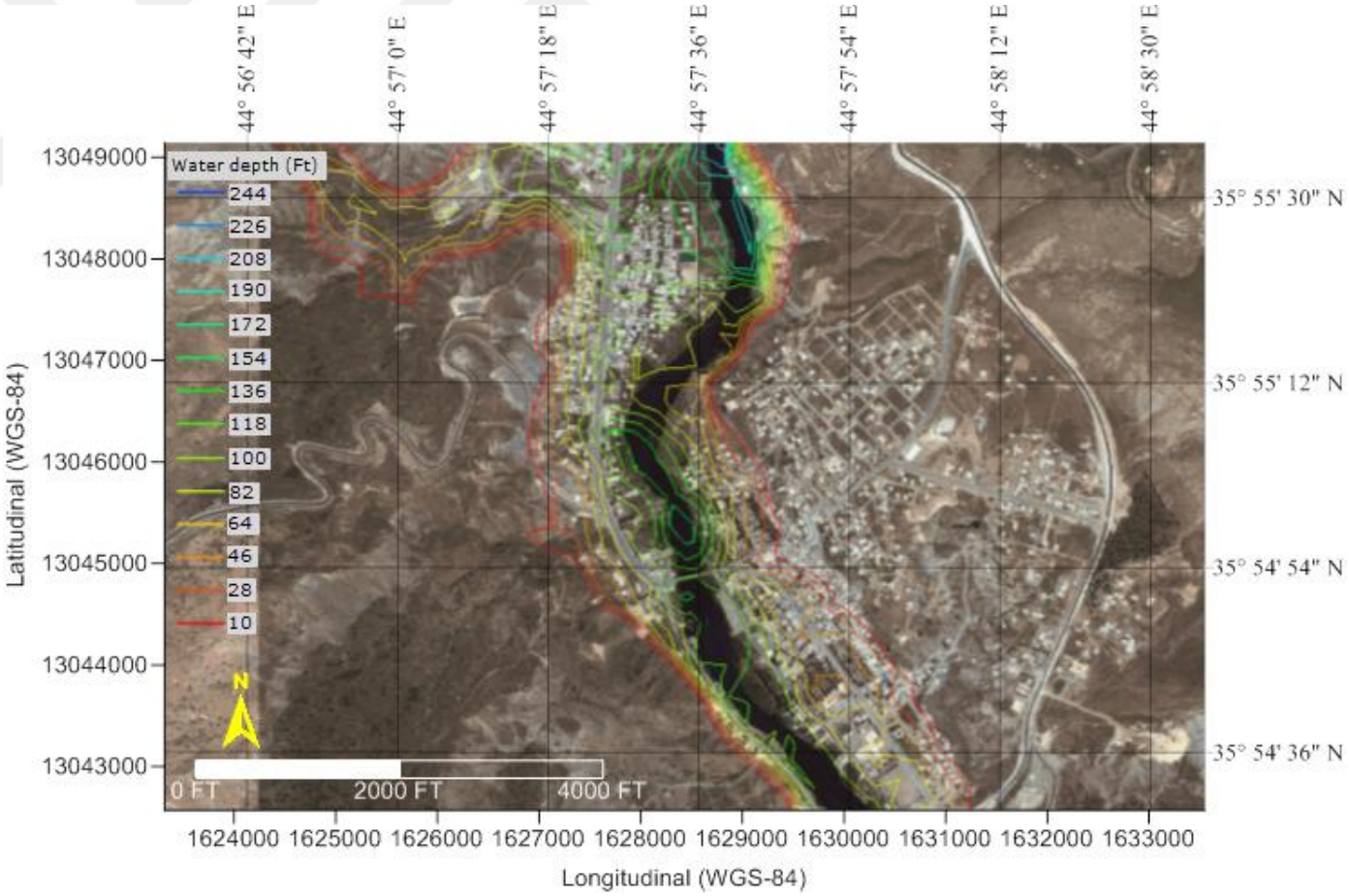

Figure 5.1. Upper part of Dukan town inundation map for first scenario

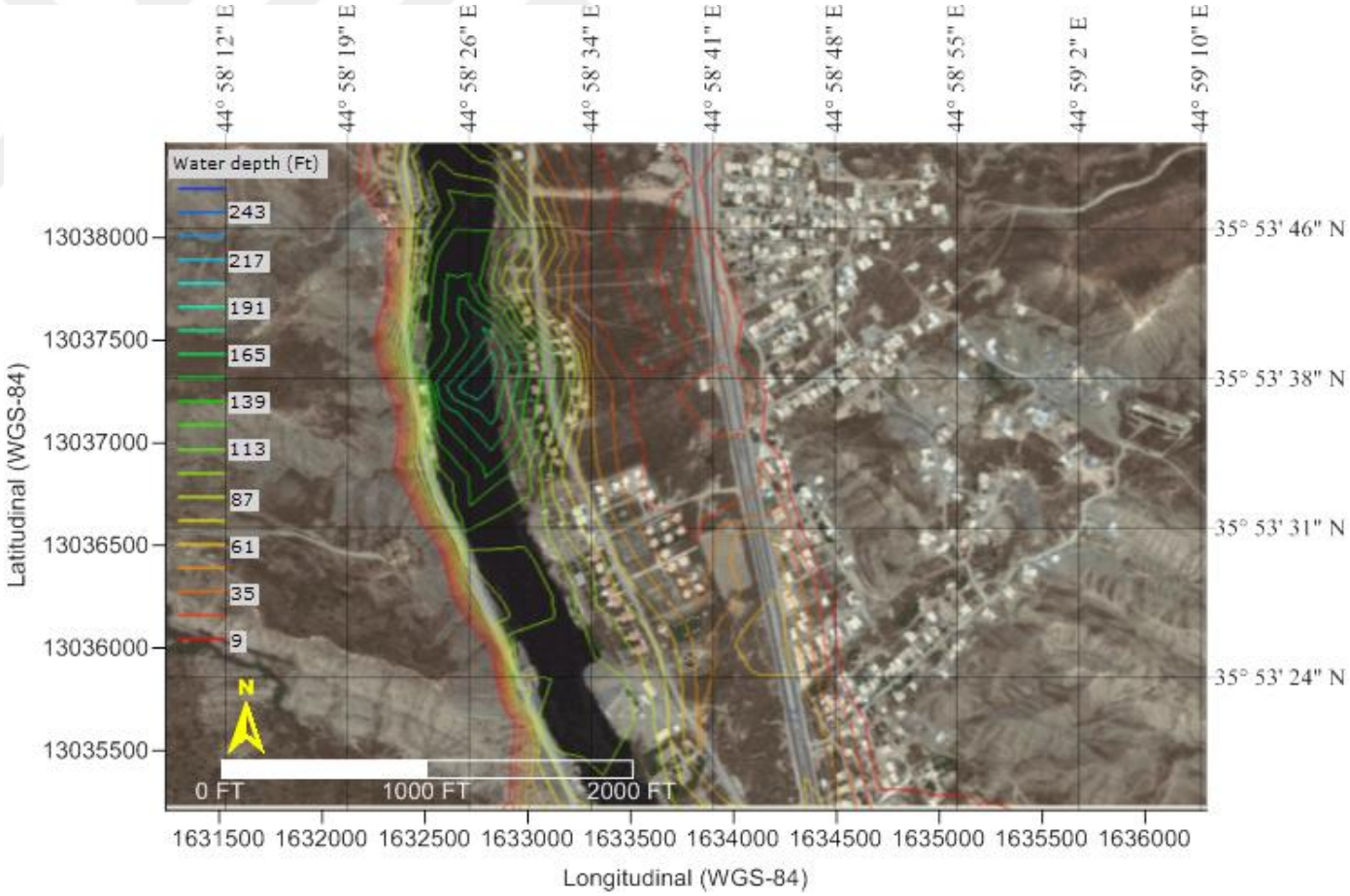

Figure 5.2. Lower part of Dukan town inundation map for first scenario

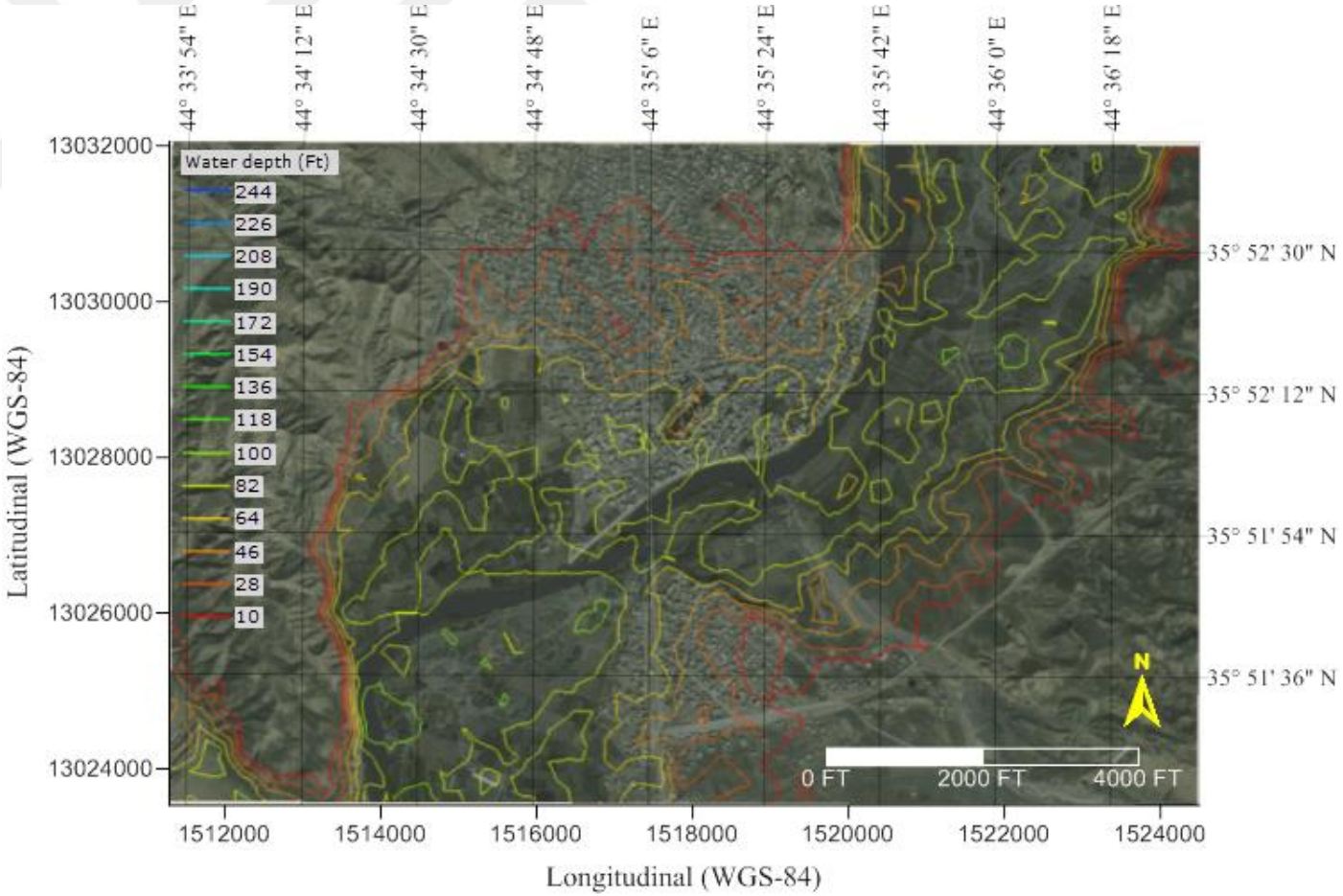

Figure 5.3. Taqtaq towns inundation map for first scenario

Figure 5.4 and 5.5 show flood depth and flood elevation maps of inundation areas along the Lesser Zab River at downstream of Dukan dam for the first scenario which is the most dangerous case. Figures 5.4 and 5.5 are very useful for the Iraqi government in future master plans around the banks of the Lesser Zab River.

After 10 hours and 15 minutes, the flood wave will reach to Tigris River carrying a large amount of water which is 236687.6m^3/s with total flooded area of 347.9653611 km^2 along the Lesser Zab River including Taqtaq and Dukan town and very good agricultural lands.

Table 5.10 shows the amount of water entering to Tigris River which will go directly to Baghdad along with 260 km of Tigris River, which is a very interesting and important subject for investigations.

Table 5.10. Amount of water entering to Tigris River

Scenario	Discharge entering to Tigris River at each scenario (M^3/s)
1	236687.6
2	219566.3
3	206250.6
4	196308.2
5	183457.5
6	167935.2
7	140641.9

Table 5.11 shows the flooded area along the Lesser Zab River for all scenarios which include very good agricultural lands on the banks of the River.

Table 5.11. Flooded area along the Lesser Zab River

Scenario	Flooded area along River (Km^2)
1	347.9653611
2	338.9274326
3	336.8323505
4	333.9761626
5	326.3741139
6	324.3691487
7	298.1395517

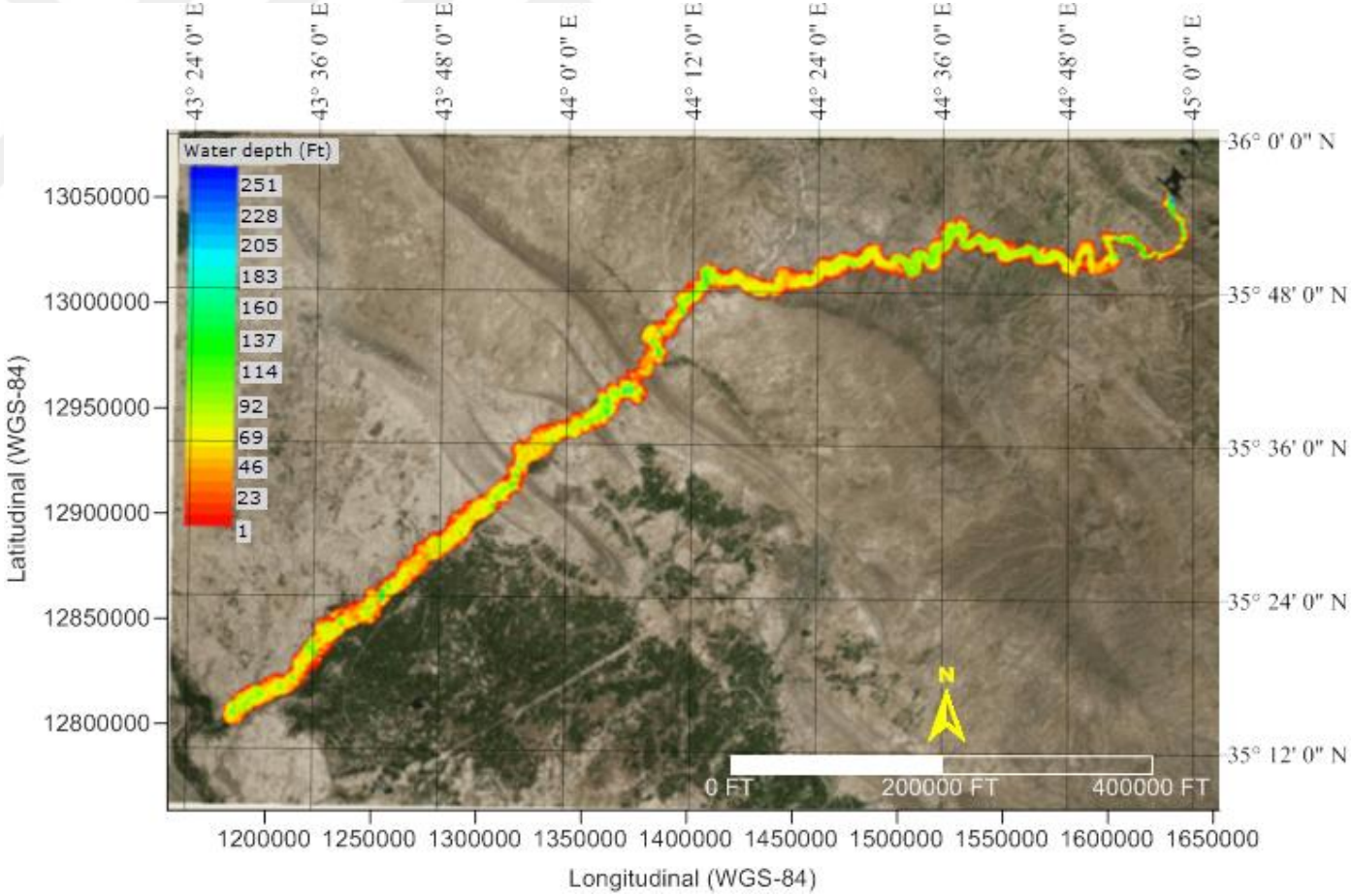

Figure 5.4. Flood depth along Lesser Zab River for first scenario

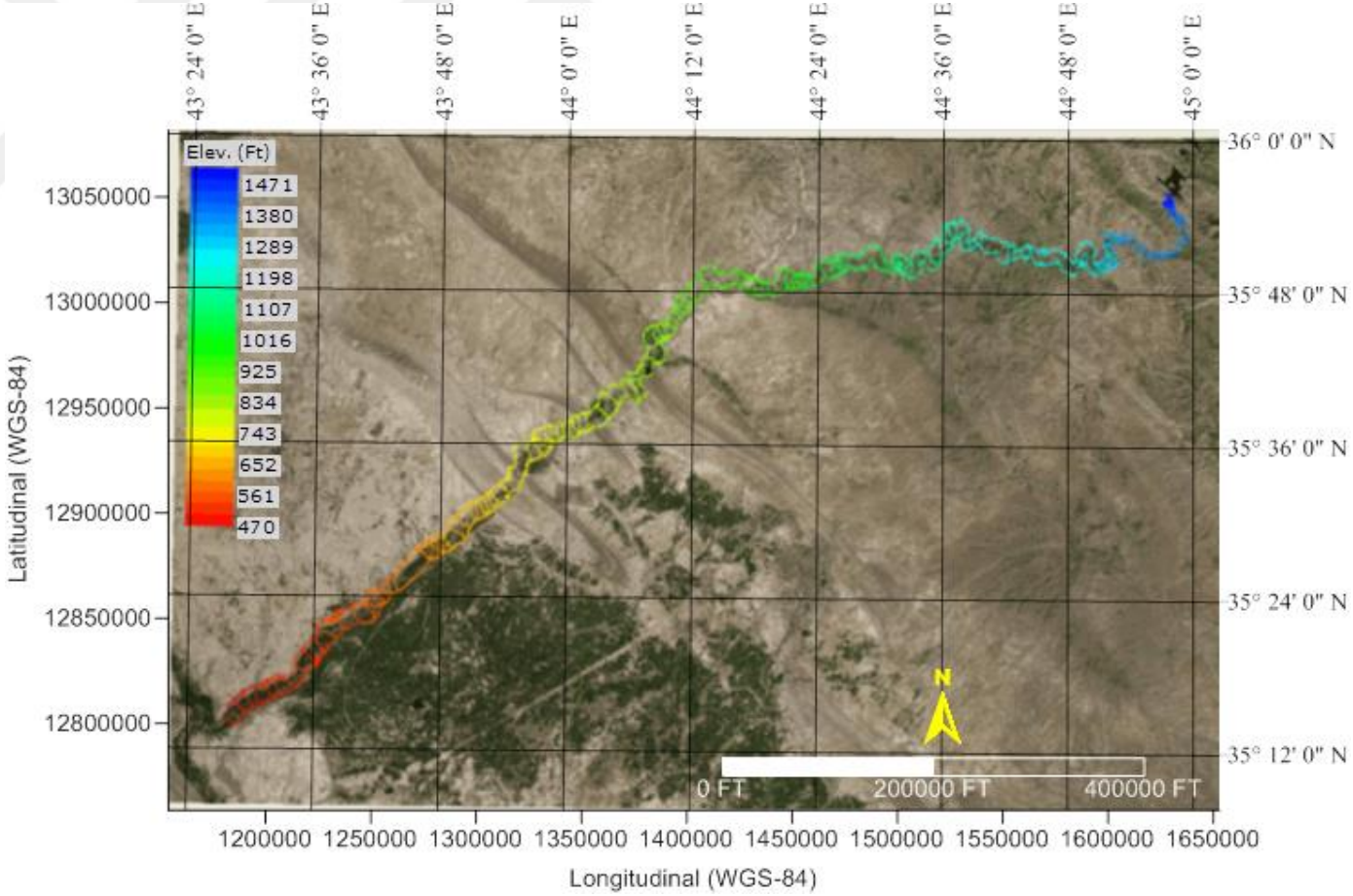

Figure 5.5. Flood elevation along Lesser Zab River for first scenario

The flood traveling time form the dam body toward the Dukan town is between (8-10) minutes for all simulated scenarios and the maximum depths of water at the natural River are shown in Table 5.12:

Table 5.12. Max. depths and elevations at the middle of Dukan town

Scenario	Max. flood depth (m)	Max flood elevation (m.a.s.l)
1	44.05	438.74
2	42.83	437.52
3	41.84	436.53
4	41	435.69
5	40.1	434.79
6	38.77	433.46
7	37.12	431.81

The flood depths in Taqtaq town for all scenarios are (29.8m, 29m, 28.3m, 27.86m, 27.2m, 26.36m, 25.42m) with the flood elevations of (354.29, 353.5, 352.8, 352.36, 351.7, 350.86, 349.921) m.a.s.l respectively. Table 5.13 shows the traveling times of the flood water from the dam body toward the Taqtaq town and the Tigris River.

Table 5.13. Times to reach the flood wave to the destination places

Scenario	Taqtaq town (hr.)	Tigris River (hr.)
1	2.14	10.25
2	2.19	10.35
3	2.22	10.5
4	2.25	10.68
5	2.29	10.92
6	2.36	11.22
7	2.47	11.82

Figures 5.6, 5.7 and 5.8 show the maximum flow, maximum depth and time to reach the flood wave respectively, along 248.8 km of the Dukan dam downstream for all the seven scenarios. And Appendix A is included tables, figures, and values of all curves separately (See Appendix A for more information).

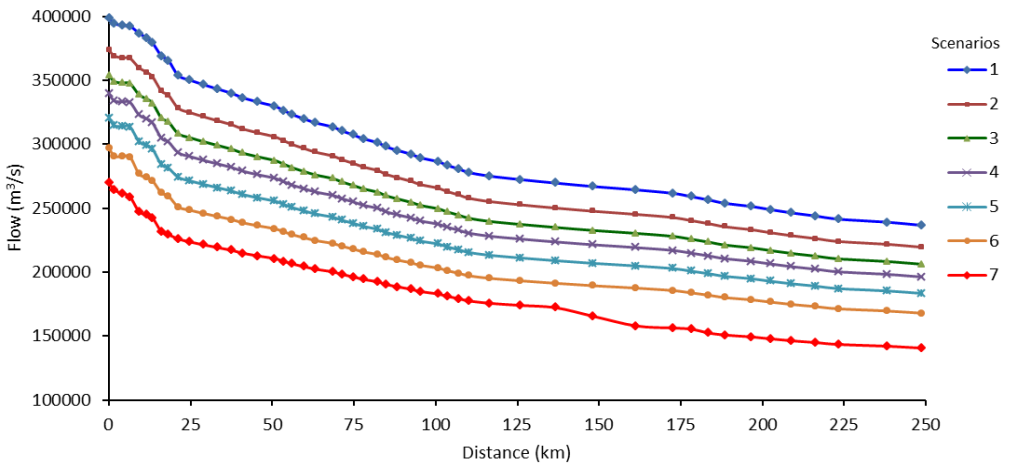

Figure 5.6. Flood discharge profiles from failed dam along the Lesser Zab River

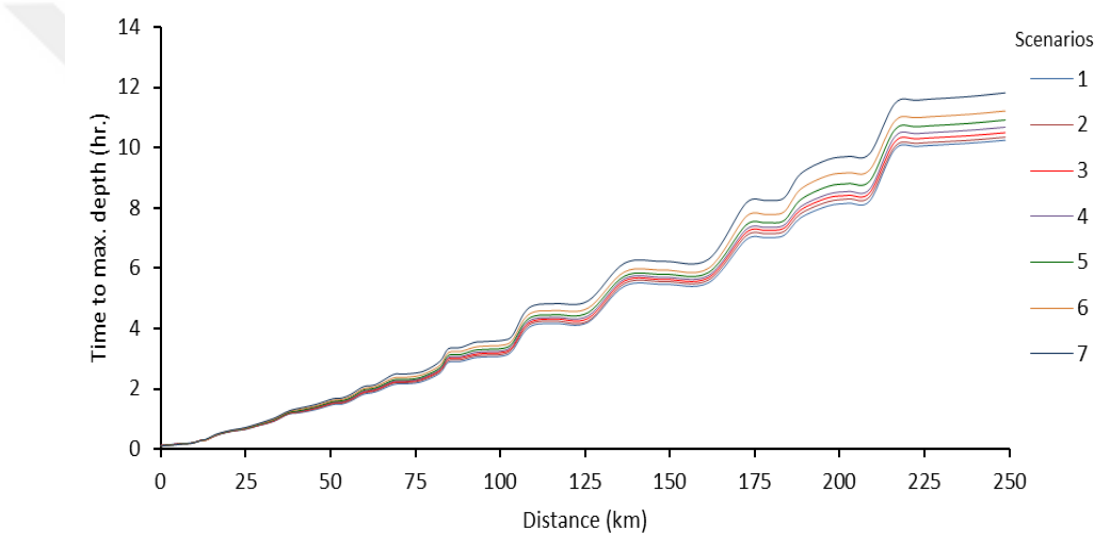

Figure 5.7. Travel time profiles of max. depth flood along the Lesser Zab River

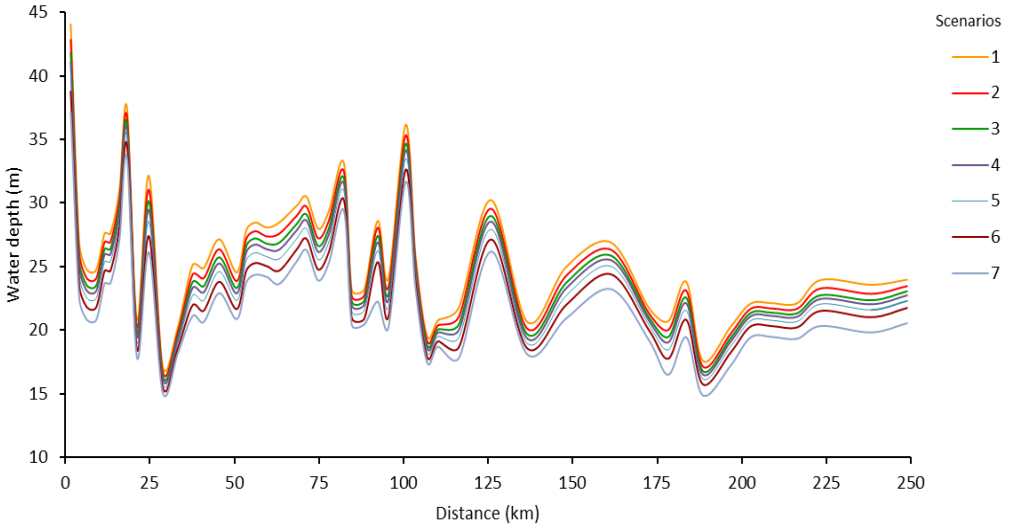

Figure 5.8. Water depth profiles of the flood wave along the Lesser Zab River

5.5. Life Losses

SMEC organization according to ANCOLD guidelines in 2006 classified the severity of Dukan dam failure category as Extreme, because of the considerable and vast dangers on the downstream of the dam including human lives and financial losses.

Graham (2001) suggests a simple procedure for estimating the loss of life from a dam failure, based on 40 dam failure cases in the US. As given in Table 5.14, the user first decides on the severity of the flood and then finds the appropriate warning time in the 2nd column and the understanding of the flood severity by those under risk in the 3rd column. The 4th column indicates the suggested multiplier and the multiplier range for the fatality rate which yields the number of fatalities when multiplied by the population of the subject settlement. This calculation presents some indicators that can be used while preparing the emergency action plans.

Table 5.14. Recommended fatality rates for estimating the loss of life due to dam failure (Graham, 2001)

FloodSeverity	WarningTime(minutes)	FloodSeverityUnderstanding	Fatality Rate (Fraction of people at risk expected todie)	
			Suggested	SuggestedRange
HIGH	nowarning	not applicable	0.75	0.30to1.00
	15to60	vague	Usethevaluesshownaboveandapplytothenumberofpeoplewhoremaininthedamfailurefloodplainafterwarningsareissued. Noguidanceisprovidedonhowmanypeoplewillremaininthefloodplain.	
		precise		
	morethan60	vague		
		precise		
MEDIUM	nowarning	notapplicable	0.15	0.03to0.35
	15to60	vague	0.04	0.01to0.08
		precise	0.02	0.005to0.04
	morethan60	vague	0.03	0.005to0.06
		precise	0.01	0.002to0.02
LOW	nowarning	notapplicable	0.01	0.0to0.02
	15to60	vague	0.007	0.0to0.015
		precise	0.002	0.0to0.004
	morethan60	vague	0.0003	0.0to0.0006
		precise	0.0002	0.0to0.0004

Flood severity: is depended on the distance between dam and place under risk.

Flood severity understanding: is depended on the warning issuers, in the case of not applicable there is no understanding of flood severity by warning issuers because of short failure time.

Fatality rate: is depended on the time of failure, if it is in night or day because all night dam failures in history have a bad reputation. Therefore, the high fatality rate is suggested for night dam failure opposite to dam failure which is occurring during day.

Table 5.14 is used to analyze the population at risk for Dukan and Taqtaq town during Dukan dam failure at day. If dam failure is at night, maximum range values should be taken in the calculations.

Solution:

- Total populations at Dukan town are 11000 individual and populations at risk are 5304 person
- Time to reach maximum flood depth to Dukan town is 8 minutes.
- Total populations at Taqtaq town are 27000 person and populations at risk are 15400 person
- Time to reach maximum flood depth to Taqtaq town is 2hr. and 15 minutes.

Table 5.15. Fatality rate calculations for Dukan and Taqtaq town

Town	Flood severity	Warning Time (Min.)	Flood severity understanding	Fatality rate	Calculation	Risk expected to die
Dukan	High	8	not applicable	0.75	0.75*5304	3978
Taqtaq	Medium	135	vague	0.03	0.03*15400	462

Total losses of the life = 4440 person

5.6. Gene Expression Programming Results

After predicting flood characteristic equations of time, discharge and water elevation by using outputs of seven scenarios along 248.8 km during Lesser Zab River by

Gene Expression Programming model in DTREG software, the equation can be used by any person in the future without requiring to use any type of dam break models which needs crew of an expert in this field, time, a lot of effort and information.

5.6.1. Predicted Equations

1. **<u>Flood Traveling Time Equation (T)</u>:** By using this equation, the user can predict the time of reaching maximum flood to any destination place during lesser Zab River by the accuracy of 99.373% as shown in Figure 5.9. The actual values are from SMPDBK model and the predicted values are from the GEP model. Variables in this equation are distance and storage.

$$T = \left(\left(0.063 * \left(\text{dist.} + (-48.643)\right)\right) - 7.194\right) + \left(\left(\frac{19.308*\left(\text{dist.} + (20.924)\right)}{S}\right) + \left(\frac{2208.905}{(\text{dist}+210.741)}\right)\right) \quad (5.1)$$

Where, T is flood traveling time along the Lesser Zab River(hr.), Dist. is the distance along the Lesser Zab River (Km), S is storage at the dam when a breakoccurs (Mm^3).

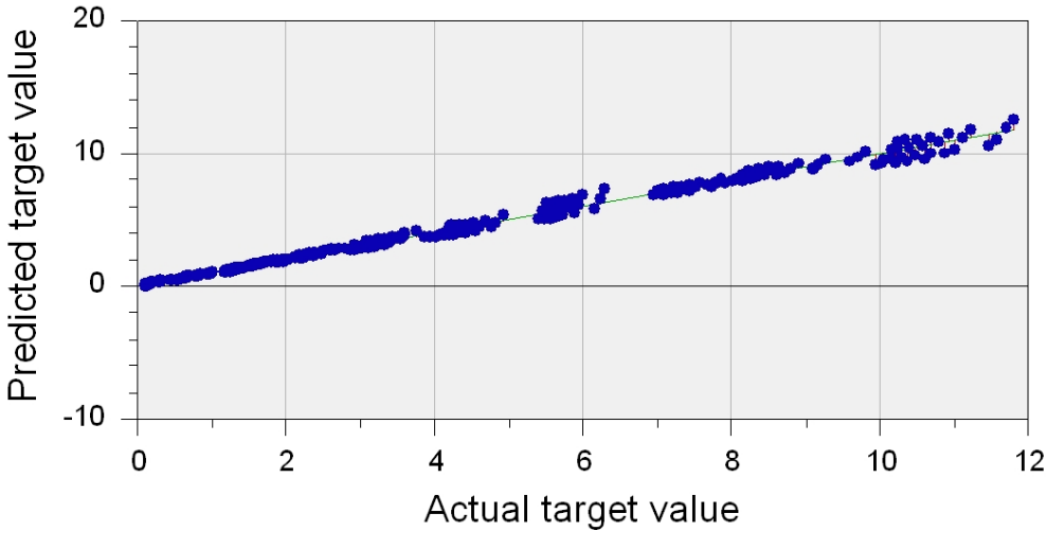

Figure 5.9. GEP chart of (Actual vs. Predicted) values of the Time

2. **<u>Flow Equation (Q)</u>:** By using this equation, the user can predict the flood flow to any destination place during Lesser Zab River by the accuracy of 98.319% as shown in Figure 5.10 which the actual values are from SMPDBK model and the predicted values are from the GEP model. Variables in this equation are distance, elevation, and storage.

$$Q = ((1.890S) - (-2719.661El)) + (-1.307 * 10^6) + (dist.((2.653dist. - 1146.201)) + El^2 \quad (5.2)$$

Where, Q is flood flow along the Lesser Zab River (M^3/s), El is elevation of water in the reservoir when a break occurs (m.a.s.l).

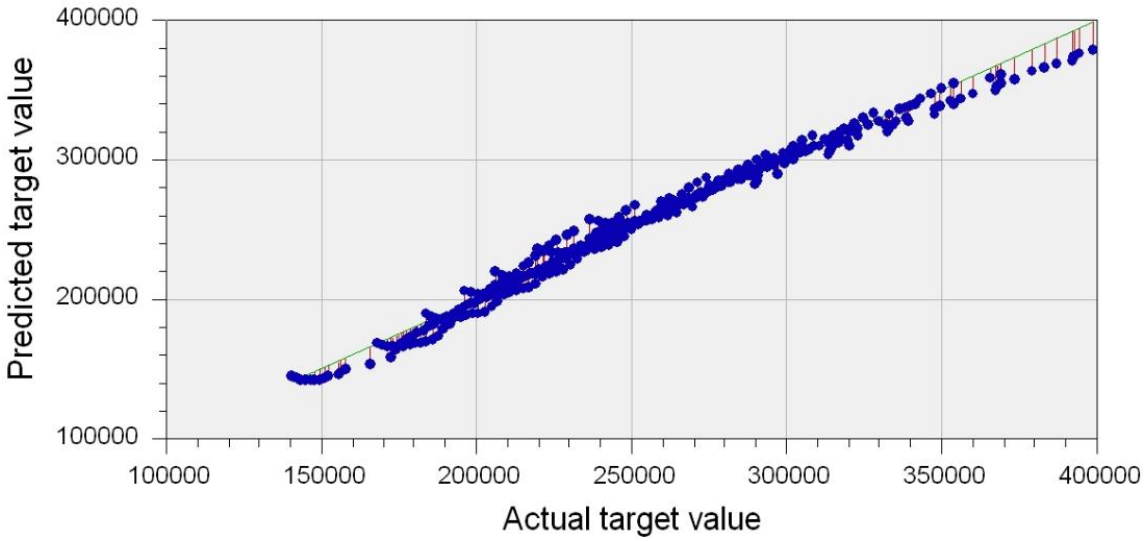

Figure 5.10. GEP chart of (Actual vs. Predicted) values of Flow

3. **<u>Flood Elevation Equation (FL)</u>:** By using this equation, the user can predict the flood elevation to any destination place during Lesser Zab River by the accuracy of 99.469% as shown in Figure 5.11. The actual values are from SMPDBK model and the predicted values are from the GEP model. Variables in this equation are distance, elevation, and storage.

$$FL = (0.143 * El) + ((-1.203) * dist.) + 359.406 \quad (5.3)$$

Where, FL is flood elevation along the Lesser Zab River (m.a.s.l).

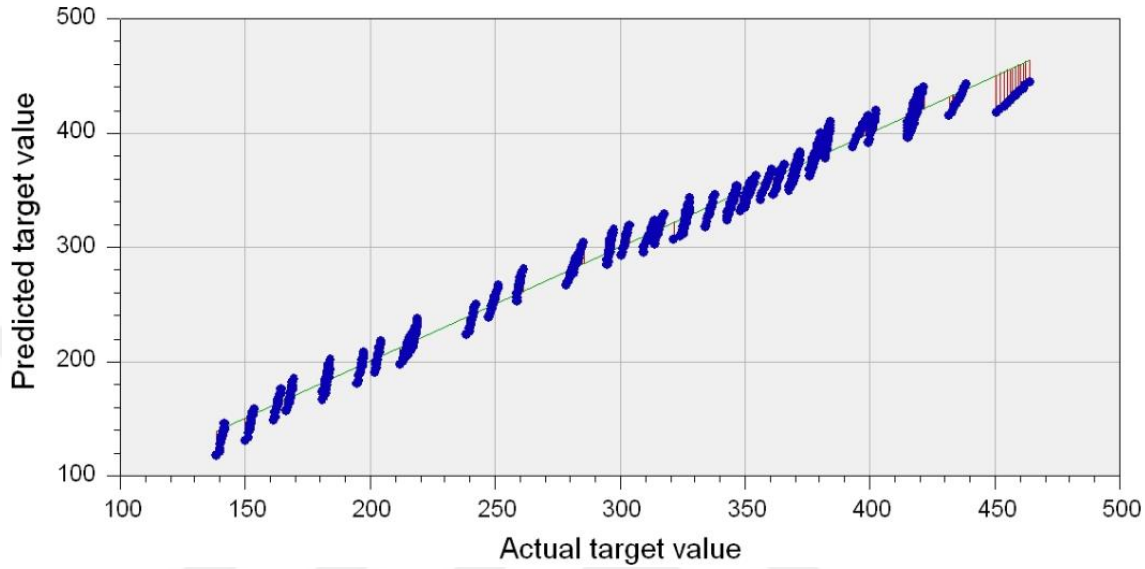

Figure 5.11. GEP chart of (Actual vs. Predicted) values of flood elevations

5.6.2. Checking GEP Predicted Equations

The idea of this point is to simulate three different scenarios by SMPDBK model and compare it with the GEP equations. It is applied for checking the validity of GEP equations.

Table 5.16. Input data of the three simulated scenarios

Checking scenarios	First checking scenario	Second Checking scenario	Third Checking scenario
Elevation of water when breach occurs (m)	498	505	513
Storage of the reservoir when breach occurs (Mm^3)	3600	5250	7500
Surface area of the reservoir (ha)	21000	26500	33000

1. **<u>Checking Flood Traveling Time equation</u>:** Figures 5.12, 5.13, and 5.14 show the accuracy of SMPDBK model versus time equation of GEP model along the Lesser Zab River for three checking scenarios.

- **First checking scenario**

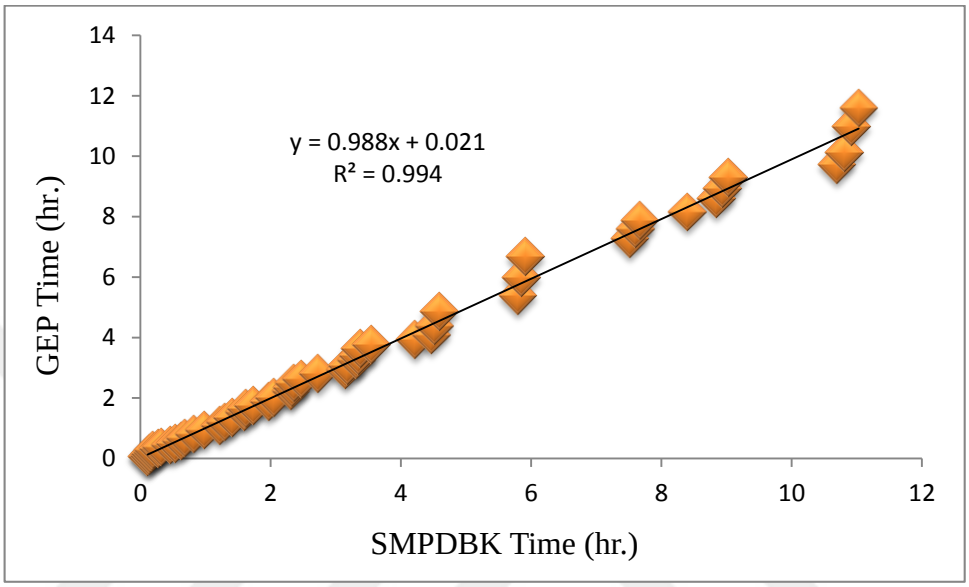

Figure 5.12. First checking scenario of flood traveling time equation

- **Second checking scenario**

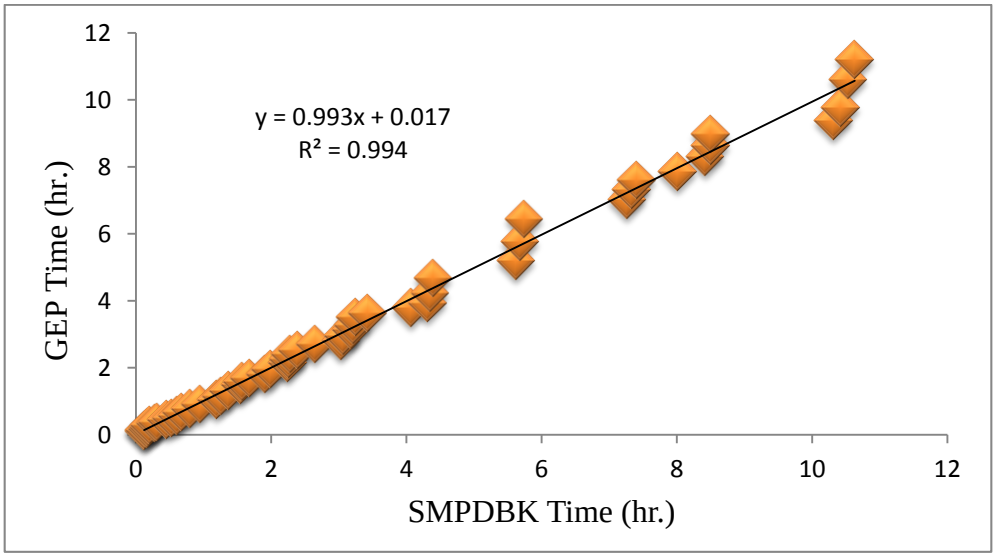

Figure 5.13. Second checking scenario of flood traveling time equation

- **Third checking scenario**

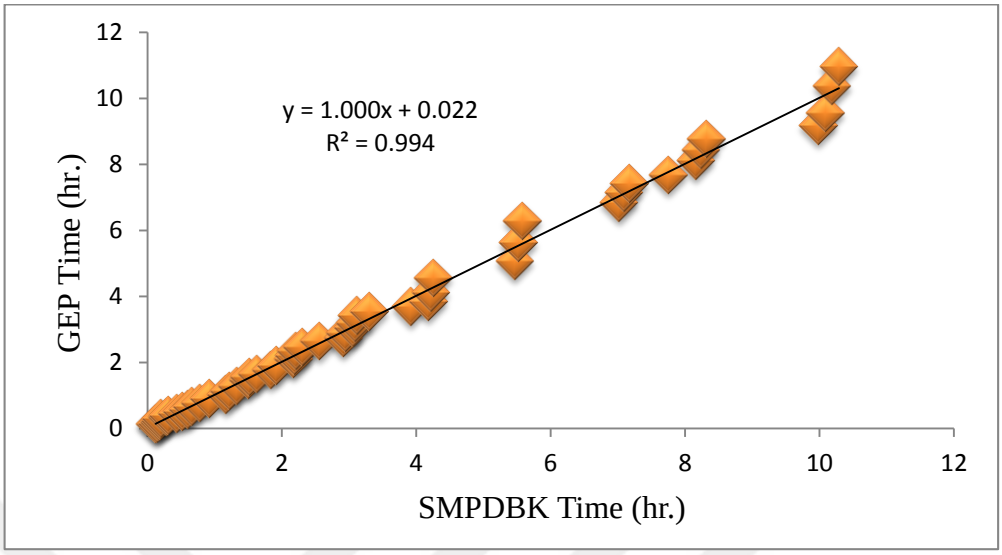

Figure 5.14. Third checking scenario of flood traveling time equation

Note: It can be noticeable that the flood traveling time equation of GEP model achieves an accuracy of 99% for any value during 248.8 km along the Lesser Zab River.

2. **<u>Checking Flood Flow Equation</u>:** Figures 5.15, 5.16, and 5.17 show the accuracy of SMPDBK model values versus flow equation of GEP model along the Lesser Zab River for three checking scenarios.

- **First checking scenario**

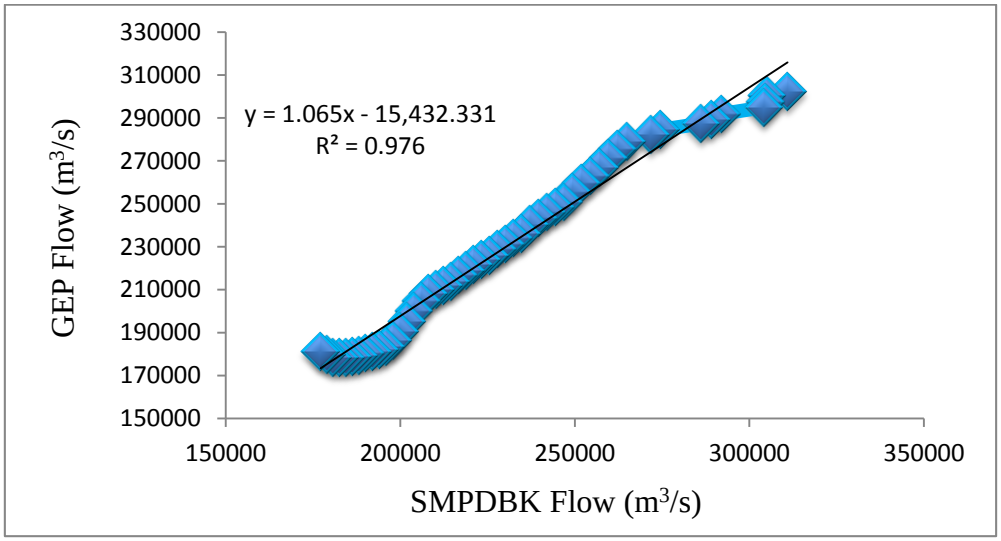

Figure 5.15. First checking scenario for flood flow equation

- **Second checking scenario**

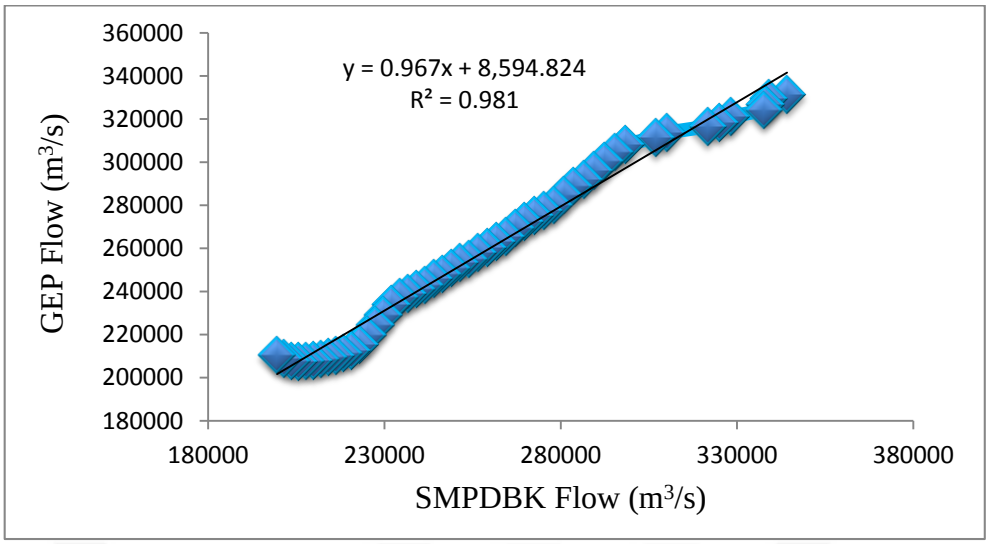

Figure 5.16. Second checking scenario for flood flow equation

- **Third checking scenario**

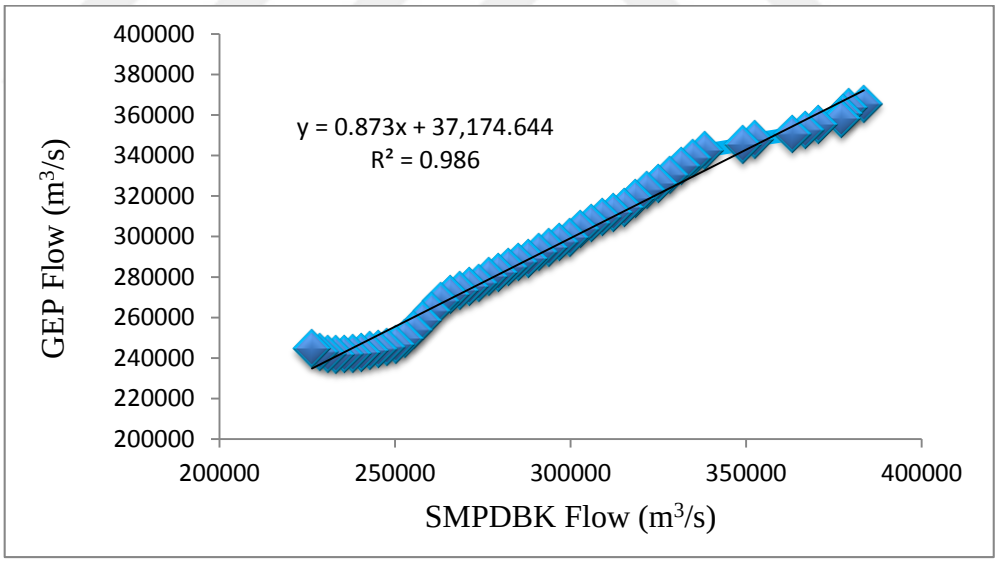

Figure 5.17. Third checking scenario for flood flow equation

Note: It can be noticeable that the flood flow equation of GEP model achieves an accuracy of (97-98) % for any value during 248.8 km along the Lesser Zab River.

3. **<u>Checking Flood Elevation Equation</u>:** Figures 5.18, 5.19, and 5.20 shows the accuracy of SMPDBK model values versus flood elevation equation of GEP model along the Lesser Zab River for three checking scenarios.

- **First checking scenario**

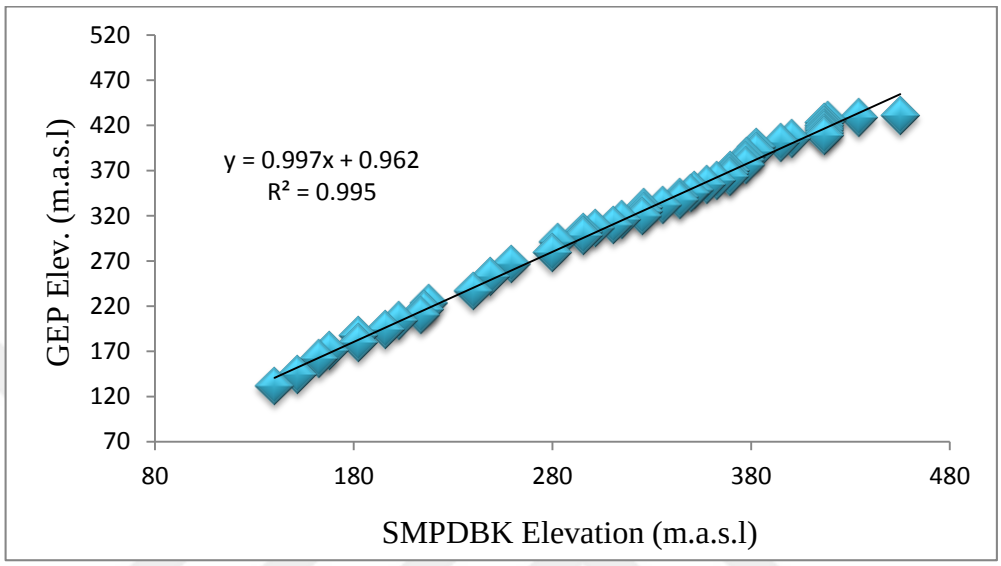

Figure 5.18. First checking scenario for flood elevation equation

- **Second checking scenario**

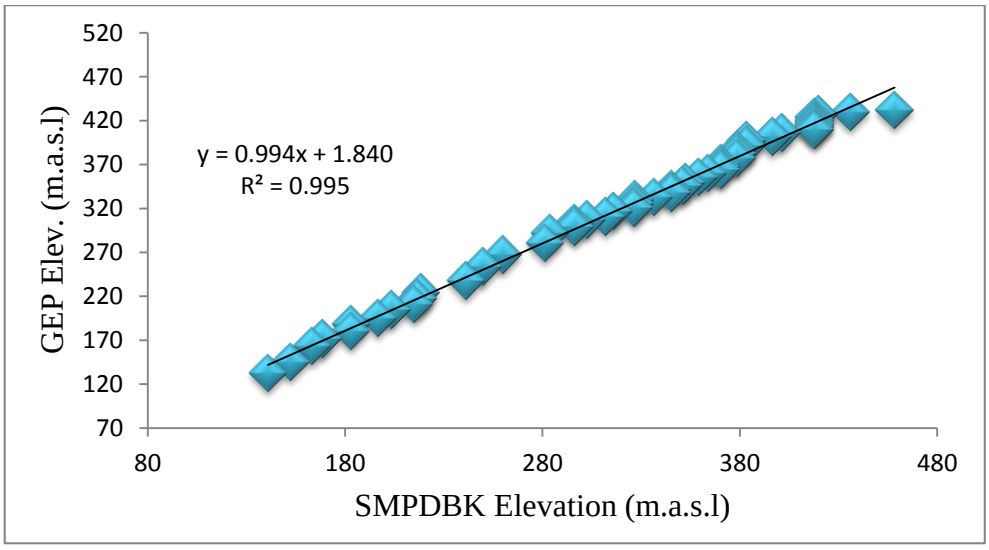

Figure 5.19. Second checking scenario for flood elevation equation

- **Third checking scenario**

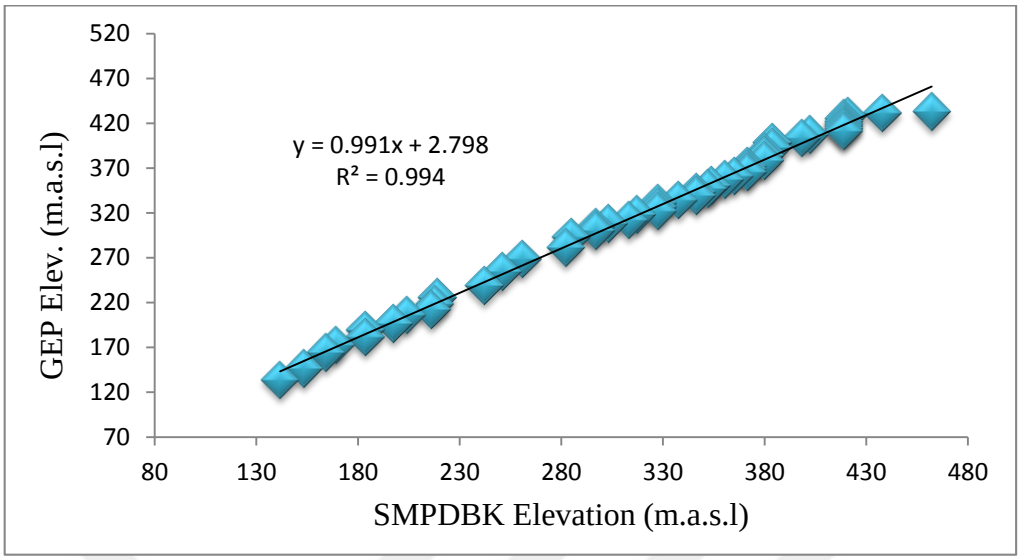

Figure 5.20. Third checking scenario for flood elevation equation

Note: It can be noticeable that the flood elevation equation of (GEP) model has an accuracy of 99% for any value during 248.8 km along the Lesser Zab River. Comparison tables of three checking scenarios of the simulated SMPDBK model and GEP model equations values can be seen in Appendix C.

CHAPTER 6

6. CONCLUSIONS AND RECOMMENDATIONS

6.1. General

In this study, the effect of dam break along downstream of a large dam was investigated. Seven scenarios of dam failure were taken for existing Dukan dam by using SMPDBK model of WMS software version 8.3. The simplified dam break model, SMPDBK was selected due to its efficiency to simulate and predict the flood wave of a hypothetical dam failure at different failure scenarios. Then GEP model was utilized to compute the dam break flood characteristics (flood discharge, flood level and flood time) based on the SMPDBK model outputs along the Lesser Zab River.

6.2. Research Methodology

Figure 6.1 shows basic general procedure of this research:

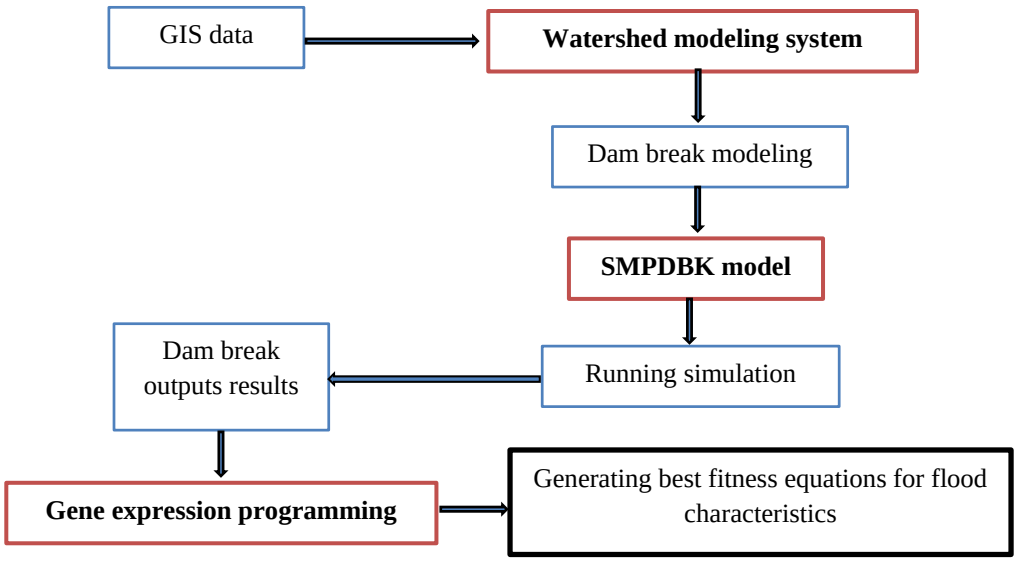

Figure 6.1. General flow chart of the research

6.3. Conclusions

Flow direction at downstream of the Dukan dam is determined by Watershed modeling system (WMS) version 8.3 and then cross sections along the Lesser Zab River are extracted. River channels geometry represented by cross-sections which are obtained from GIS facilities. Then breach parameters in the dam are predicted by empirical equations. And then the dam failure scenarios were taken.

Dam break analysis, even before construction of the dam is a scientific strategy to study the effect and boundary of a possible drowning areas along the downstream of the dam, in additional, to Guarantee the future lives located at downstream of the dam.

The main findings of this research can be summarized as:

- The flood wave will reach to the Dukan town after 8 minutes and 24 seconds of the break. At the middle of Dukan town in the natural river, the depth of water will record 43.29 m which is 438.744 m.a.s.l.Total population in Dukan town is 11000. Almost 48% of the total population is at risk of the deadly flood in the case of the insufficient warnings, as shown in Figure 5.1.
- 56% of 27000 people in Taqtaq town which is 68.413213 Km far from Dukan dam after 2hr. and 8 min. will face 29.8 m depth of flood water which is equal to 354.2995 m.a.s.l,in the middle of natural River in the worst case of dam break which is the first scenario.
- The last point of Lesser Zab river, according to seven analysis scenarios of Dukan dam break, shows the amount of water entering to Tigris River (236687.6, 219566.34, 206250.6, 196308.2, 183457.5, 167935.2, and 140641.9) m^3/s after (10.25, 10.35, 10.5, 10.68, 10.92, 11.22, and 11.82) hours respectively, which will go directly to capital Baghdad along with the 260 Km of Tigris River, which is an interesting and significant subject for investigations.
- Flooded areas along the Lesser Zab River are (347.9653611, 338.9274326, 336.8323505, 333.9761626, 326.3741139, 324.3691487, and 298.1395517) Km^2 respectively for seven scenarios including private and public property and very good agricultural lands.

- Using GEP model to predict the flood characteristics equations (flood discharge, flood elevation, and flood travel time) along the Lesser Zab River with the accuracy of (98%-99%). Any person in the future can use these equations without using any type of flood simulation software and without needs of an expert crew in this field, time, a lot of effort and information.

6.4. Recommendations

1. Immediate relocation in sensitive areas of Dukan town that is affected by the flood as shown in scaled inundation map Figure 5.1 and 5.2;
2. Setting up an accurate evacuation emergency action plan for Taqtaq town to repel any possible failure of Dukan dam according to scaled inundation map Figure 5.5;
3. Taking into account the large amount of water that will flow toward the Capital Baghdad and Setting up an accurate evacuation emergency action plan especially for the locations which are near to the banks of the river are strongly recommended.

6.5. General Notes

1. For using SMPDBK model, its manual empirical equations must be used for predicting breach parameter, because all simplifications in the Simplified Dam Break (SMPDBK) Flood Forecasting Model are taken into account during empirical equations preparations by National Weather Service (NWS).
2. Using better resolution than 1 arc-second Resolution which is the best free resolution till now in 2016 is recommended.

REFERENCE

Petchprayoon, p. (2001). The Prediction of Flash Flood Caused by Dam Failure a case study at the the tha Dan Dam, Thailand. In Paper presented at the 22nd Asian Conference on Remote Sensing, 9.

Kerisel, J. (1985). 'The History of Geotechnical Engineering up Until 1700'; in: Proc. 11th Int. Conf. on Soil Mechanics and Foundation Engineering, San Francisco, CA, Golden Jubilee Volume, 3-93.

Costa and John, E. (1985). Floods from Dam Failures, U.S. Geological Survey Open-File Report 85-560, Denver, Colorado, pp: 54.

Fread, D. (1981). Some Limitations of Dam Breach Flood Routing Models.

Attalla, T.A. (2002). A review on dams and breach parameters estimation. Master of science hydrosystem engineering. Dept. of civil and environment. Virgina polytechnic institute and state University. Blacksburge. V.A.

Singh, V. (2013). Dam breach modeling technology. Springer Science & Business Media.

Wetmore, J. N. and Fread, D. L. (1983). The NWS simplified dam-break flood forecasting model. *National Weather Service*, Silver Spring, Maryland, 164-197.

Cook, A. and Merwade, V. (2009). Effect of topographic data, geometric configuration and modeling approach on flood inundation mapping. *Journal of Hydrology*, **377**, 131-142.

Martins, R. (2000). Dam safety and protection of human lives. International European–Asian Workshop Ecosystem and Flood, Hanoi.

Wikipedia (2016). Bento Rodrigues dam disaster [online].Wikipedia, the free encyclopedia available at: https://en.wikipedia.org/wiki/Bento_Rodrigues_dam_disaster#External_links [Accessed: 23 may 2016].

Lodhi, M. S. and Agrawal, D. K. (2012). Dam-break flood simulation under various likely scenarios and mapping using GIS: Case of a proposed dam on River Yamuna, India. *Journal of Mountain Science*, **9**, 214-220.

Ritter, A. (1892). Die fortpfazung der wasser-wellen. *Zeitschrift des Vereins deutscher ingenieure*, **36**, 947-954.

Hicks, F. E. and Steffler, P. M. (1997). One dimensional dam break solutions for Variable width channel. *Journal of Hydraulic Engineering*, **123**, 464-468.

Sanders, B. F. (2001). High-resolution and non-oscillatory solution of the St.Venant equations in non-rectangular and no prismatic channels. *Journal of hydraulic Research*, **39**, 321-330.

Macchione, F. and Viggiani, G. (2004). Simple modeling of dam failure in a natural river. *Journal of Water Management*, **157**, 53-60.

Akanbi, A. A. and Katapodes, N. D. (1988). Model for flood propagation on initially dry land. *Journal of Hydraulic Engineering*, **114**, 689-706.

Zhao, D. H. (1996). Approximate Riemann Solver in FVM for 2D Hydraulic Shock Wave Modeling. *Journal of Hydraulic Engineering*, **122**, 692-702.

Sarma, A. K. (1999). A study of two-dimensional flow propagating from an opening in the river dike. PhD thesis, Gauhati University, Assam, India.

Zoppou, C. and Roberts, S. (2000). Numerical solution of the two dimensional unsteady dam break. *Applied Mathematical Model*, **24**, 457-475.

ASCFJUSCOLD (1975). Lessons from Dam Incidents, USA, American Society of CivilEngineers, New York.

ICOLD (1973). Lessons from Dam Incidents, Abridged Edition, USCOLD, Boston, MA.Jarrett, R.D. (1984). Hydraulics of High-Gradient Streams. *J. Hydraul. Div*., ASCE, **110**, 1519-1539.

Gibson, C. (2006). Our 10 greatest natural disasters. *American Heritage*, **57**, 26-37.

Osnos and Evan (2011). Faust, China, and Nuclear Power," The New Yorker, Wednesday October 12.

Cheng, C.,Qian X.,Zhang Y.,Wang Q. and Sheng, J. (2011). Estimation of the evacuation clearance time based on dam-break simulation of the Huaxi dam in Southwestern China. *Natural Hazards*, **57**, 227-243.

Tofiq, F. A.and Guven, A. (2014). Computational Dam Break Analysis Using PMF from Statistical Downscaling. European users conference, Vienna, Austria.

EXSCIMAP (2007). (A European Exchange Circle on Flood Mapping) Handbook onGood Practices for Flood Mapping in Europe.

Moel, H., van Alphen, J. and Aerts, J.C.J.H.(2009). Flood maps in Europe – methods, availability and use. *Natural Hazards and Earth System Sciences*, **9**, 289–301.

Ellingwood, B., Corotis, R., Boland, J. and Jones, N. (1993). Assessing Cost of Dam Failure. *Journal of Water Resources Planning and Management*, ASCE, **119**, 64-82.

NFIP(2002). National Flood Insurance Program – Program Description, Federal Emergency Management Agency.

Wahl, T. L. (1998). DSO-98-004 Dam Safety Research Report.

Brown, C.A. and Graham W.J. (1988). Assessing the Threat to Life from Dam Failure. *Water Resources Bulletin*, **24**, 6-10.

Dekay, M.L., and McClelland G.H. (1991). Setting Decision Thresholds for Dam Failure Warnings: A Practical Theory-Based Approach, CRJP Technical Report No. 328, Center for Research on Judgment and Policy, University of Colorado, Boulder, Colorado.

Fread, D.L. 1988 (revised 1991), BREACH: An Erosion Model for Earthen Dam Failures, National Weather Service, National Oceanic and Atmospheric Administration, Silver Spring, Maryland.

Graham, W. (2001). Human and Economic Consequences of Dam Failure, Proceedings Fema Workshop, Oklahoma City.

Froelich, D. (1995). Embankment Dam Breach Parameters Revisited. *Journal of Water Resources Planning and Management*, **121**, 90-97.

Dewey, R.L. andGillette, D.R. (1993). Prediction of Embankment Dam Breaching for Hazard Assessment. ASCE Specialty Conference on Geotechnical Practice in Dam Rehabilitation. Raleigh, NC.

Von Thun, J. L. andGillette, D. R. (1990). Guidance on Breach Parameters, [Internal Memorandum]. Denver, CO: U.S. Department of the Interior, Bureau of Reclamation.

USBR. (1988). ACER Technical Memorandum No. 11: Downstream Hazard Classification Guidelines. Denver,CO: USBR.

MacDonald, T. C. and Langridge-Monopolis, J. (1984). Breaching Characteristics of Dam Failures. *Journal of Hydraulic Engineering*, **110**, 576-586. ASCE.

FEMA (2013). Federal Guidelines for Inundation Mapping of Flood Risks Associated with Dam Incidents and Failures.

Wahl, T. L. (2004). Uncertainty of Predictions of Embankment Dam Brach Parameters. *Journal of Hydraulic Engineering*, **130**, 389-397.

Fread, D.L. (2001). Some Existing Capabilities and Future Directions for Dam-Breach Modeling/Flood Routing. Proceedings of the FEMA Workshop. Oklahoma City, OK.

Fread, D. L. (1988). The NWS DAMBRK Model: Theoretical Background/User Documentation, National Weather Service, Silver Spring, Maryland.

Fread, D.L. andLewis, J. M. (1998). NWS FLDWAV Model: Theoretical Description and User Documentation. Hydrologic Research Laboratory, Office of Hydrology, National Weather Service.

Wahl, T. L. (1997). Predicting Embankment Dam breach Parameters – A Needs Assessment. Proceedings of the U.S. Bureau of Reclamation, XXVIIth IAHR Congress. San Francisco, CA.

Evans, S. G. (1986). The maximum discharge of outburst floods caused by the breaching of man-made and natural dams. *Canada Geotechnical Journal*, **23**, 385-387.

Singh, K. P. and Snorrason, A. (1984). Sensitivity of outflow peaks and flood stage to the selection of dam breach parameters and simulation models. *Journal of Hydrology*, **68**, 295-310.

State of Colorado Department of Natural Resources. (2010). Guidelines for Dam Breach Analysis. Division of Water Resources. Retrieved January 19, 2011, from http://water.state.co.us/DWRIPub/Documents/GuidelinesForDamBreachAnalysis021010.pdf

Hagen, V. K. (1982). Re-evaluation of design floods and dam safety. Proceedings of the 14th Congress of International Commission on Large Dams, International Commission on Large Dams. Paris, France.

SCS (Soil Conservation Service). (1981). Simplified Dam Breach Routing Procedure, Technical Release No. 66 (Rev. 1).

Kirkpatrick, G. (1977). Evaluation Guidelines for Spillway Adequacy. The Evaluation of Dam Safety, Engineering Foundation Conference, Pacific Grove, California, ASCE.

FEMA (2012). National Dam Safety Program TechnicalSeminar No. 22 -Dam Breach Modelingand Consequence Assessment, Overview of FEMA Dam Breach Tools.

DHI. A modeling system for Rivers and channels (MIKE11), User Guide manual, (2005). DHI water & Environment, Denmark.

DHI. "Flow model (MIKE21), User Guide manual", (2005). DHI water & Environment, Denmark.

O'Brien, K. (2013). Pocket Guide Basic FLO-2D Model manuals, FLO-2D Software, Inc.

Wahl, T. (2010). Dam Breach Modeling- An Overview of Analysis Methods. Published in the Joint Federal Interagency Conference on Sedimentation and Hydrologic Modeling, June 27 – July 1, 2010, Las Vegas, NV. Published by Tony L.

Wahl, Hydraulic Engineer, U.S. Bureau of Reclamation, Denver. http://www.usbr.gov/pmts/hydraulics_lab/pubs/PAP/PAP-1018.pdf.

Wahl, T. (2009). "Evaluation of New Models for Simulating Embankment Dam Breach," Dam Safety '09, Annual Meeting of the Association of State Dam Safety Officials (ASDSO), Sept. 27-Oct. 1, 2009, Hollywood, FL.

Wahl, Tony L., Jean-Robert Courivaud, Rene Kahawita, Gregory J. Hanson, Mark W. Morris, and Jeffrey T. McClenathan. (2008). Development of Next-Generation Embankment Dam Breach Models. Retrieved January 19, 2011.

Visser, K., Hanson, G. J., Temple, D., and Neilsen, M. (2013). Earthen embankment overtopping analysis using the WinDAM B software. National Dam Safety Program Technical Seminar No. 20, Overtopping of Dams February 20-21, 2013 FEMA National Emergency Training Center, Emmitsburg, MD.

Bernedo, C. (2011). Predictive models and available software, USSD Workshop,on Dam Break Analysis, Denver, Colorado.http://www.infomine.com/publications/docs/Bernedo2011.pdf

Munson, B. R.,Young D. F.,Okiishi T. H., andHuebsch W. W. (2009). Fundamentals ofFluid Mechanics, Sixth Edition, John Wiley & Sons, New York, NY.

Fourie, A. (2011). "Providing realistic data for calibration of models: results from South Africa (Merriespruit), Chile (Maule), and Australia (submarine landslides)," USSD Workshop, Denver, CO. http://www.infomine.com/publications/docs/Fourie2011.pdf

Fread, D. L. (1984). DAMBRK: The NWS Dam-Break Flood Forecasting Model, Officeof Hydrology, National Weather Service, Silver Spring, MD.

Browne, R. (2011). "Tailings dam break models in Nevada – A practitioner's perspective," *USSD Workshop*, Denver, CO. http://www.infomine.com/publications/docs/Browne2011.pdf

O'Brien, J. S., Julien, P. Y., and Fullerton, W. T. (1993). "Two-Dimensional Water Flood and Mudflow Simulation. *Journal of Hydraulic Engineering*, ASCE, New York, **119**, 244-261.

Breitkreutz, W., (2011). Overview of USACE Dam Break Modeling, Mapping andConsequence Analysis, USSD Workshop, Denver, CO.http://www.infomine.com/publications/docs/Breitkreutz2011.pdf

McDougall, S. (2006). A new continuum dynamic model for the analysis of extremely rapid landslide motion across complex 3D terrain. University of British Columbia.

Fread, D. L., and Lewis, J. M. (1988). FLDWAV: A Generalized Flood Routing Model,National Weather Service (NWS), Silver Spring, MD.

Fread, D. L. (1993). NWS FLDWAV Model: The Replacement of DAMBRK for Dam- Break Flood Prediction, National Weather Service (NWS), Silver Spring, MD.

Fread, D. (2000). NWS FLDWAV Model: Theoretical Description, Hydrologic ResearchLaboratory, Office of Hydrology, National Weather Service, NOAA.

Kunkel, J. (2011b). "Downstream Modeling of Tailings Flow from Failure of a 380 ft High Tailing Dam," *USSD Workshop*, Denver, CO. http://www.infomine.com/publications/docs/Kunkel2011a.pdf.

Hegedus, P. (2011). "October 4, 2010 Red Sludge Tailings Sam Failure at Kolontar, Hungary," USSD Workshop, Denver, CO.http://www.infomine.com/publications/docs/Hegedus2011.pdf

Soderstrom, A. and N. Isaksson (2011). "Dambreak Modeling Using Combined 1-D and 2-D Models," *USSD Workshop*, Denver, CO. http://www.infomine.com/publications/docs/Soderstrom2011.pdf

Bozkuş, Z. and Kasap, A. (1998). Comparison of physical and numerical dam-break simulations. Turkish Journal of Engineering and Environmental Sciences, 22, 429-444.

Wurbs, R. A. (1987). Dam breach flood wave models. *Journal of Hydraulic Engineering*. **113**, 29-46.

Westphal, Jerome A., and David, B. Thompson, (1987). NWS Dam break or NWS Simplified Dam Breac Computational Hydrology. *Proceedings of the First International Conference*, Anaheim, California.17-23.

Lewis, J. M. and Paquier, A. (1999). Discussion and Closure: Simplified Dam-Break Wave Model. *Journal of Hydraulic Engineering*, **125**, 314-315.

Fread, D.L., Lewis, J. M. and Wiele, S. M. (1991). The NWS Simplified Dam Breach, Lighthouse Publications First international conference (Hromadka and McCuen, Eds), Anaheim, California.

Fread, D.L. (1993). Chapter 10, Flow Routing, Handbook of Hydrology, editor D.R. Maidment, McGraw-Hill book Co., New York.

Hu, H.H. and Walton, R., (2008). Advanced Guidance on Use of Steady HEC-RAS. In: World Environmental and Water Resources Congress 2008. Hawaii, USA.

Zhou, R.D., Judge, D.G.C. and Donnely, R. (2005) Comparison of HEC-RAS withFLDWAV and DAMBRK models for dam break analysis. Canadian Dam.

Gee, D.M. and Brunner, G.W. (2005). Dam Break Flood Routing using HEC-RAS andNWS-FLDWAV. EWRI/ASCE.

Moreda, F., Gutierrez, A., Reed, S. and Aschwanden, C. (2009). Transitioning NWS Operational Hydraulics Models from FLDWAV to HEC-RAS. In: World Environmental and Water Resources Congress 2009: Great Rivers. Kansas City, Missouri, USA, ASCE.

Ferreira, C. (2001a). Gene expression programming in problem solving. 6th Online World Conference on Soft Computing in Industrial Applications (invited tutorial).

Ferreira, C. (2006). Gene expression programming: mathematical modeling by an artificial intelligence, 2nd edn.Springer, Berlin (DE).

Aytek, A., Kisi, O., Guven, A. (2014). A genetic programming technique for lake level modeling. *Hydrol Res* **45**, 529–539.

Seckin, N., Guven, A. (2012). Estimation of peak flood discharges at ungauged sites across turkey. *Water Resour Manag* **26**, 2569–2581.

Tofiq, F., Guven, A. (2014) Prediction of design flood discharge by statistical downscaling and General Circulation Models. *J. Hydraul.*, **517**, 1145–1153

Guven, A., Kisi, O. (2011) Estimation of suspended sediment yield in natural rivers using machine-coded linear genetic programming. *Water Resour. Manag.*, **25**, 691–704.

Kisi, O., Guven, A. (2010) A machine code-based genetic programming for suspended sediment concentration estimation. *Adv Eng Softw*., **41**, 939–945.

Traore, S., Guven, A. (2013) New algebraic formulations of evapotranspiration extracted from gene-expression programming in the tropical seasonally dry regions of West Africa. *Irrig Sci*., **31**, 1–10.

Guven, A. (2009) Linear genetic programming for time-series modeling of daily flow rate. *J. Earth Syst*., **118**, 137–146.

Guven, A., Kisi, O. (2011) Estimation of suspended sediment yield in natural rivers using machine-coded linear genetic programming. *Water Resour Manag*., **25**, 691–704.

Al-Juboori, A. M., & Guven, A. (2016). Hydropower Plant Site Assessment by Integrated Hydrological Modeling, Gene Expression Programming and Visual Basic Programming. *Water Resources Management*, **30**, 2517-2530.

Guven, A., and Azamathulla, H.Md. (2012). Gene-Expression programming for flip-bucket spillway scour. *Water Science & Technology*, **65**, 1982–1987.

Moussa, Y.A.M. (2013). Modeling of local scour depth downstream hydraulic structures in trapezoidal channel using GEP and ANNs. *Ain Shams Engineering Journal*, **4**, 717–722.

Azamathulla, H.Md., AbGhani, A., Leow, C.S., Chang, C.K., and Zakaria, N.A. (2011). Gene expression programming for the development of a stage-discharge curve of the Pahang River. *Water Resources Management*, **25**, 2901–2916.

Guven, A., Aytek, A. (2009) New approach for stage–discharge relationship: Gene-expression programming. *J. Hydrol Eng*., **14**, 812–820.

Zakaria, N.A, Azamathulla, H.Md, Chang, C.K and AbGhani, A. (2010). Gene-Expression programming for total bed material load estimation – A Case Study. *Science of the Total Environment*, **408**, 5078–5085.

Azamathulla, H.Md., and Jarrett, R. (2013). Use of Gene-Expression programming to estimate manning's roughness coefficient for high gradient streams. *Water Resources Management*, **27**, 715–729.

Azamathulla, H.Md., Ahmad, Z., and AbGhani, A. (2012). Computation of discharge through side sluice gate using gene-expression programming. *Irrig. and Drain. Engrg*., ASCE, **62**, 115–119.

Kisi, O., Emiroğlu, ME., Bilhan, O., Guven, A. (2012) Prediction of lateral outflow over triangular labyrinth side weirs under subcritical conditions using soft computing approaches. *Expert Syst. Appl*., **39**, 3454–3460.

Karbasi, M., & Azamathulla, H. M. (2015). GEP to predict characteristics of a hydraulic jump over a rough bed. *KSCE Journal of Civil Engineering*, 1-6.

Zorn CR, Shameldin AY (2015) Peak flood estimation using gene expression programming. *J Hydraul*.., **531**, 1122–1128.

Wang, C.Y., Shih, H.P, Hong, J.H. and Rajkumar, V.R. (2013). Prediction of bridge pier scour using genetic programming. *J. Marine Science and Technology*, **21**, 483–492.

TALAB, A. A. (2011) Evaluation of some irrigation projects in Dukan watershed as controlling and conservation of water resources. URL: http://goo.gl/szTkz6[Accessed: 1 march 2016].

SMEC (2006) Consultancy services for dukan and derbendikhan dam inspection. URL: http://goo.gl/l0mbWi[Accessed: 19 may 2016].

Watershed Modeling System (WMS). (2008). Available from: Environmental Modeling Systems Incorporated (EMSI).

Reed, S.and Halgren, J. (2011).Validation of a New GIS Tool to Rapidly Develop Simplified Dam Break Models. NOAA, National Weather Service Office of Hydrologic Development and Riverside Technology, Inc.

Ferreira, C. 2001a Gene expression programming in problem solving. 6th Online World Conference on Soft Computing in Industrial Applications (invited tutorial).

Ferreira, C. 2001b Gene expression programming: A new adaptive algorithm for solving problems. *Complex Syst*., 13, 87–129.

Shahraki, A., Zadbar, A., Motevalli, M., and Aghajani, F. (2012). Modeling of Earth Dam Break with SMPDBK Case Study: Bidekan Earth Dam. *World Applied Sciences Journal*, **19**, 376-386.

APPENDICES

Appendix A

Output Data of SMPDBK Model

1st scenario: V= 8400MCM, AS=34000 ha

Table A-1. 1st scenario results of dam break

RVR KM FROM DAM	MAX. FLOW (CMS)	MAX. ELEV. (M-MSL)	MAX. DEPTH (M)	TIME (HR) AT MAX.DEPTH
0	398602.7	463.625	67.059	0.13
1.609	394616.8	438.744	44.055	0.14
4.119	392807.6	421.480	26.822	0.17
6.421	392345.5	419.371	24.743	0.19
9.173	386947.2	419.371	24.774	0.21
11.603	383077.7	419.371	27.611	0.29
13.357	379247	419.371	27.642	0.31
15.996	369197.3	419.371	31.062	0.44
18.217	365505.4	419.371	37.505	0.52
21.195	353808	402.670	20.836	0.6
24.703	350269.8	399.175	32.150	0.65
28.791	346767	384.173	17.178	0.78
33.232	343299.3	384.173	20.223	0.92
37.578	339866.4	380.606	25.106	1.16
40.893	336467.9	380.353	24.883	1.21
45.528	333103	380.353	27.154	1.31
50.710	329772.1	372.054	24.554	1.48
53.478	326474.3	372.054	27.861	1.5
56.149	323209.6	372.054	28.468	1.61
59.642	319977.5	365.507	28.084	1.82
63.263	316777.7	360.980	28.480	1.9
68.413	313609.9	354.299	29.800	2.14
71.309	310473.8	352.610	30.492	2.17
74.753	307369.2	346.990	27.983	2.19
77.908	304295.4	346.990	29.367	2.28
82.301	301252.5	338.001	33.180	2.53
84.683	298239.8	327.961	23.170	2.88
88.320	295257.5	327.961	23.201	2.91
92.360	292304.9	327.961	28.602	3.03
95.482	289382	317.583	24.085	3.06

Table A-1 continued

100.632	286488.1	313.837	36.155	3.09
103.528	283623.2	303.513	25.862	3.26
106.972	280787	297.158	19.537	3.87
110.175	277979.2	297.158	20.787	4.13
116.339	275199.4	285.433	21.805	4.17
125.882	272447.4	282.735	30.236	4.21
136.616	269722.9	261.146	20.647	5.41
148.171	267025.7	251.478	25.021	5.47
161.336	264355.4	242.392	26.892	5.52
172.473	261711.9	219.267	21.771	6.95
178.218	259094.7	218.181	20.717	7.02
183.561	256503.8	216.432	23.810	7.09
188.453	253938.8	204.389	17.602	7.67
196.613	251399.4	197.763	20.263	8.07
202.567	248885.4	183.888	22.098	8.16
208.892	246396.5	183.888	22.128	8.24
216.295	243932.6	169.481	22.125	9.95
223.344	241493.2	164.729	23.966	10.05
238.278	239078.3	153.820	23.579	10.15
248.787	236687.6	142.018	23.981	10.25

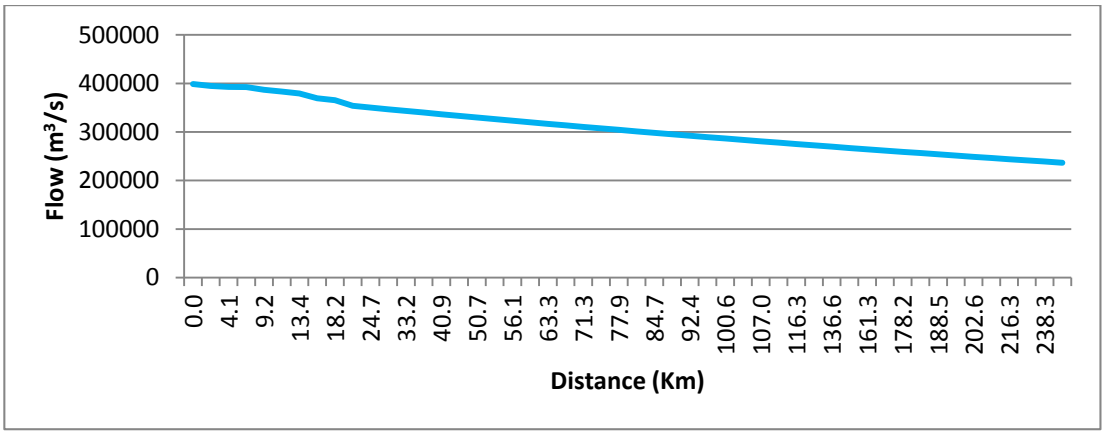

Figure A-1. Flood discharge curve from the failed Dukan dam along the Lesser Zab River for 1st scenario

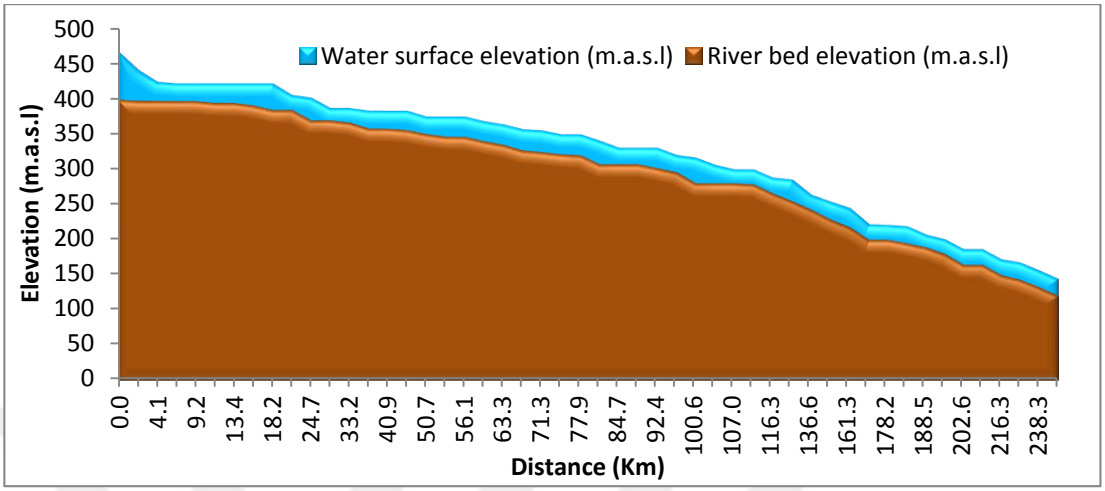

Figure A-2.Water elevation curve of the flood wave along the Lesser Zab River for 1st scenario

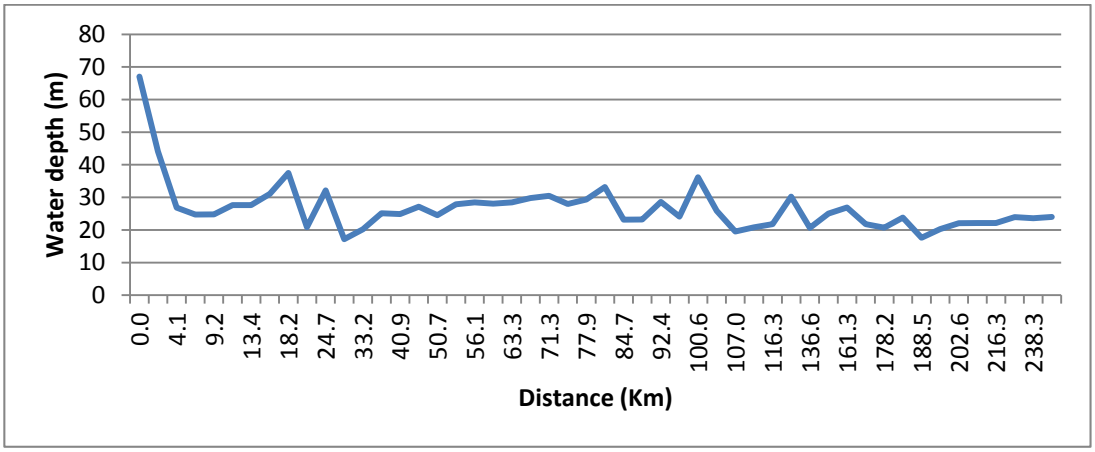

Figure A-3.Water depth curve of the flood wave along the Lesser Zab River for the 1st scenario

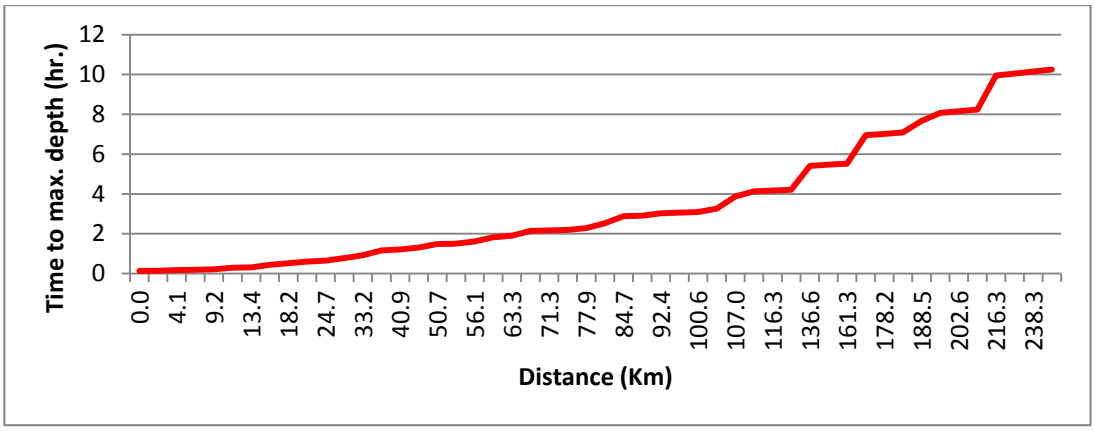

Figure A-4.Time curve to reach max. depth of the flood wave along the Lesser Zab River for the 1st scenario

2nd scenario: V= 7000MCM, AS=32000 ha

Table A-2. 2nd scenario results of dam break

RVR KM FROM DAM	MAX. FLOW (CMS)	MAX. ELEV. (M-MSL)	MAX. DEPTH (M)	TIME (HR) AT MAX.DEPTH
0	373583.029	461.302	64.736	0.12
1.609	369148.045	437.525	42.836	0.14
4.119	367725.406	420.724	26.066	0.16
6.421	367245.719	418.694	24.067	0.19
9.173	359935.442	418.694	24.097	0.2
11.603	356336.087	418.694	26.932	0.29
13.357	352772.695	418.694	26.965	0.31
15.996	341772.733	418.694	30.385	0.44
18.217	338354.889	418.694	36.828	0.53
21.195	328214.627	402.098	20.263	0.6
24.703	324932.421	398.071	31.046	0.66
28.791	321683.063	383.782	16.788	0.79
33.232	318466.269	383.782	19.833	0.93
37.578	315281.756	379.863	24.362	1.17
40.893	312128.958	379.564	24.094	1.23
45.528	309007.592	379.564	26.365	1.34
50.710	305917.375	371.377	23.878	1.51
53.478	302858.306	371.377	27.185	1.53
56.149	299829.819	371.377	27.791	1.64
59.642	296831.348	364.802	27.380	1.86
63.263	293863.17	360.099	27.599	1.94

Table A-2 continued

68.413	290924.454	353.507	29.007	2.19
71.309	288015.181	351.839	29.721	2.21
74.753	285135.075	346.240	27.233	2.23
77.908	282283.710	346.240	28.617	2.33
82.301	279460.888	337.340	32.519	2.58
84.683	276666.270	327.477	22.686	2.94
88.320	273899.601	327.477	22.716	2.97
92.360	271160.597	327.434	28.075	3.09
95.482	268449.004	316.873	23.375	3.12
100.632	265764.511	313.014	35.332	3.15
103.528	263106.861	303.053	25.402	3.33
106.972	260475.801	296.759	19.138	3.95
110.175	257871.048	296.759	20.388	4.21
116.339	255292.346	284.704	21.076	4.25
125.882	252739.412	282.052	29.553	4.25
136.616	250212.020	260.610	20.110	5.5
148.171	247709.916	250.786	24.329	5.56
161.336	245232.814	241.828	26.328	5.61
172.473	242780.490	218.852	21.357	7.08
178.218	240352.689	217.493	20.028	7.15
183.561	237949.155	215.740	23.119	7.22
188.453	235569.662	203.938	17.151	7.81
196.613	233213.984	197.208	19.708	8.21
202.567	230881.836	183.477	21.686	8.3
208.892	228573.022	183.477	21.717	8.38
216.295	226287.315	169.048	21.692	10.04
223.344	224024.430	164.061	23.298	10.15
238.278	221784.200	153.110	22.869	10.25
248.787	219566.339	141.512	23.475	10.35

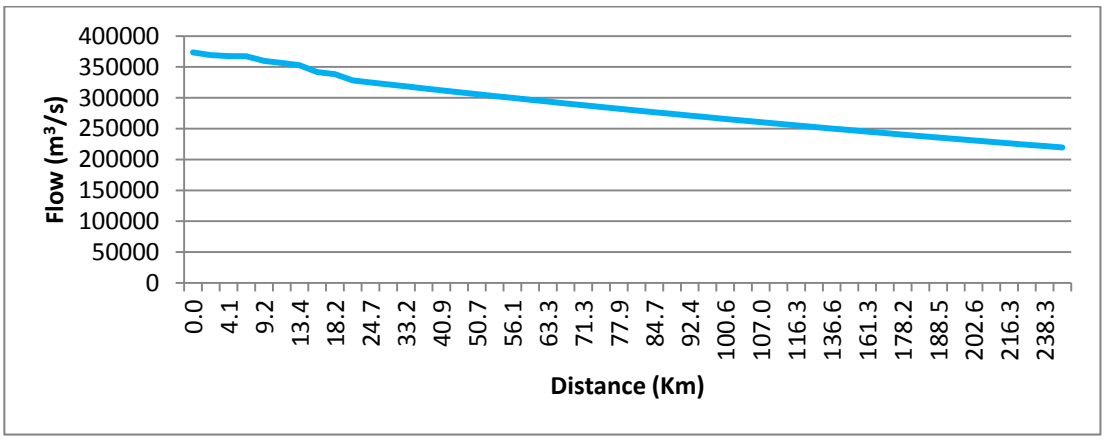

Figure A-5. Flood discharge curve from the failed dam along the Lesser Zab River for 2nd scenario

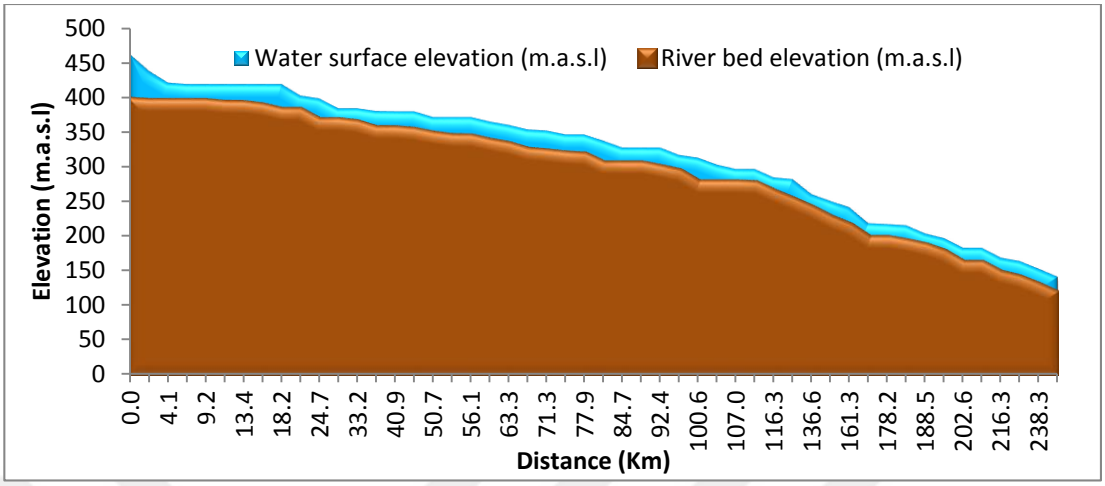

Figure A-6. Water elevation curve of the flood wave along the Lesser Zab River for the 2nd scenario

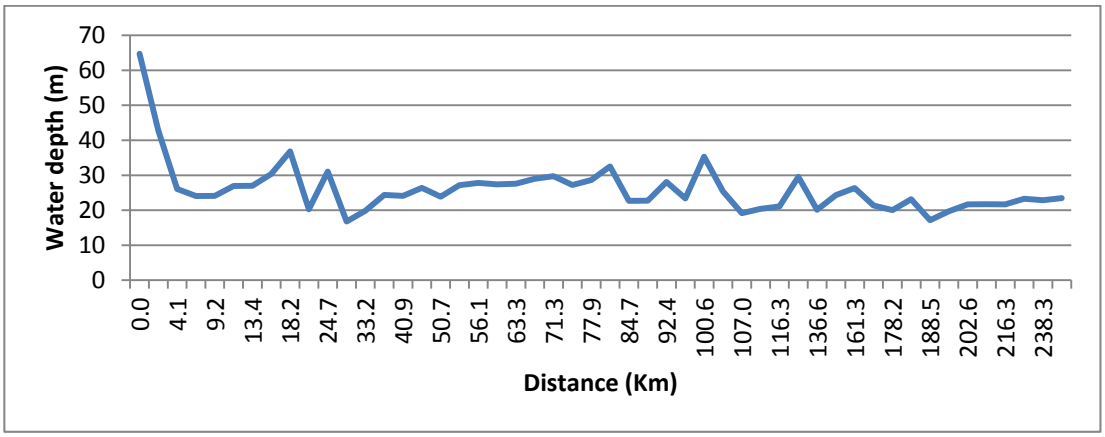

Figure A-7. Water depth curve of the flood wave along the Lesser Zab River for the 2nd scenario

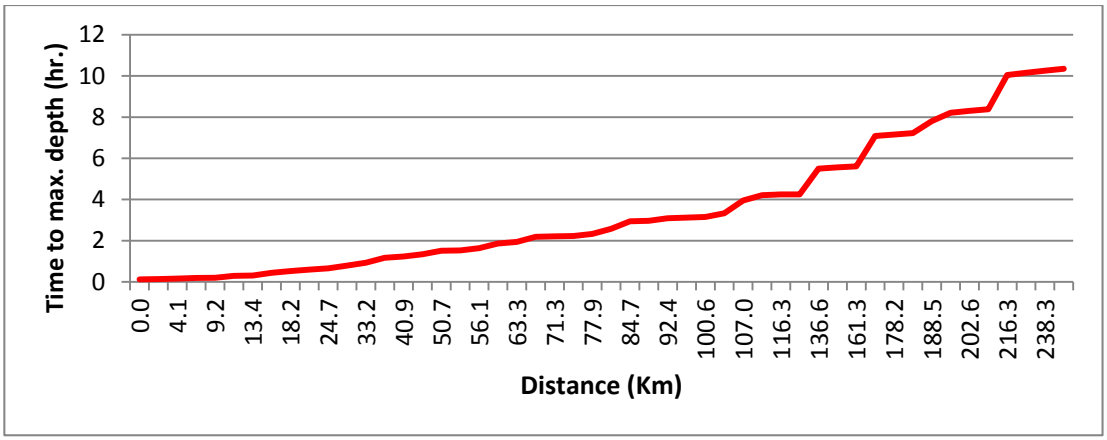

Figure A-8. Time curve to reach maximum depth of the flood wave along the Lesser Zab River for the 2nd scenario

3rd scenario: V= 6000MCM, AS=28500 ha

Table A-3. 3rd scenario results of dam break

RVR KM FROM DAM	MAX. FLOW (CMS)	MAX. ELEV. (M-MSL)	MAX. DEPTH (M)	TIME (HR) AT MAX.DEPTH
0	353913.298	459.400	62.834	0.12
1.609	349162.297	436.534	41.845	0.13
4.119	348002.722	420.102	25.444	0.16
6.421	347518.221	418.136	23.509	0.19
9.173	338832.595	418.136	23.53	0.2
11.603	335444.201	418.136	26.377	0.29
13.357	332089.787	418.136	26.407	0.31
15.996	320645.533	418.136	29.827	0.45
18.217	317438.934	418.136	36.271	0.53
21.195	308309.582	401.650	19.815	0.61
24.703	305226.444	397.178	30.153	0.67
28.791	302174.171	383.468	16.474	0.79
33.232	299152.480	383.468	19.519	0.94
37.578	296161.088	379.268	23.768	1.19
40.893	293199.429	378.933	23.463	1.25
45.528	290267.503	378.933	25.734	1.36
50.710	287364.743	370.828	23.329	1.54
53.478	284491.149	370.810	26.618	1.56
56.149	281646.184	370.810	27.224	1.67
59.642	278829.734	364.232	26.810	1.89
63.263	276041.431	359.392	26.892	1.97
68.413	273281.019	352.863	28.364	2.22

Table A-3 continued

71.309	270548.217	351.214	29.096	2.24
74.753	267842.741	345.637	26.630	2.27
77.908	265164.307	345.637	28.014	2.37
82.301	262512.661	336.804	31.982	2.62
84.683	259887.547	327.077	22.286	3
88.320	257288.684	327.077	22.317	3.03
92.360	254715.787	326.788	27.428	3.14
95.482	252168.630	316.303	22.805	3.18
100.632	249646.958	312.352	34.671	3.21
103.528	247150.488	302.687	25.036	3.38
106.972	244678.993	296.442	18.821	4.02
110.175	242232.220	296.442	20.071	4.27
116.339	239809.912	284.113	20.485	4.32
125.882	237411.815	281.488	28.989	4.34
136.616	235037.702	260.177	19.677	5.58
148.171	232687.347	250.228	23.771	5.63
161.336	230360.467	241.368	25.868	5.69
172.473	228056.863	218.523	21.028	7.19
178.218	225776.309	216.938	19.473	7.26
183.561	223518.550	215.179	22.558	7.33
188.453	221283.360	203.578	16.791	7.93
196.613	219070.540	196.867	19.366	8.34
202.567	216879.835	183.148	21.357	8.42
208.892	214711.019	183.148	21.387	8.51
216.295	212563.923	168.694	21.339	10.2
223.344	210438.290	163.528	22.765	10.3
238.278	208333.896	152.604	22.363	10.4
248.787	206250.569	141.101	23.064	10.5

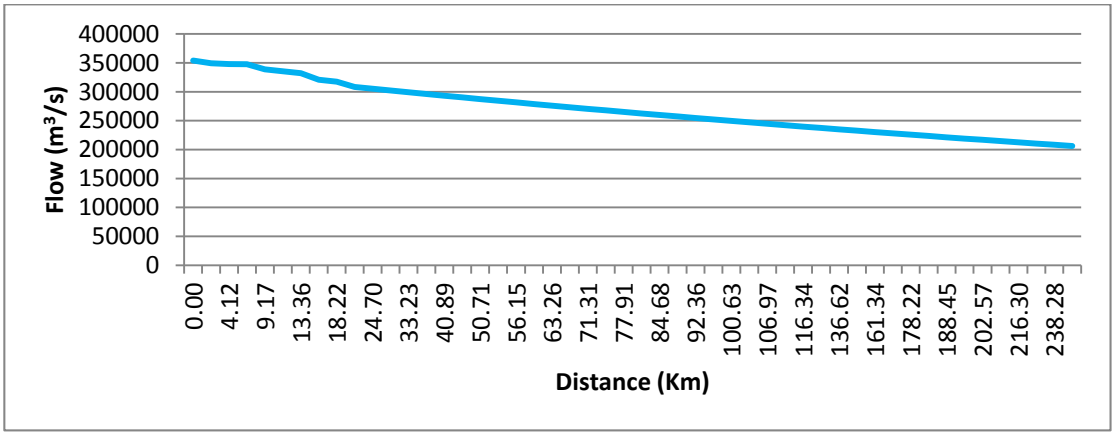

Figure A-9. Flood discharge curve from the failed dam along the Lesser Zab River for the 3rd scenario

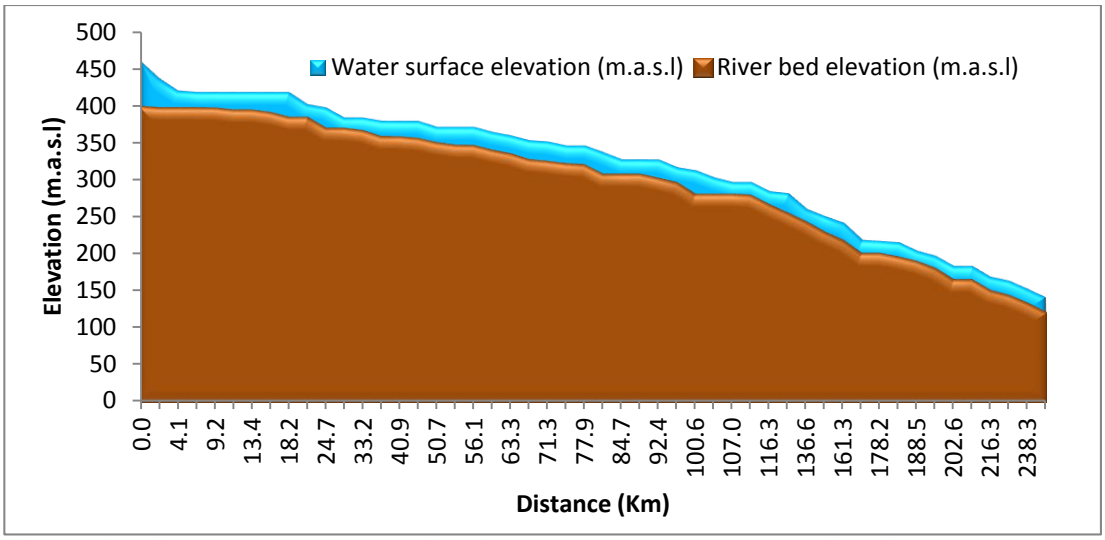

Figure A-10. Water elevation curve of the flood wave along the Lesser Zab River for the 3rd scenario

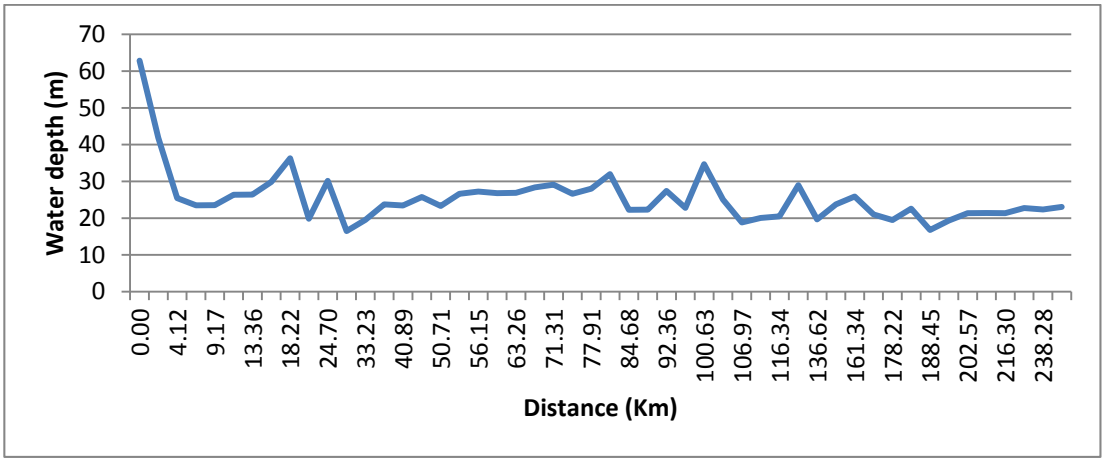

Figure A-11. Water depth curve of the flood wave along the Lesser Zab River for the 3rd scenario

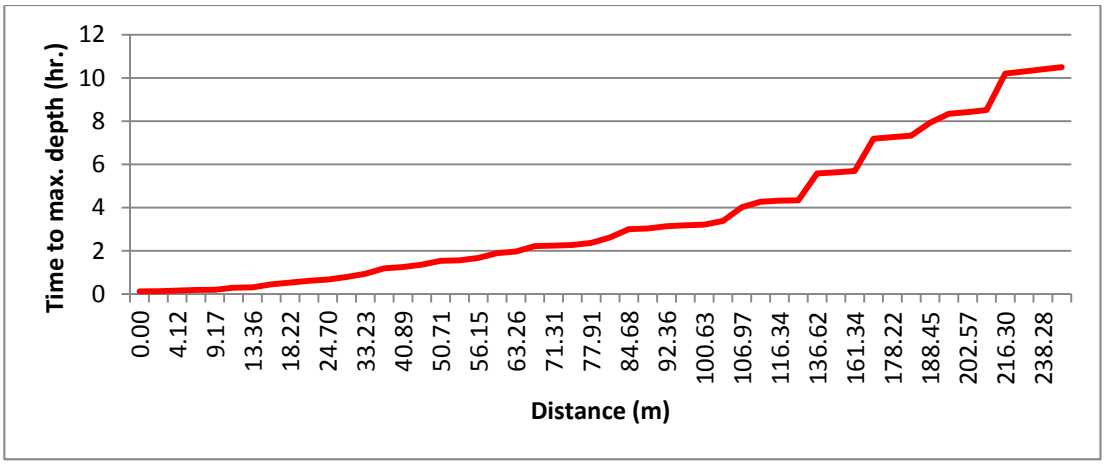

Figure A-12. Time curve to reach maximum depth of the flood wave along the Lesser Zab River for the 3rd scenario

4th scenario: V= 5000MCM, AS=25900 ha

Table A-4. 4th scenario results of dam break

RVR KM FROM DAM	MAX. FLOW (CMS)	MAX. ELEV. (M-MSL)	MAX. DEPTH (M)	TIME (HR) AT MAX.DEPTH
0	339376.845	457.983	61.417	0.11
1.609	334034.022	435.787	41.099	0.13
4.119	333285.608	419.636	24.978	0.16
6.421	332846.130	417.716	23.088	0.18
9.173	323037.457	417.716	23.119	0.2
11.603	319807.072	417.716	25.956	0.28
13.357	316608.967	417.716	25.987	0.31
15.996	304921.188	417.716	29.407	0.45
18.217	301872.030	417.716	35.850	0.53
21.195	293447.485	401.311	19.476	0.61
24.703	290513.010	396.492	29.468	0.67
28.791	287607.985	383.231	16.236	0.8
33.232	284731.843	383.231	19.281	0.95
37.578	281884.527	378.811	23.311	1.2
40.893	279065.698	378.448	22.978	1.26
45.528	276275.045	378.448	25.249	1.38
50.710	273512.283	370.411	22.911	1.56
53.478	270777.159	370.325	26.133	1.58
56.149	268069.389	370.325	26.740	1.69
59.642	265388.689	363.794	26.371	1.92
63.263	262734.806	358.853	26.353	2

Table A-4 continued

68.413	260107.456	352.367	27.867	2.25
71.309	257506.384	350.739	28.620	2.27
74.753	254931.334	345.173	26.167	2.29
77.908	252382.025	345.173	27.550	2.4
82.301	249858.201	336.389	31.568	2.66
84.683	247359.608	326.757	21.966	3.04
88.320	244886.018	326.757	21.997	3.07
92.360	242437.149	326.291	26.932	3.2
95.482	240012.774	315.864	22.366	3.23
100.632	237612.638	311.840	34.158	3.26
103.528	235236.514	302.404	24.752	3.44
106.972	232884.149	296.204	18.583	4.09
110.175	230555.315	296.204	19.833	4.33
116.339	228249.757	283.662	20.034	4.37
125.882	225967.278	281.043	28.544	4.42
136.616	223707.593	259.838	19.339	5.65
148.171	221470.534	249.798	23.341	5.7
161.336	219255.817	241.008	25.508	5.76
172.473	217063.272	218.270	20.775	7.29
178.218	214892.644	216.511	19.046	7.36
183.561	212743.707	214.746	22.125	7.43
188.453	210616.290	203.313	16.526	8.04
196.613	208510.111	196.596	19.095	8.46
202.567	206425.029	182.892	21.101	8.55
208.892	204360.787	182.892	21.131	8.63
216.295	202317.160	168.417	21.061	10.37
223.344	200294.007	163.238	22.475	10.47
238.278	198291.071	152.287	22.046	10.58
248.787	196308.155	140.781	22.744	10.68

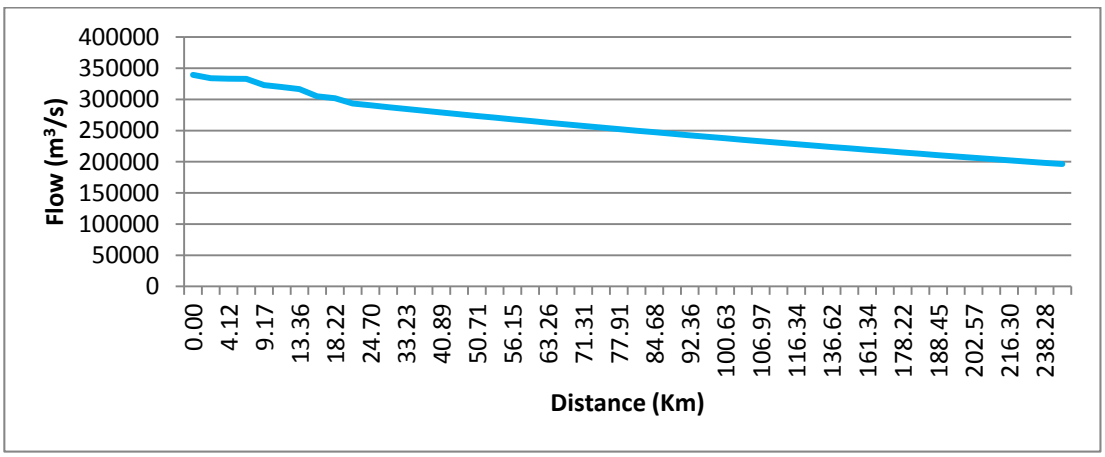

Figure A-13. Flood discharge curve from the failed dam along the Lesser Zab River for the 4th scenario

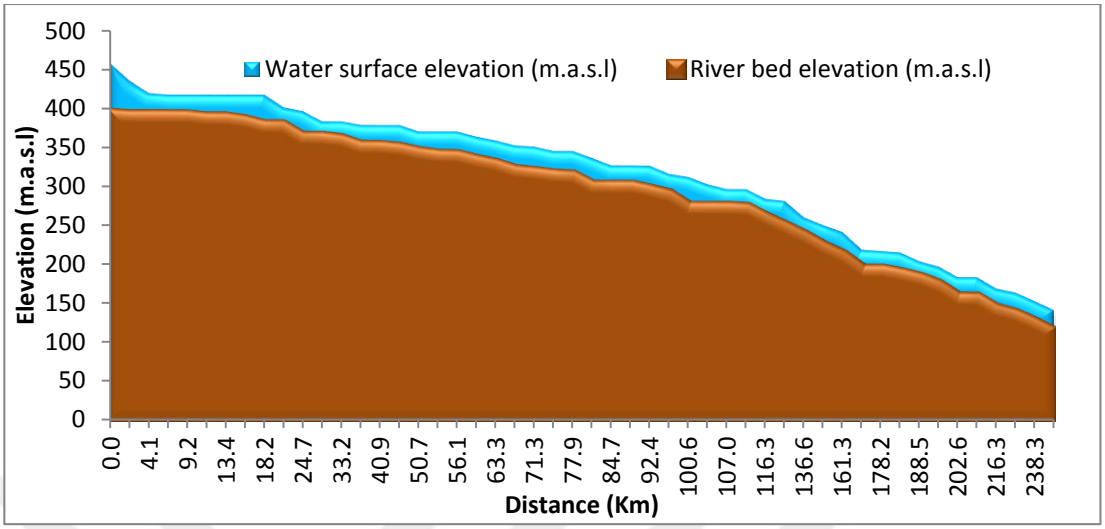

Figure A-14. Water elevation curve of the flood wave along the Lesser Zab River for the 4th scenario

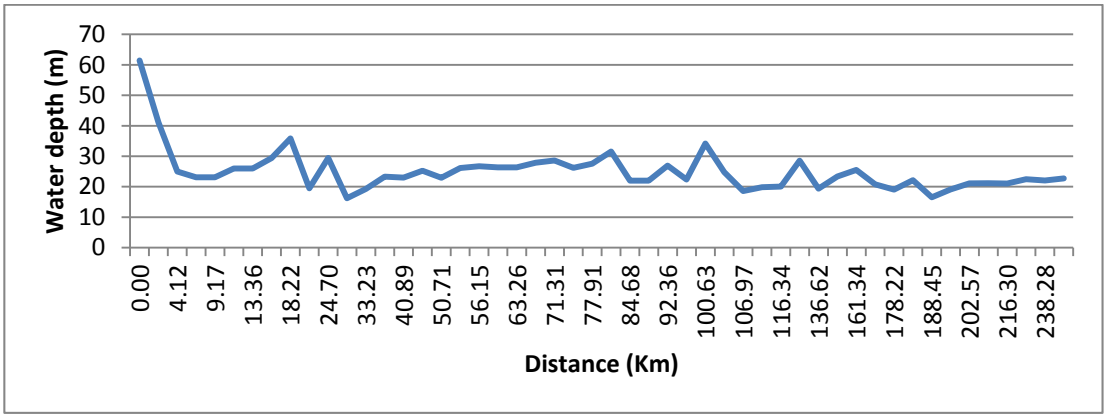

Figure A-15. Water depth curve of the flood wave along the Lesser Zab River for the 4th scenario

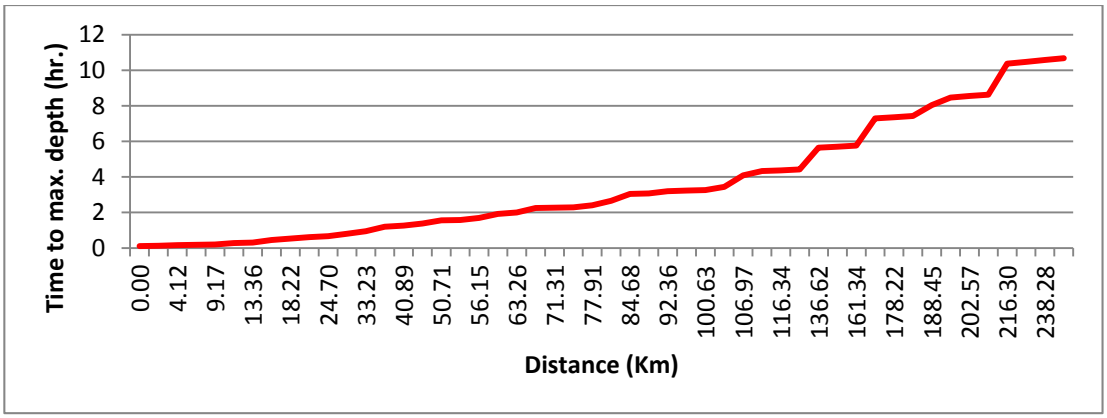

Figure A-16. Time curve to reach maximum depth of the flood wave along the Lesser Zab River for the 4th scenario

5th scenario: V= 4000MCM, AS=22500 ha

Table A-5. 5th scenario results of dam break

RVR KM FROM DAM	MAX. FLOW (CMS)	MAX. ELEV. (M-MSL)	MAX. DEPTH (M)	TIME (HR) AT MAX.DEPTH
0	320330.367	456.050	59.484	0.11
1.609	314648.875	434.794	40.105	0.13
4.119	314044.876	418.996	24.338	0.15
6.421	313667.413	417.146	22.518	0.18
9.173	302234.203	417.146	22.549	0.2
11.603	299211.946	417.146	25.386	0.28
13.357	296219.704	417.146	25.417	0.32
15.996	284273.676	417.146	28.837	0.46
18.217	281431.033	417.146	35.280	0.54
21.195	274237.902	400.863	19.028	0.62
24.703	271495.529	395.575	28.550	0.68
28.791	268780.566	382.917	15.922	0.81
33.232	266092.76	382.917	18.967	0.97
37.578	263431.825	378.208	22.707	1.21
40.893	260797.509	377.811	22.341	1.28
45.528	258189.528	377.811	24.612	1.4
50.710	255607.626	369.856	22.357	1.58
53.478	253051.549	369.679	25.487	1.61
56.149	250521.042	369.679	26.093	1.72
59.642	248015.822	363.202	25.779	1.96
63.263	245535.663	358.130	25.630	2.03
68.413	243080.309	351.705	27.206	2.29

Table A-5 continued

71.309	240649.506	350.102	27.983	2.31
74.753	238243.027	344.555	25.548	2.33
77.908	235860.618	344.555	26.932	2.44
82.301	233501.994	335.822	31.001	2.71
84.683	231166.987	326.306	21.515	3.11
88.320	228855.313	326.306	21.546	3.14
92.360	226566.745	325.626	26.267	3.28
95.482	224301.086	315.279	21.781	3.31
100.632	222058.080	311.167	33.485	3.34
103.528	219837.501	301.983	24.332	3.51
106.972	217639.123	295.893	18.272	4.17
110.175	215462.747	295.893	19.522	4.42
116.339	213308.118	283.061	19.434	4.46
125.882	211175.038	280.434	27.934	4.53
136.616	209063.281	259.457	18.958	5.74
148.171	206972.648	249.222	22.765	5.8
161.336	204902.941	240.523	25.024	5.86
172.473	202853.906	217.938	20.442	7.44
178.218	200825.372	215.941	18.476	7.51
183.561	198817.141	214.170	21.549	7.58
188.453	196828.959	202.975	16.187	8.27
196.613	194860.683	196.221	18.720	8.72
202.567	192912.059	182.541	20.750	8.81
208.892	190982.946	182.541	20.781	8.9
216.295	189073.116	168.051	20.695	10.6
223.344	187182.400	162.836	22.073	10.7
238.278	185310.572	151.848	21.607	10.81
248.787	183457.461	140.348	22.311	10.92

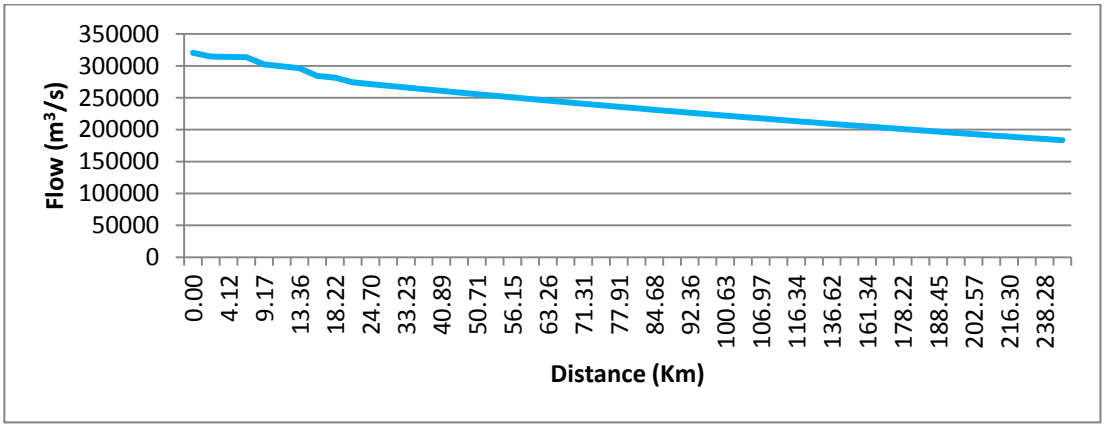

Figure A-17. Flood discharge curve from the failed dam along the Lesser Zab River for the 5th scenario

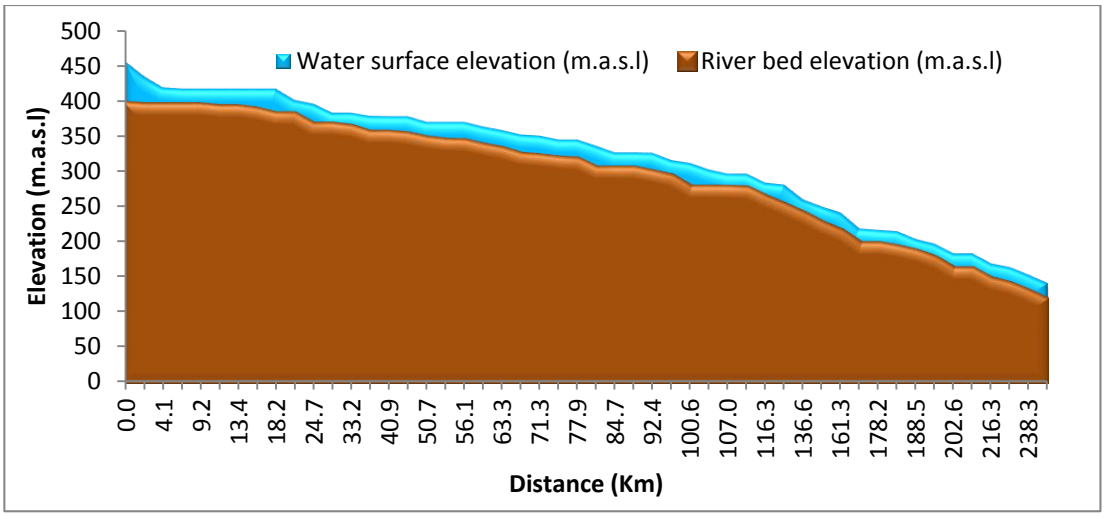

Figure A-18. Water elevation curve of the flood wave along the Lesser Zab River for the 5th scenario

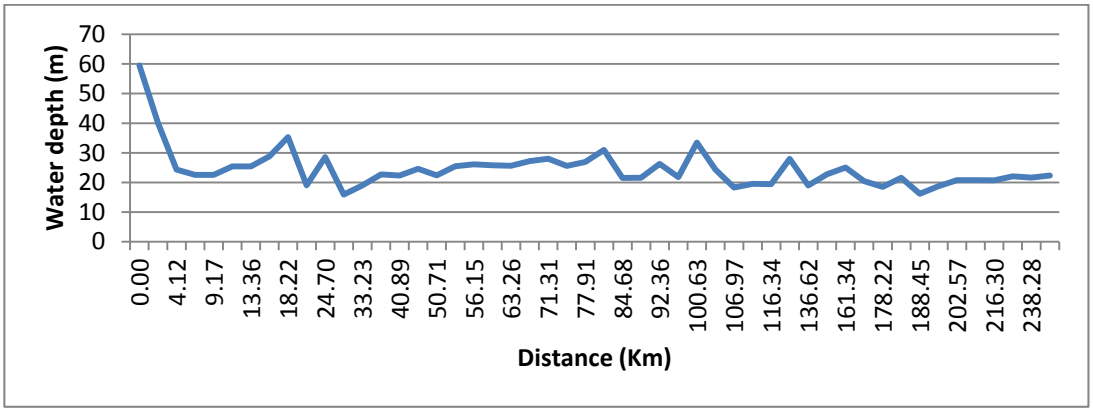

Figure A-19. Water depth curve of the flood wave along the Lesser Zab River for the 5th scenario

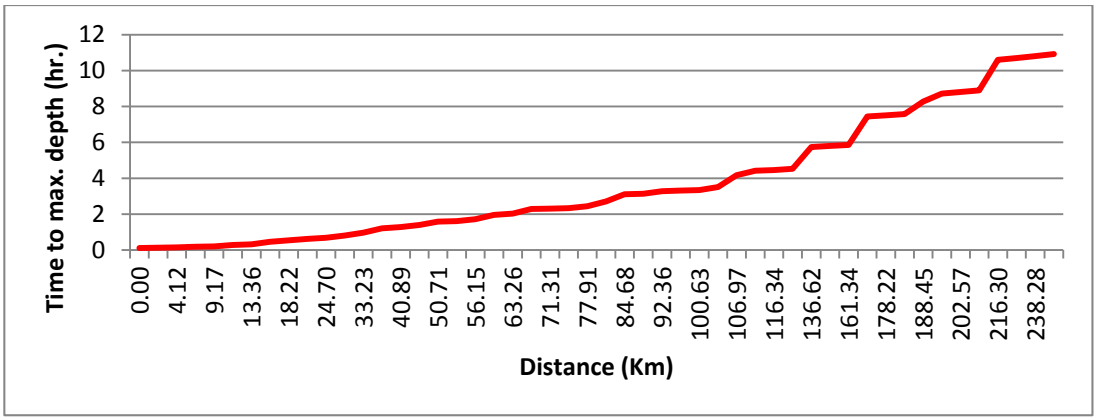

Figure A-20. Time curve to reach maximum depth of the flood wave along the Lesser Zab River for the 5th scenario

6th scenario: V= 3000MCM, AS=18000 ha

Table A-6. 6th scenario results of dam break

RVR KM FROM DAM	MAX. FLOW (CMS)	MAX. ELEV. (M-MSL)	MAX. DEPTH (M)	TIME (HR) AT MAX.DEPTH
0	297008.6	453.639	57.073	0.1
1.609	290759.1	433.465	38.776	0.12
4.119	290505.4	418.197	23.539	0.15
6.421	290160.5	416.426	21.799	0.17
9.173	276876.7	416.426	21.829	0.19
11.603	274107.9	416.426	24.667	0.28
13.357	271366.8	416.426	24.697	0.3
15.996	262118.5	416.426	28.117	0.46
18.217	259497.3	416.426	34.561	0.55
21.195	251034.7	400.299	18.464	0.63
24.703	248524.4	394.426	27.401	0.69
28.791	246039.2	382.533	15.538	0.83
33.232	243578.8	382.533	18.583	0.99
37.578	241143	377.455	21.954	1.24
40.893	238731.5	377.013	21.543	1.32
45.528	236344.2	377.013	23.814	1.43
50.710	233980.8	369.167	21.668	1.62
53.478	231641	368.869	24.676	1.65
56.149	229324.6	368.869	25.283	1.77
59.642	227031.4	362.456	25.033	2
63.263	224761	357.198	24.697	2.08
68.413	222513.4	350.867	26.368	2.36

Table A-6 continued

71.309	220288.3	349.309	27.191	2.38
74.753	218085.4	343.783	24.777	2.41
77.908	215904.6	343.783	26.160	2.51
82.301	213745.5	335.100	30.278	2.79
84.683	211608.1	325.776	20.985	3.2
88.320	209492	325.648	20.887	3.24
92.360	207397.1	324.721	25.362	3.38
95.482	205323.1	314.538	21.040	3.42
100.632	203269.9	310.310	32.628	3.45
103.528	201237.2	301.456	23.804	3.61
106.972	199224.8	295.506	17.885	4.3
110.175	197232.6	295.506	19.135	4.56
116.339	195260.2	282.308	18.681	4.6
125.882	193307.6	279.635	27.136	4.68
136.616	191374.6	259.058	18.559	5.88
148.171	189460.8	248.488	22.030	5.94
161.336	187566.2	239.902	24.402	6
172.473	185690.6	217.526	20.031	7.72
178.218	183833.7	215.234	17.769	7.79
183.561	181995.3	213.448	20.826	7.87
188.453	180175.4	202.539	15.752	8.62
196.613	178373.6	195.730	18.230	9.08
202.567	176589.9	182.093	20.302	9.17
208.892	174824	182.093	20.333	9.27
216.295	173075.7	167.58	20.229	10.89
223.344	171345	162.293	21.531	11
238.278	169631.5	151.269	21.028	11.11
248.787	167935.2	139.793	21.756	11.22

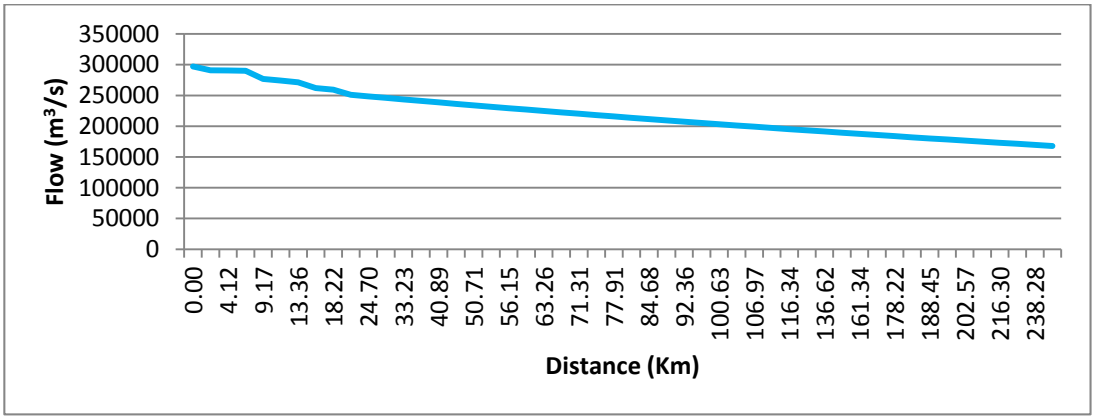

Figure A-21. Flood discharge curve from the failed dam along the Lesser Zab River for the 6th scenario

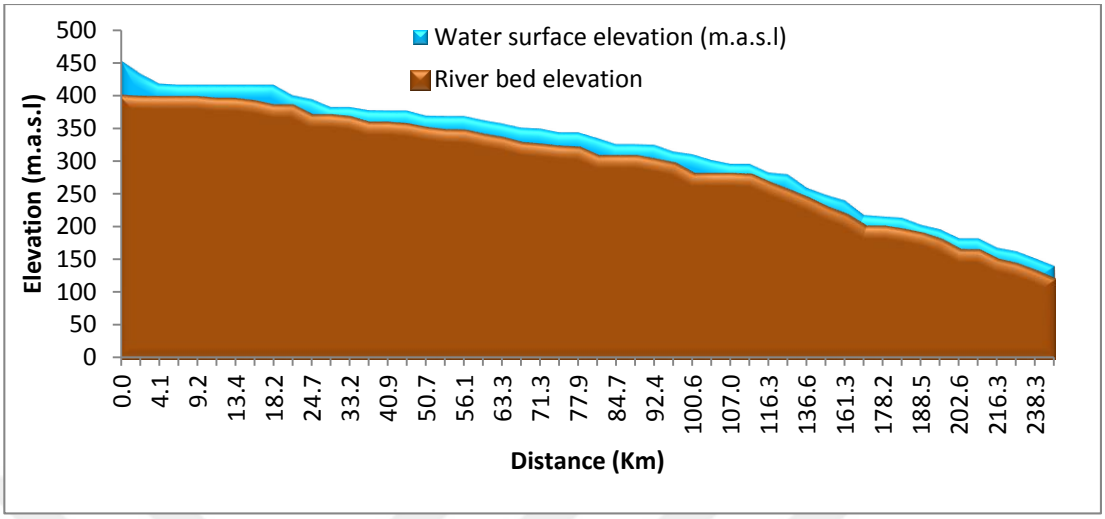

Figure A-22. Water elevation curve of the flood wave along the Lesser Zab River for the 6th scenario

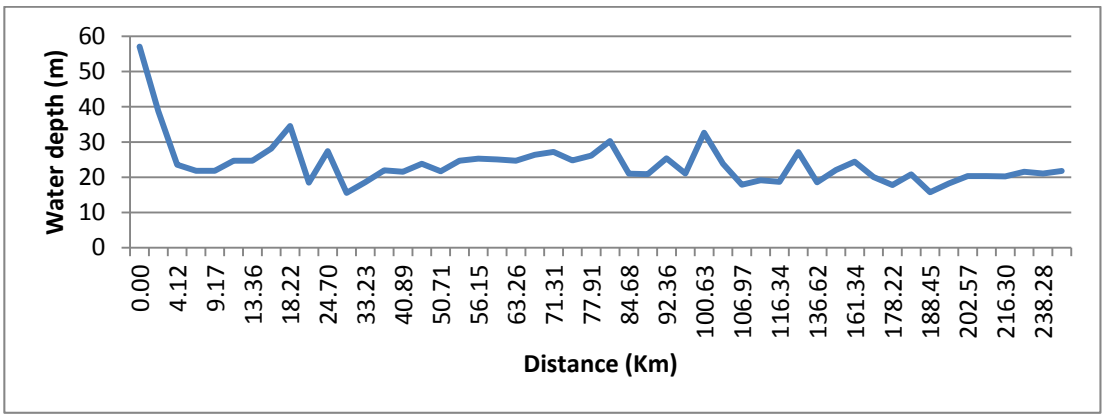

Figure A-23. Water depth curve of the flood wave along the Lesser Zab River for the 6th scenario

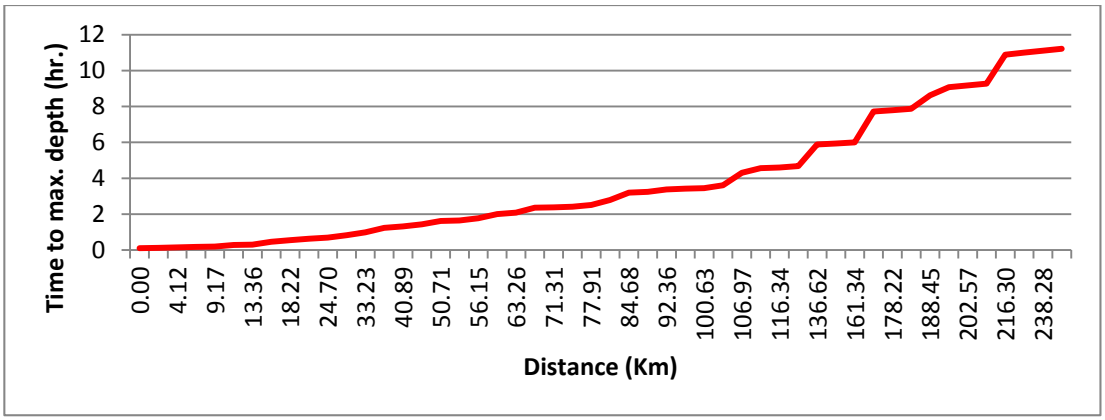

Figure A-24. Time curve to reach maximum depth of the flood wave along the Lesser Zab River for the 6th scenario

7th scenario: V= 2000MCM, AS=12600 ha

Table A-7. 7th scenario results of dam break

RVR KM FROM DAM	MAX. FLOW (CMS)	MAX. ELEV. (M-MSL)	MAX. DEPTH (M)	TIME (HR) AT MAX.DEPTH
0	269716.070	450.665	54.098	0.1
1.609	264264.709	431.813	37.124	0.12
4.119	261603.095	417.167	22.509	0.14
6.421	258987.072	415.442	20.814	0.17
9.173	247372.209	415.442	20.845	0.19
11.603	244898.477	415.442	23.682	0.28
13.357	242449.495	415.442	23.713	0.33
15.996	231732.673	415.442	27.133	0.48
18.217	229415.335	415.442	33.576	0.56
21.195	225987.581	399.672	17.836	0.64
24.703	223727.698	393.161	26.136	0.71
28.791	221490.441	382.106	15.111	0.85
33.232	219275.525	382.106	18.156	1.02
37.578	217082.782	376.610	21.110	1.26
40.893	214911.956	376.117	20.647	1.36
45.528	212762.820	376.117	22.917	1.48
50.710	210635.206	368.387	20.887	1.67
53.478	208528.857	367.951	23.759	1.7
56.149	206443.576	367.951	24.365	1.83
59.642	204379.136	361.605	24.182	2.07
63.263	202335.340	356.149	23.649	2.14
68.413	200311.988	349.919	25.420	2.47

Table A-7 continued

71.309	198308.882	348.416	26.298	2.49
74.753	196325.797	342.924	23.917	2.52
77.908	194362.533	342.924	25.301	2.61
82.301	192418.921	334.255	29.434	2.92
84.683	190494.735	325.212	20.421	3.33
88.320	188589.776	325.212	20.452	3.37
92.360	186703.874	321.618	22.259	3.54
95.482	184836.831	313.706	20.208	3.57
100.632	182988.477	309.344	31.662	3.61
103.528	181158.586	300.889	23.237	3.76
106.972	179347.015	295.086	17.465	4.5
110.175	177553.54	295.086	18.714	4.78
116.339	175778.017	281.464	17.836	4.83
125.882	174020.220	278.690	26.191	4.92
136.616	172280.037	258.589	18.089	6.17
148.171	165560.392	247.418	20.961	6.23
161.336	157966.805	238.728	23.228	6.3
172.473	156387.121	216.737	19.242	8.17
178.218	155465.153	213.972	16.507	8.25
183.561	152416.901	212.076	19.455	8.33
188.453	150892.718	201.670	14.883	9.13
196.613	149383.799	194.709	17.209	9.61
202.567	147889.972	181.240	19.449	9.71
208.892	146411.068	181.240	19.479	9.81
216.295	144946.945	166.692	19.336	11.47
223.344	143497.491	161.105	20.342	11.58
238.278	142062.506	150.074	19.833	11.7
248.787	140641.878	138.595	20.558	11.82

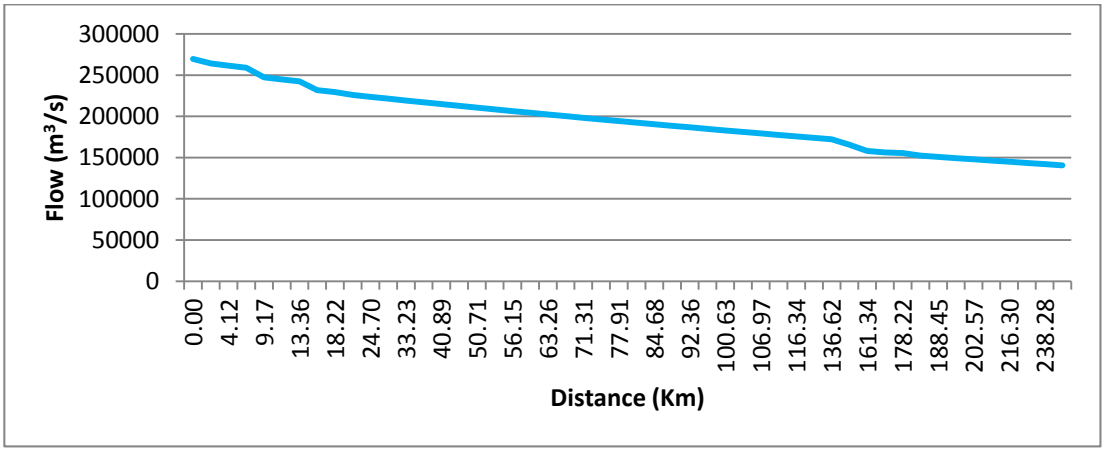

Figure A-25. Flood discharge curve from the failed dam along the Lesser Zab River for the 7th scenario

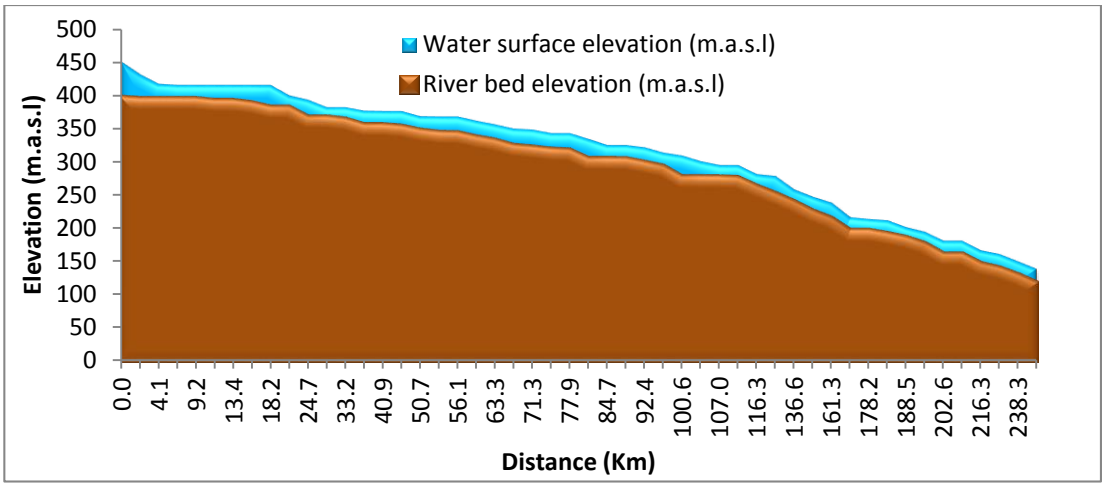

Figure A-26. Water elevation curve of the flood wave along the Lesser Zab River for the 7th scenario

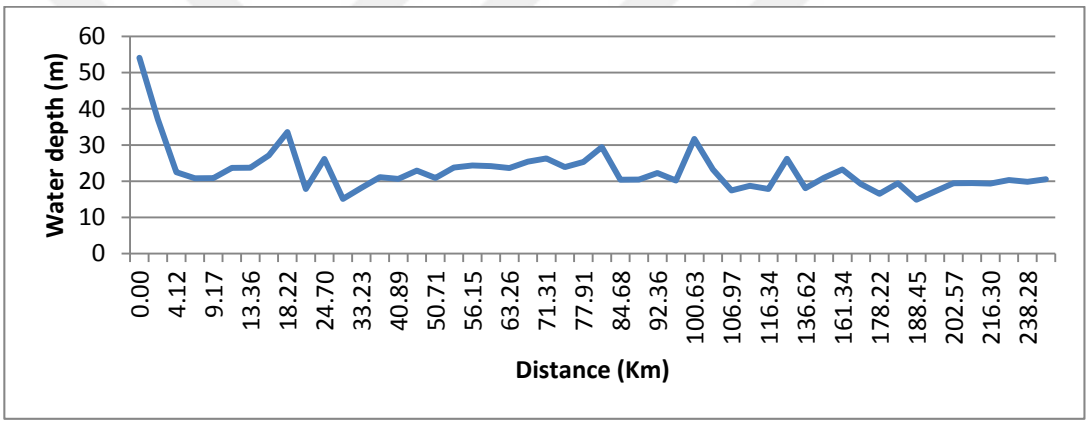

Figure A-27. Water depth curve of the flood wave along the Lesser Zab River for the 7th scenario

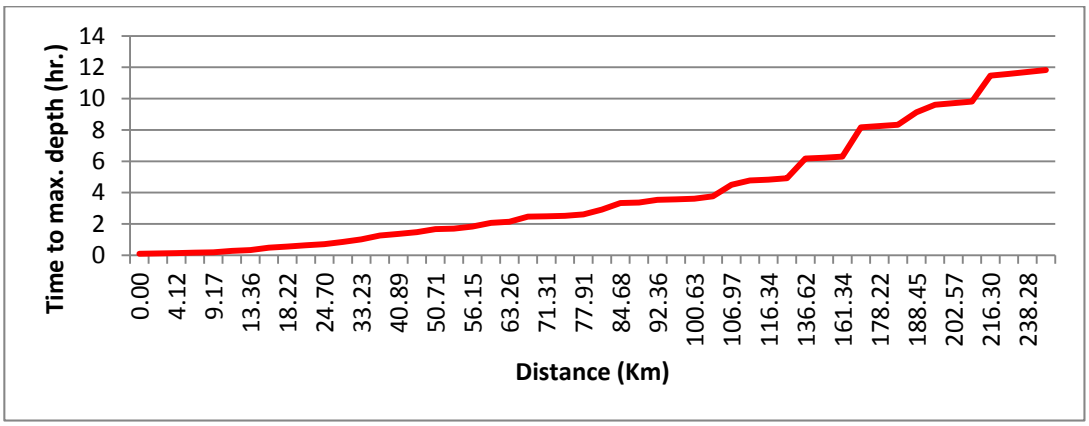

Figure A-28. Time curve to reach maximum depth of the flood wave along thezLesser Zab River for the 7th scenario

Appendix B

Figures of Extracting Cross Sections and Flood Water Elevations

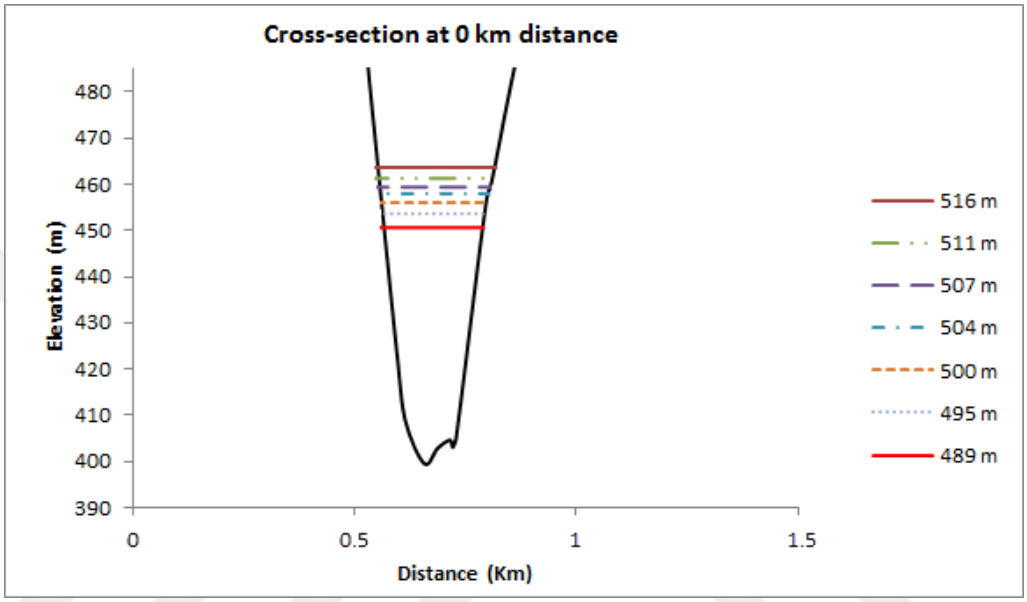

Figure B-1. Cross section number 1

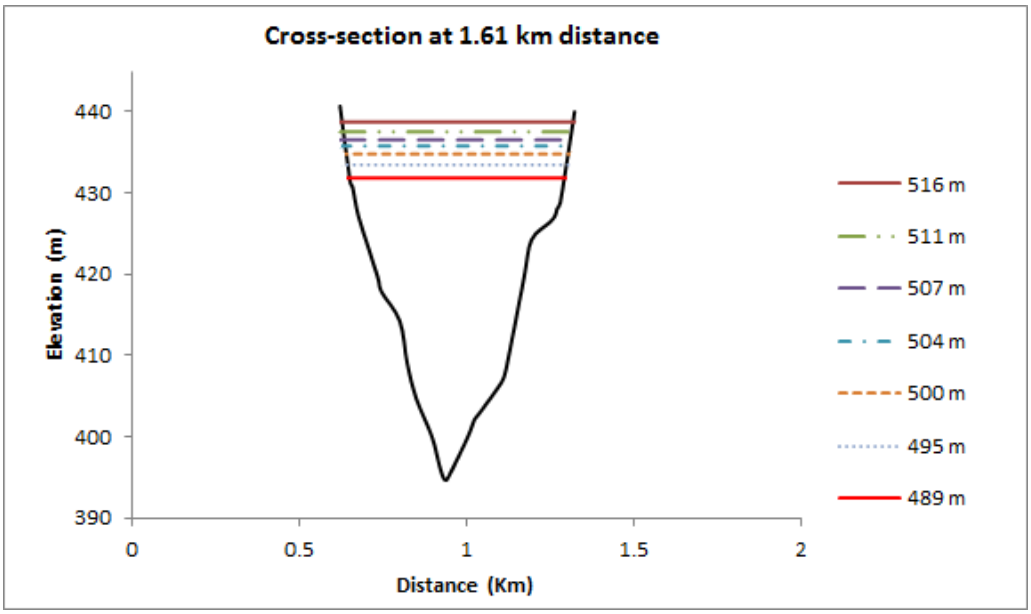

Figure B-2. Cross section number 2

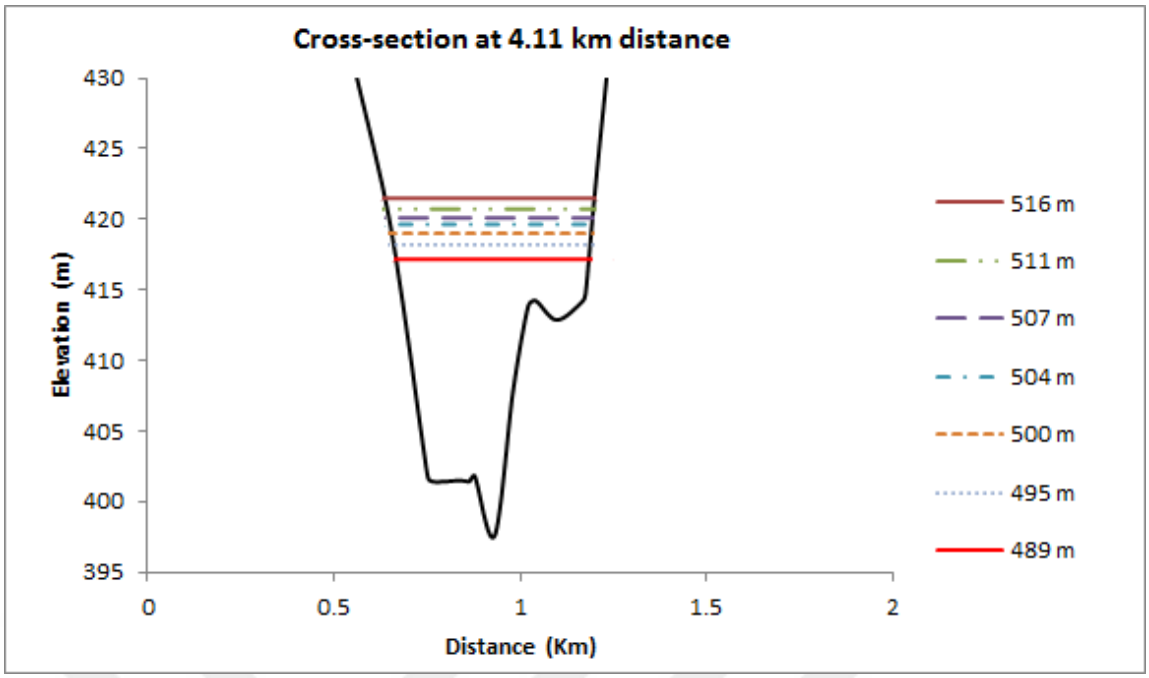

Figure B-3. Cross section number 3

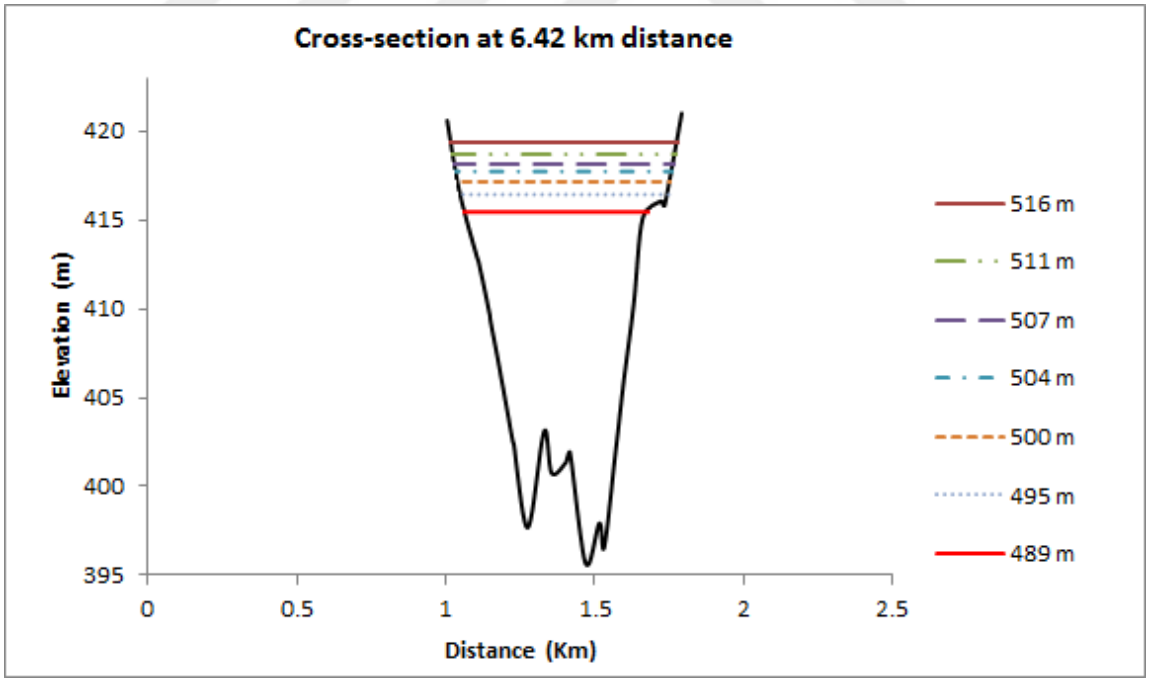

Figure B-4. Cross section number 4

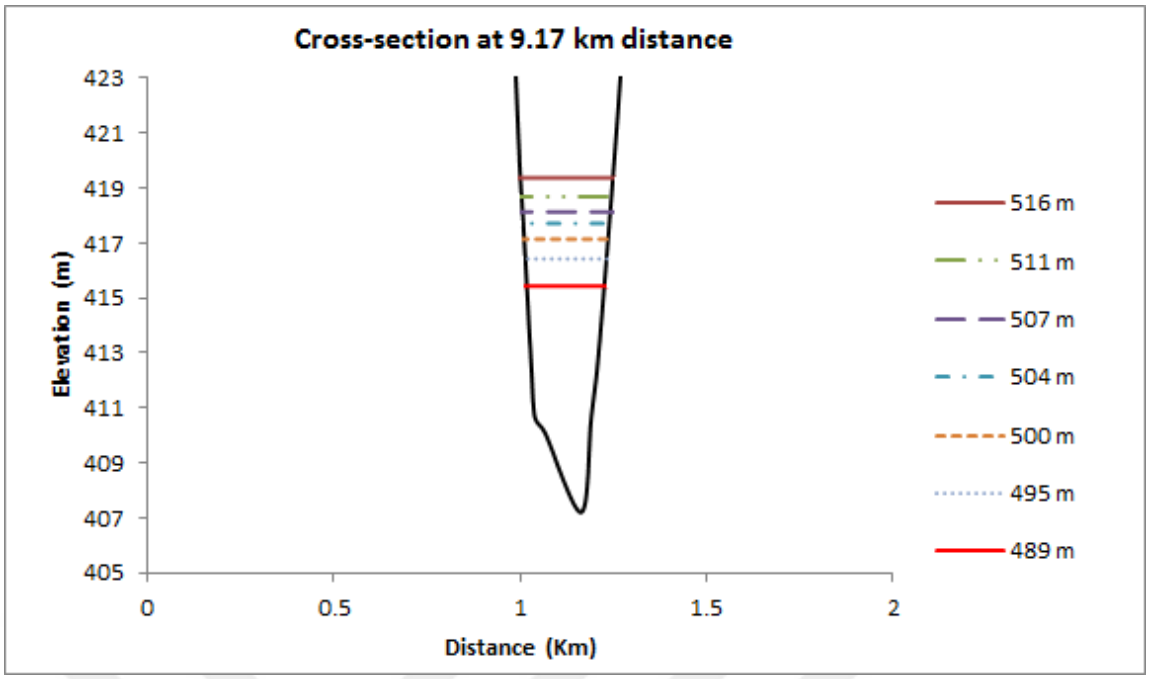

Figure B-5. Cross section number 5

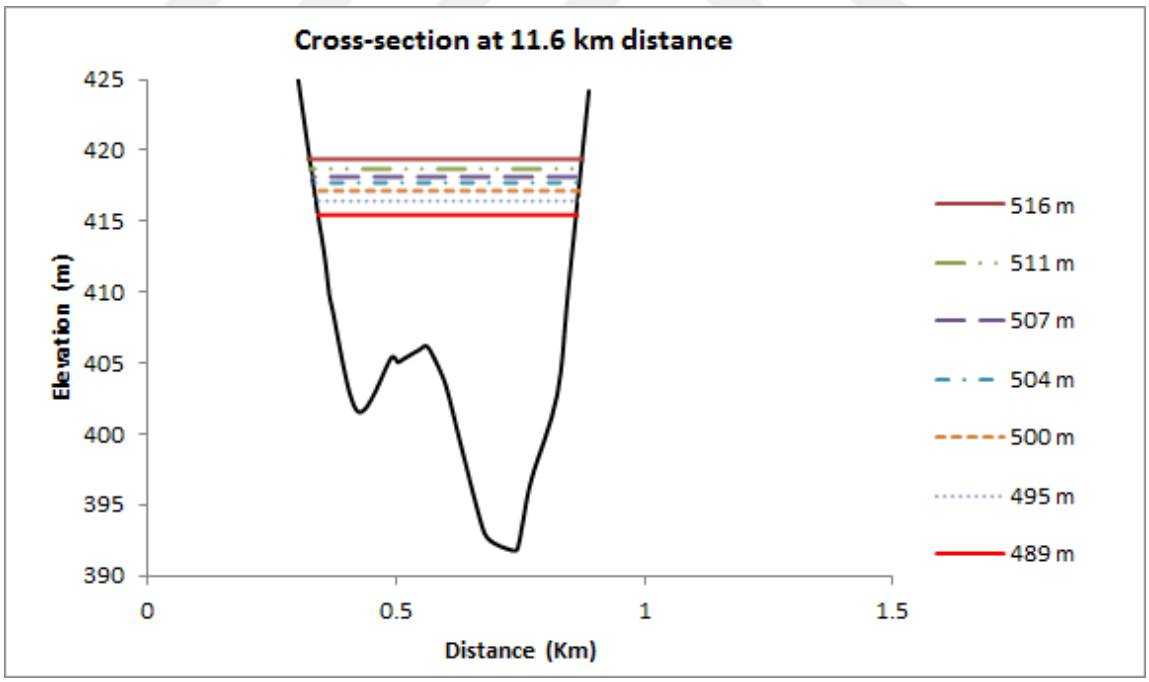

Figure B-6. Cross section number 6

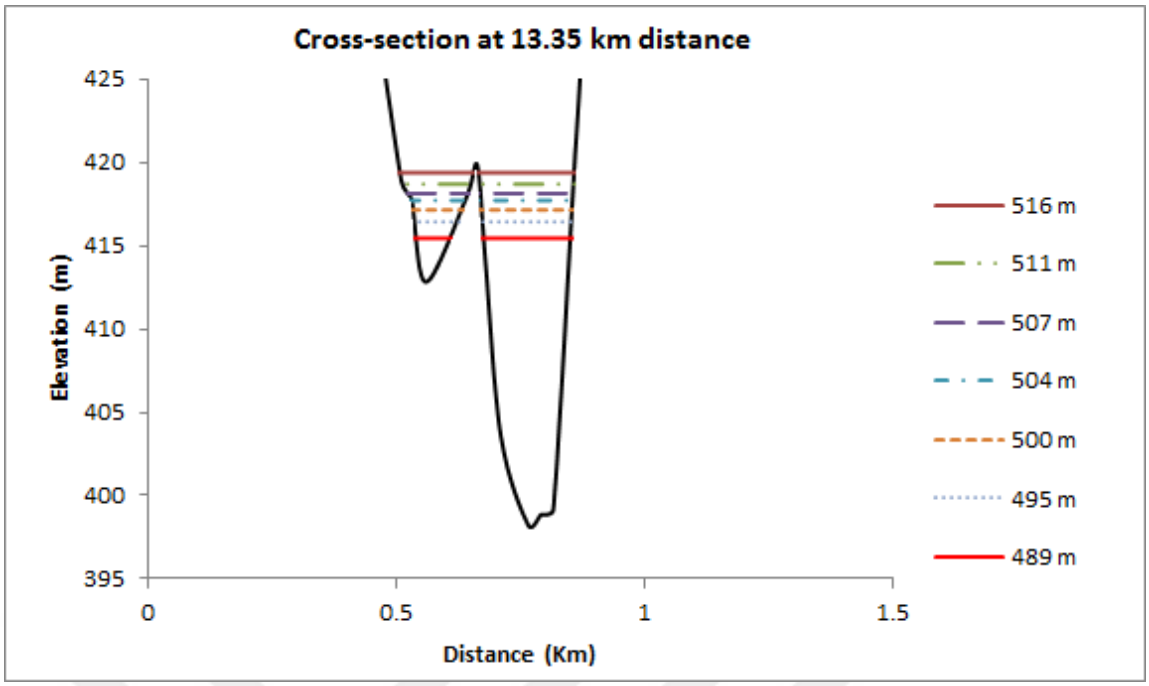

Figure B-7: Cross section number 7

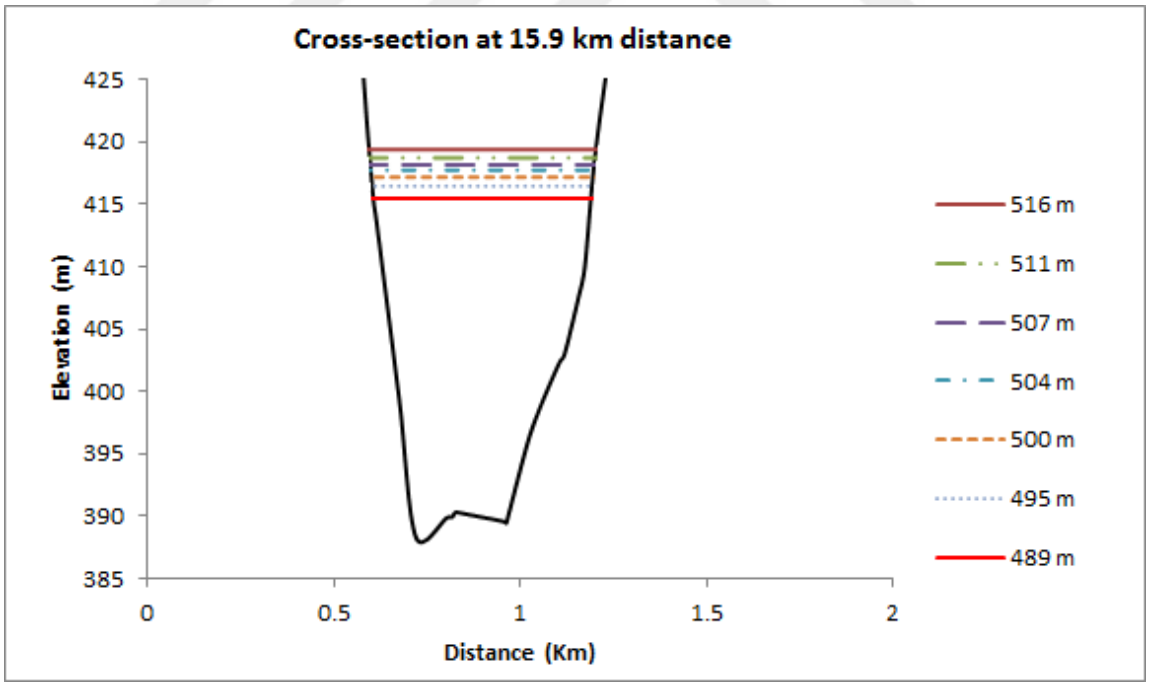

Figure B-8. Cross section number 8

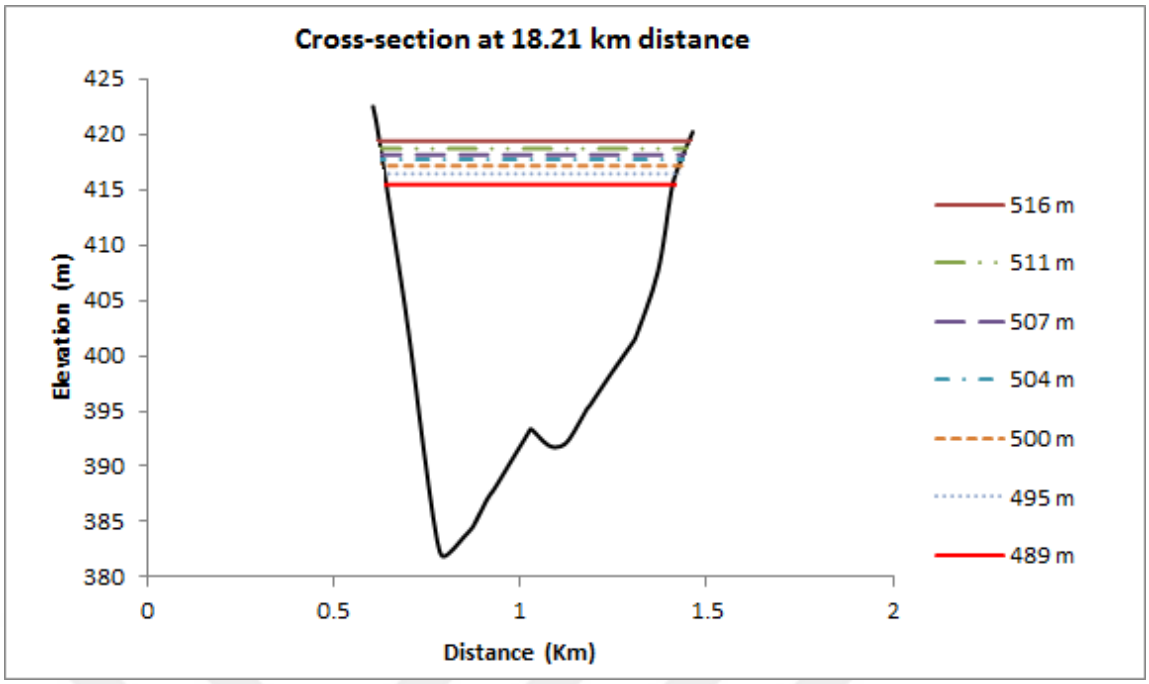

Figure B-9. Cross section number 9

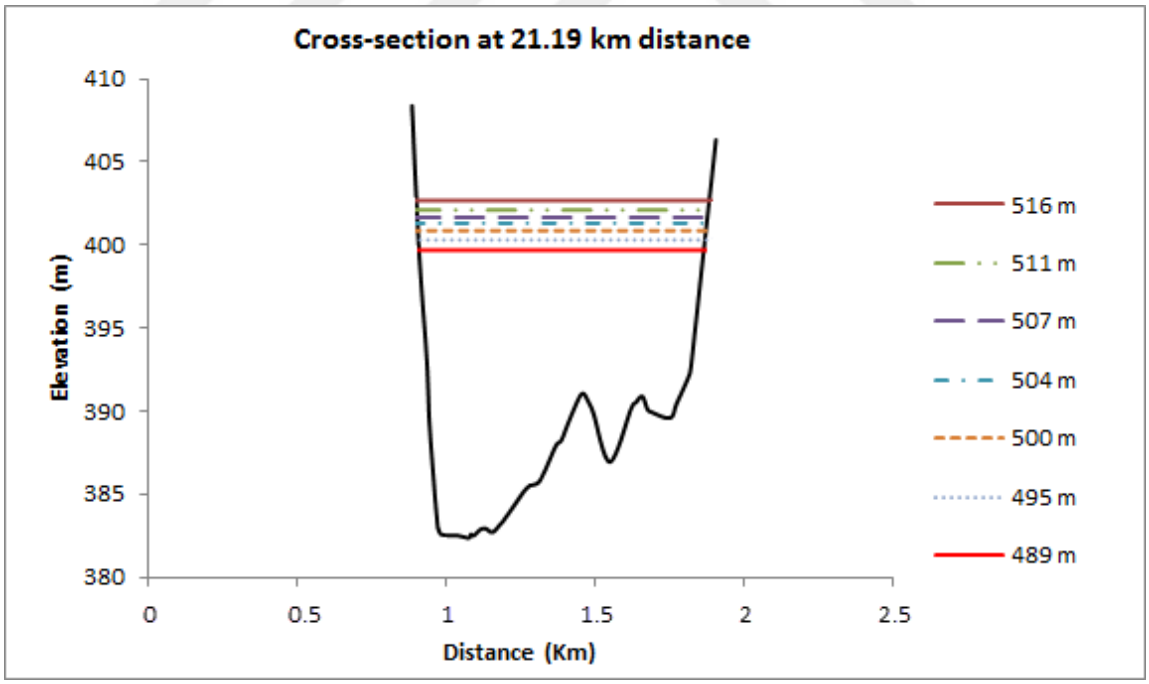

Figure B-10. Cross section number 10

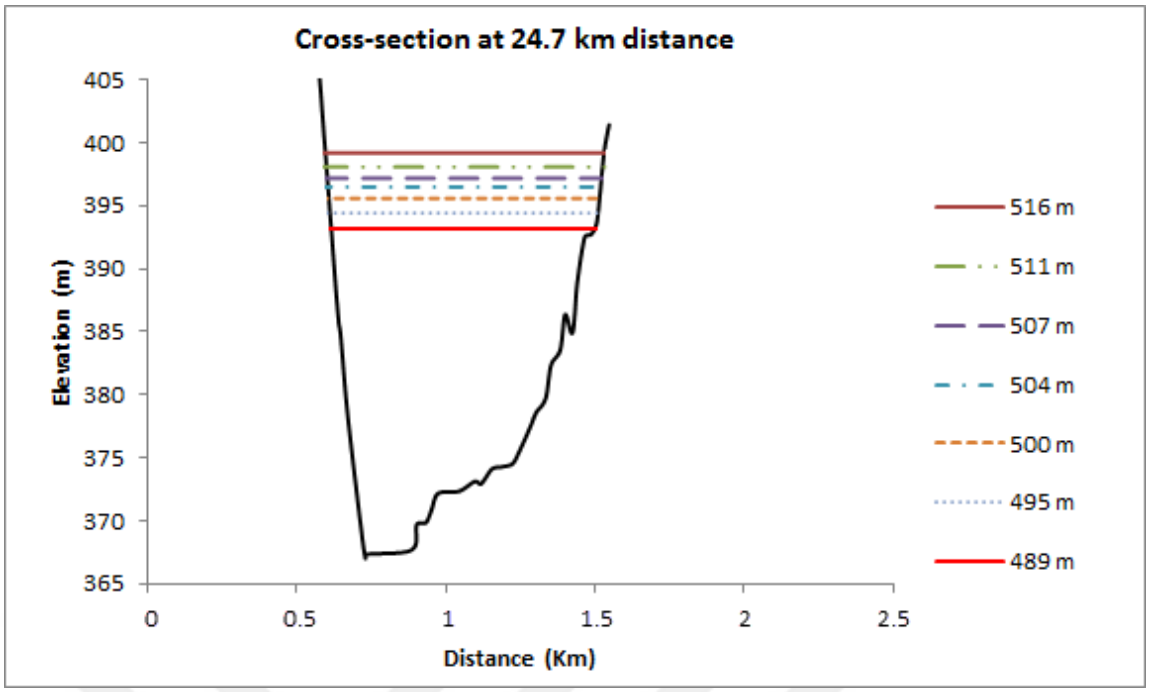

Figure B-11. Cross section number 11

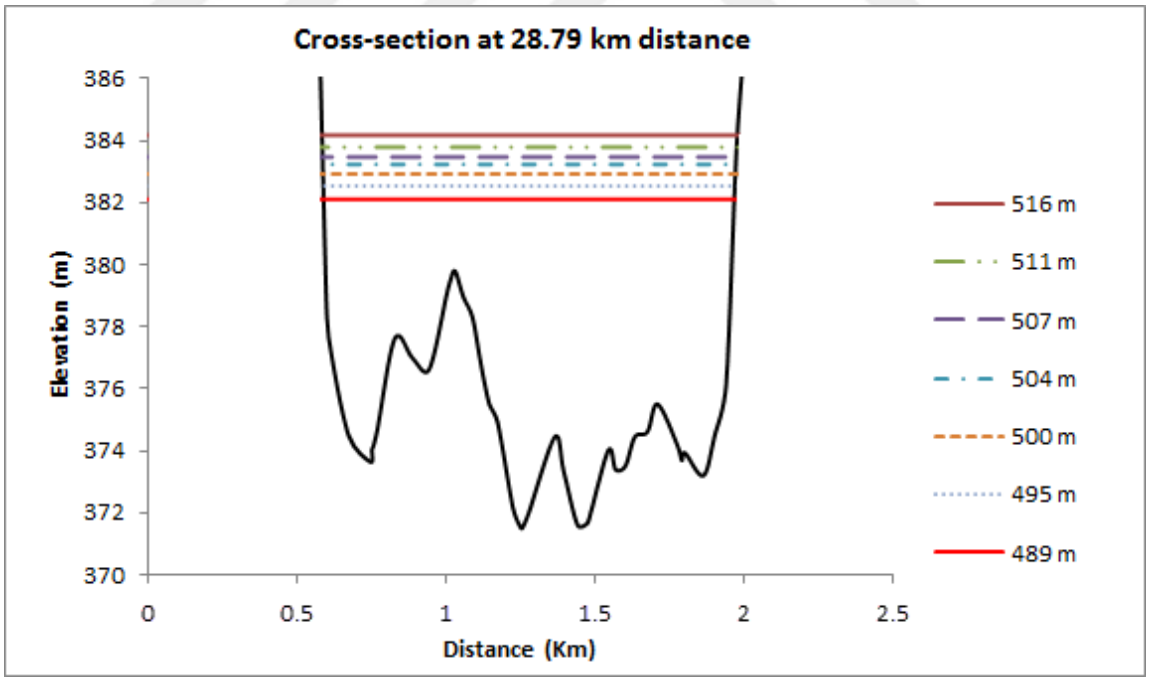

Figure B-12. Cross section number 12

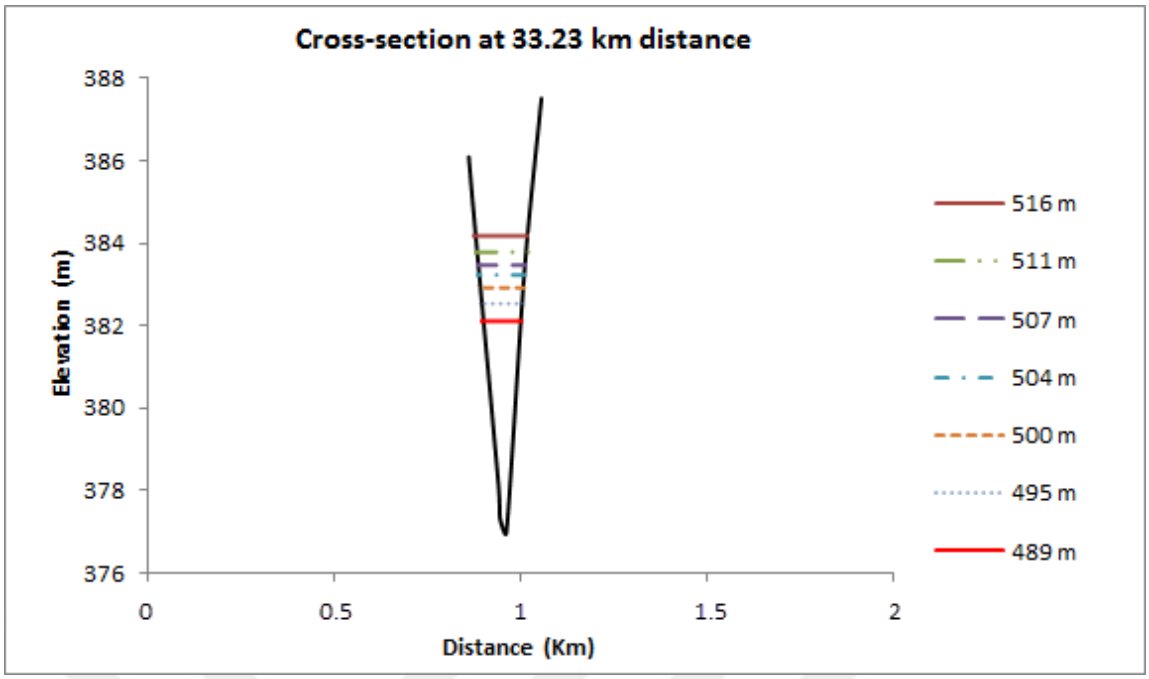

Figure B-13. Cross section number 13

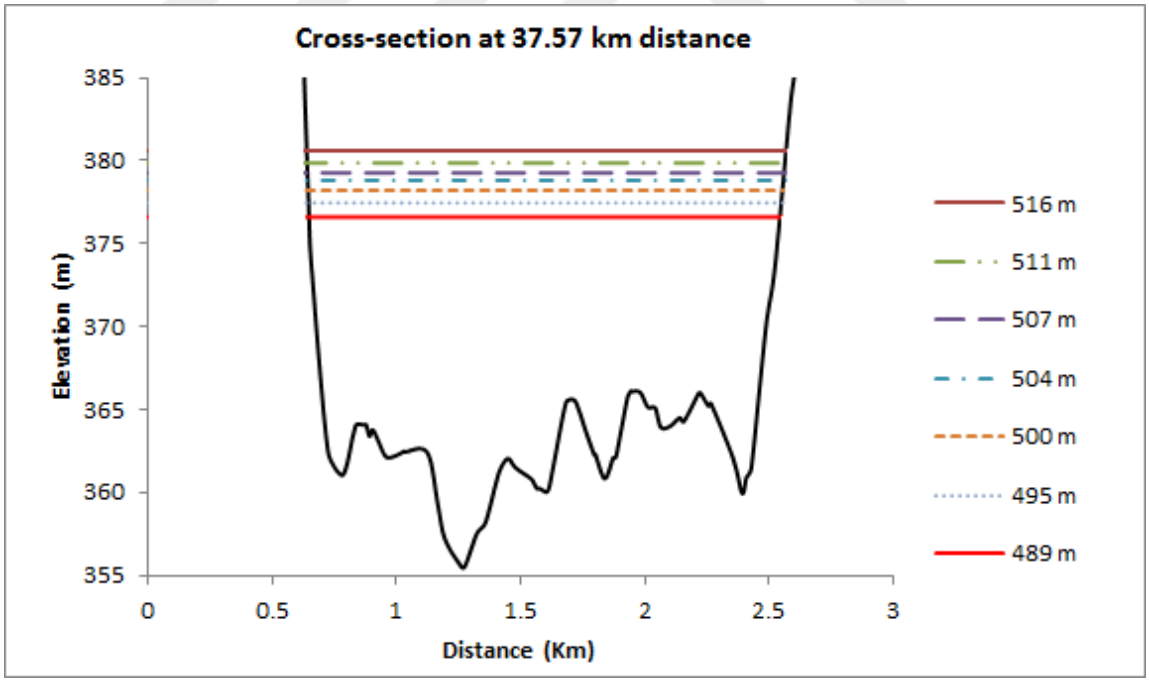

Figure B-14. Cross section number 14

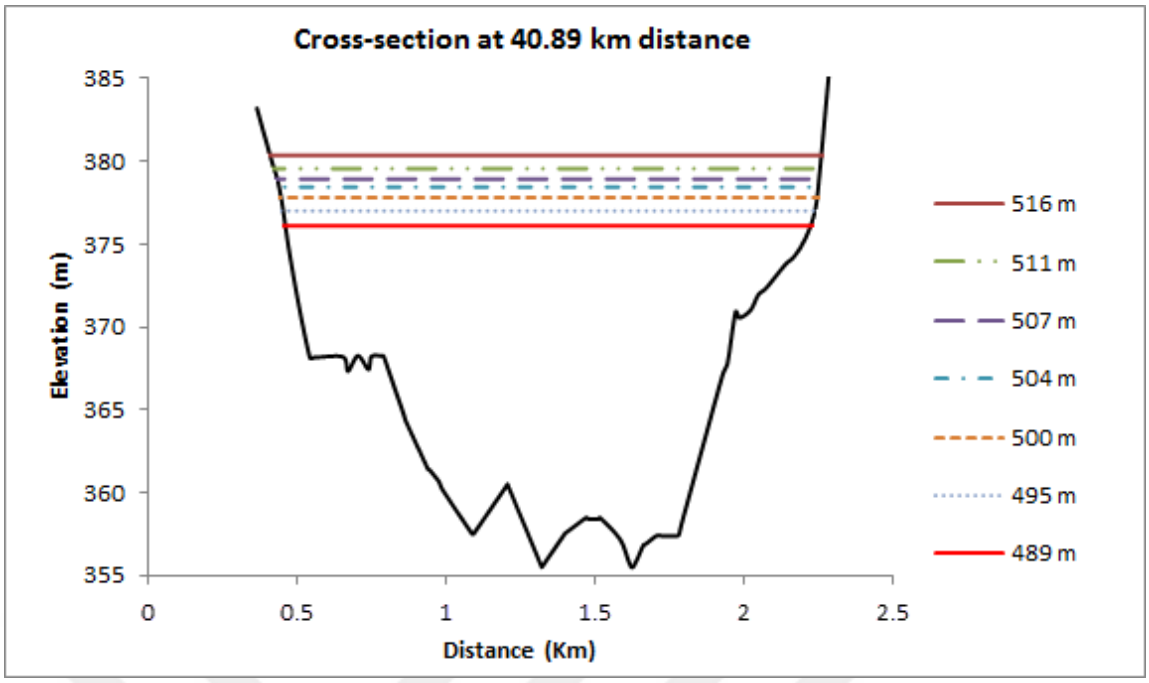

Figure B-15. Cross section number 15

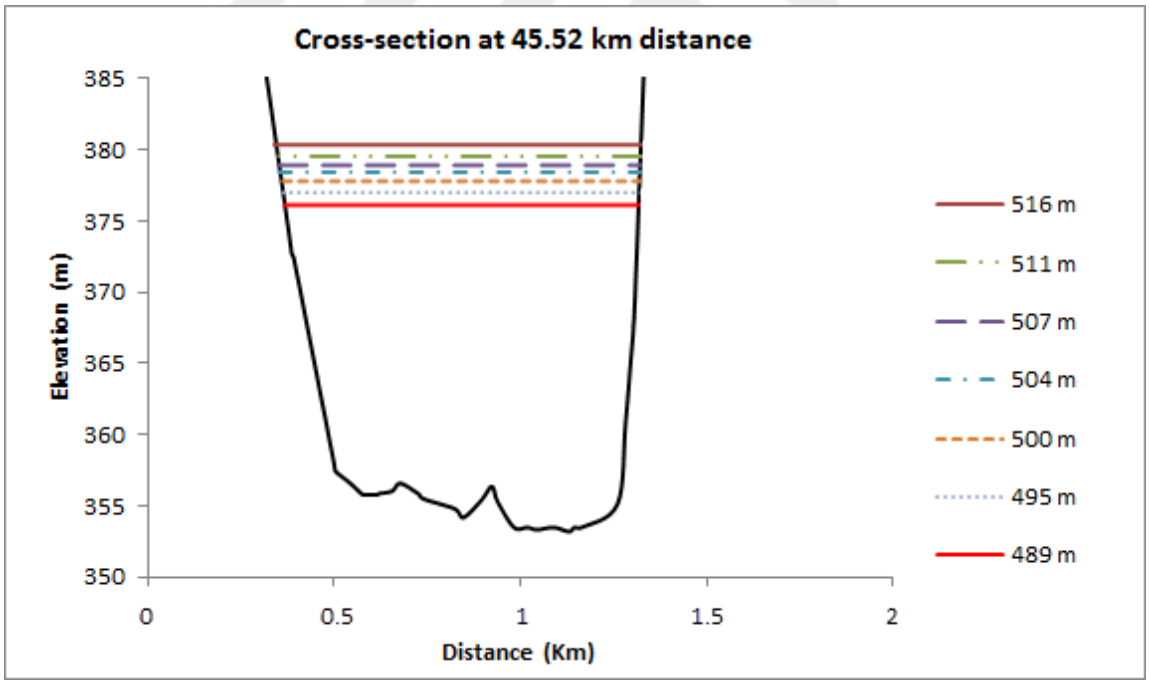

Figure B-16. Cross section number 16

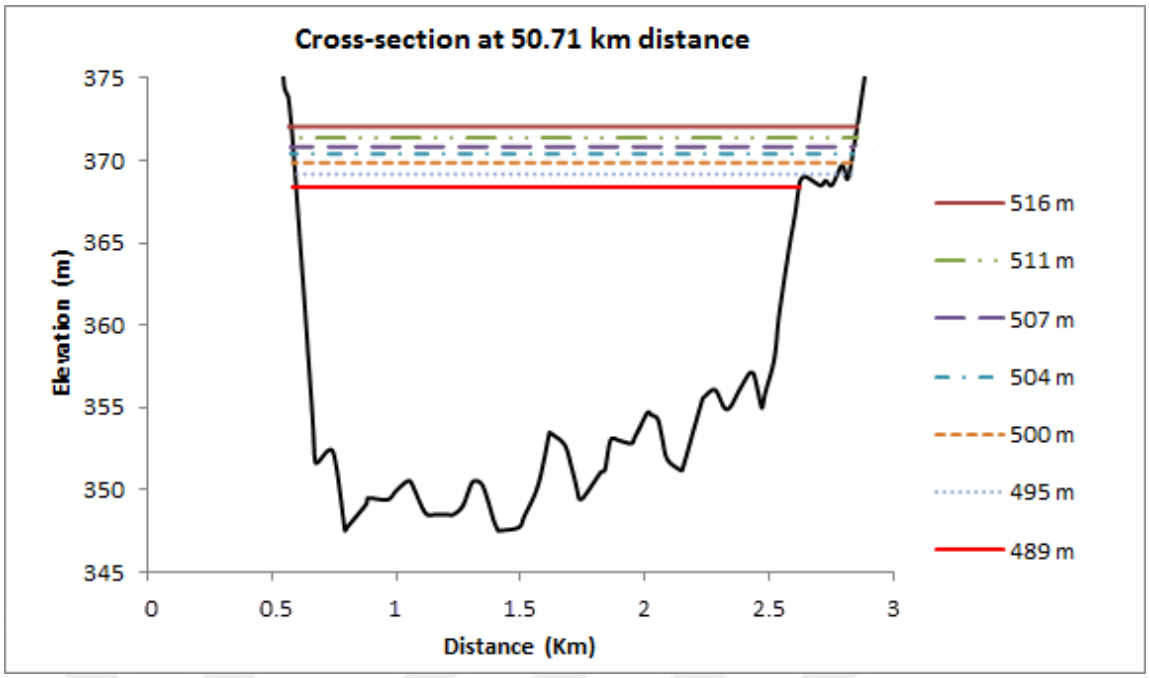

Figure B-17. Cross section number 17

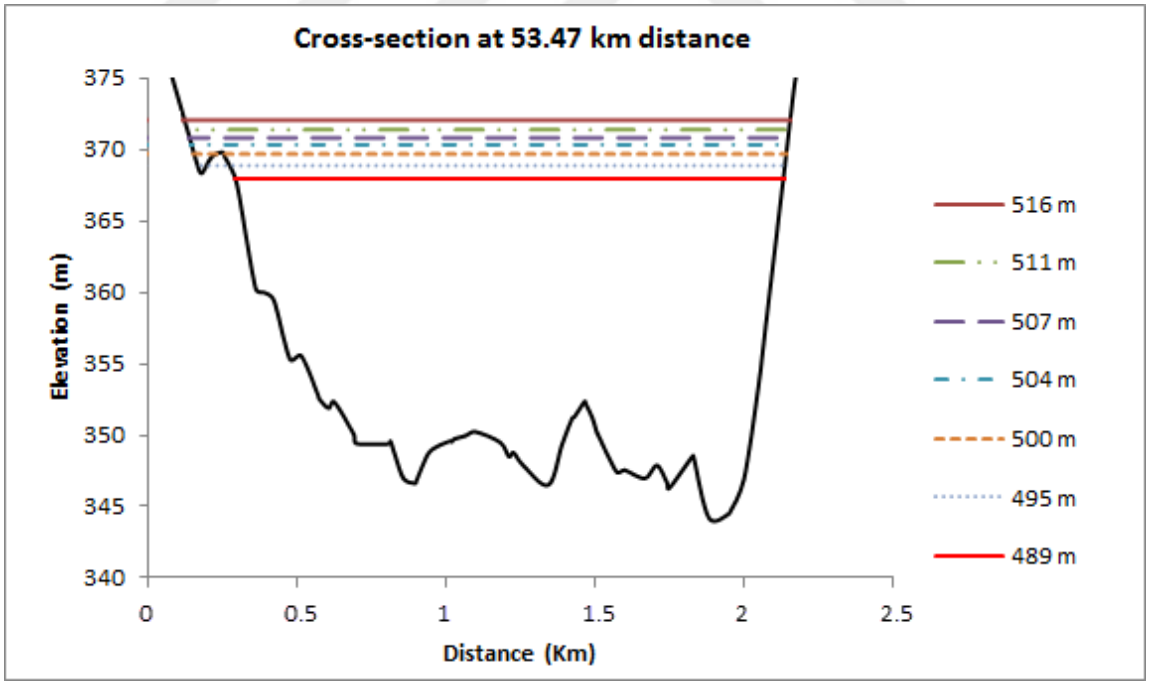

Figure B-18. Cross section number 18

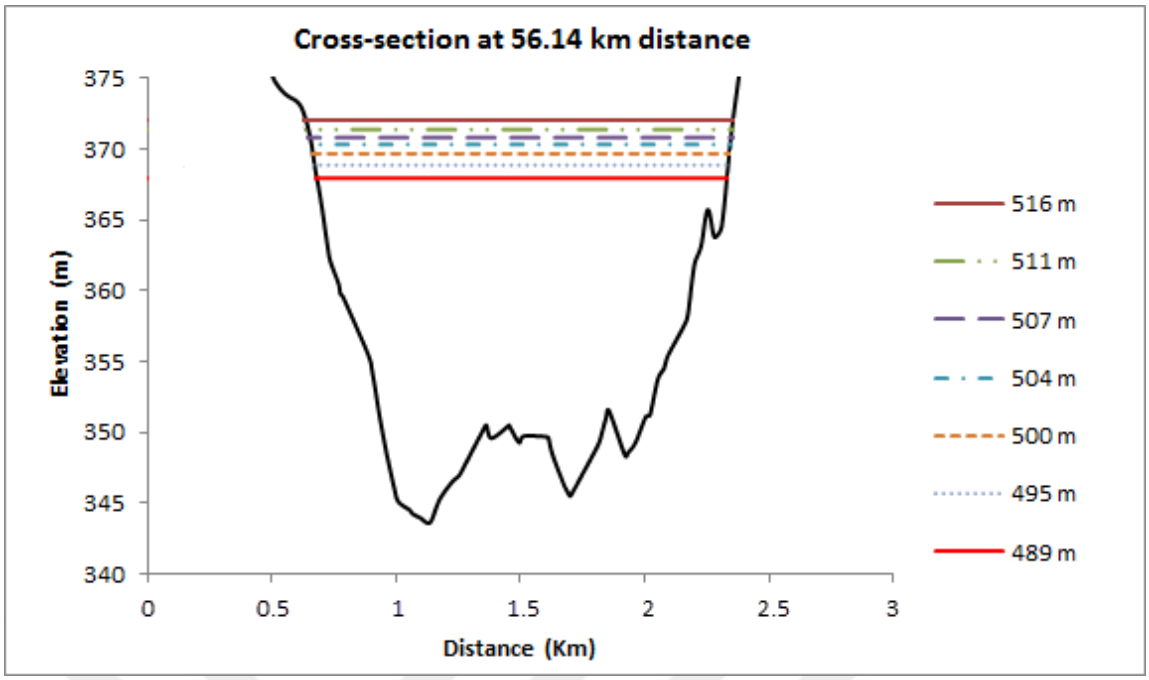

Figure B-19. Cross section number 19

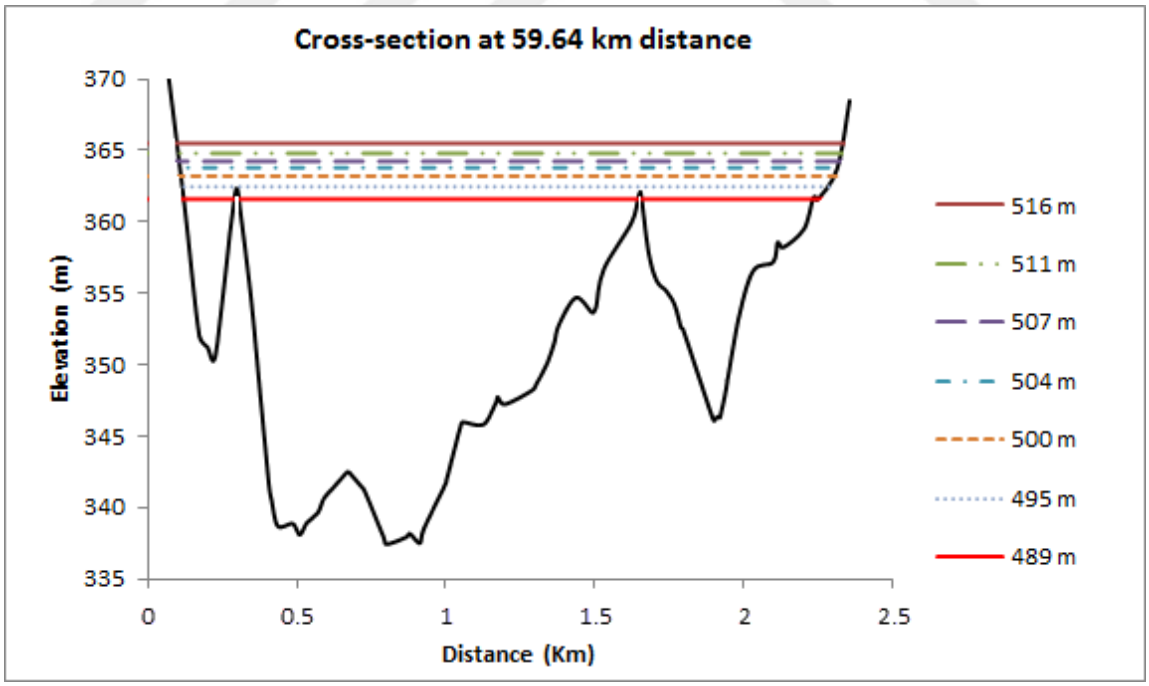

Figure B-20. Cross section number 20

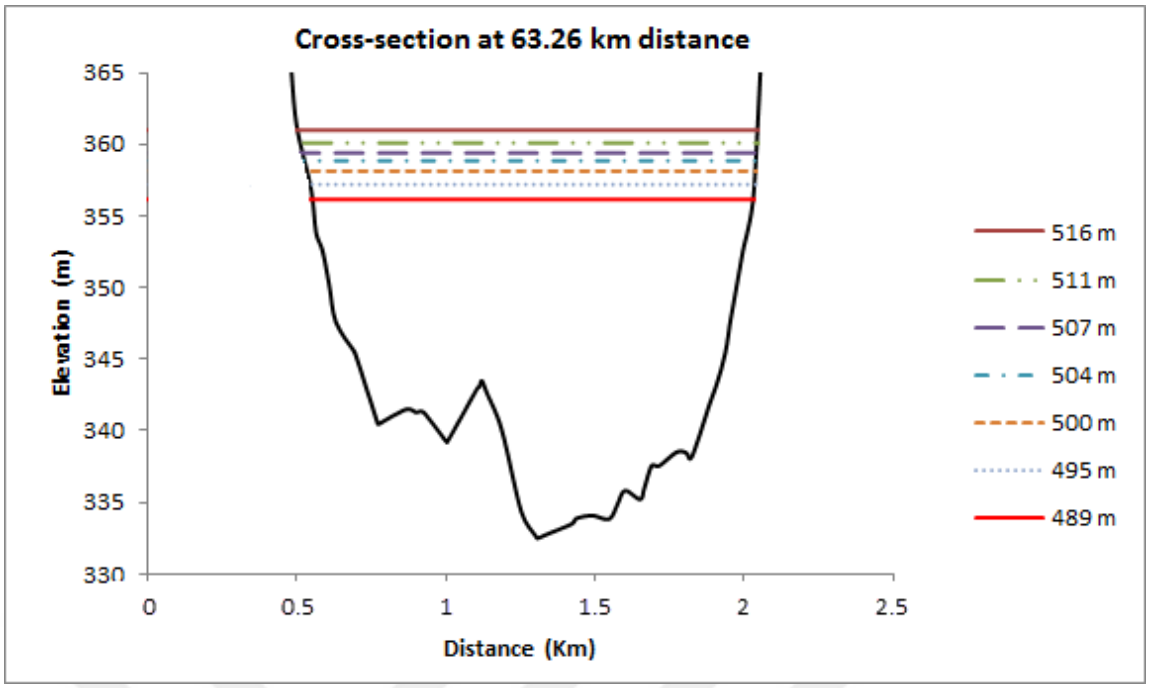

Figure B-21. Cross section number 21

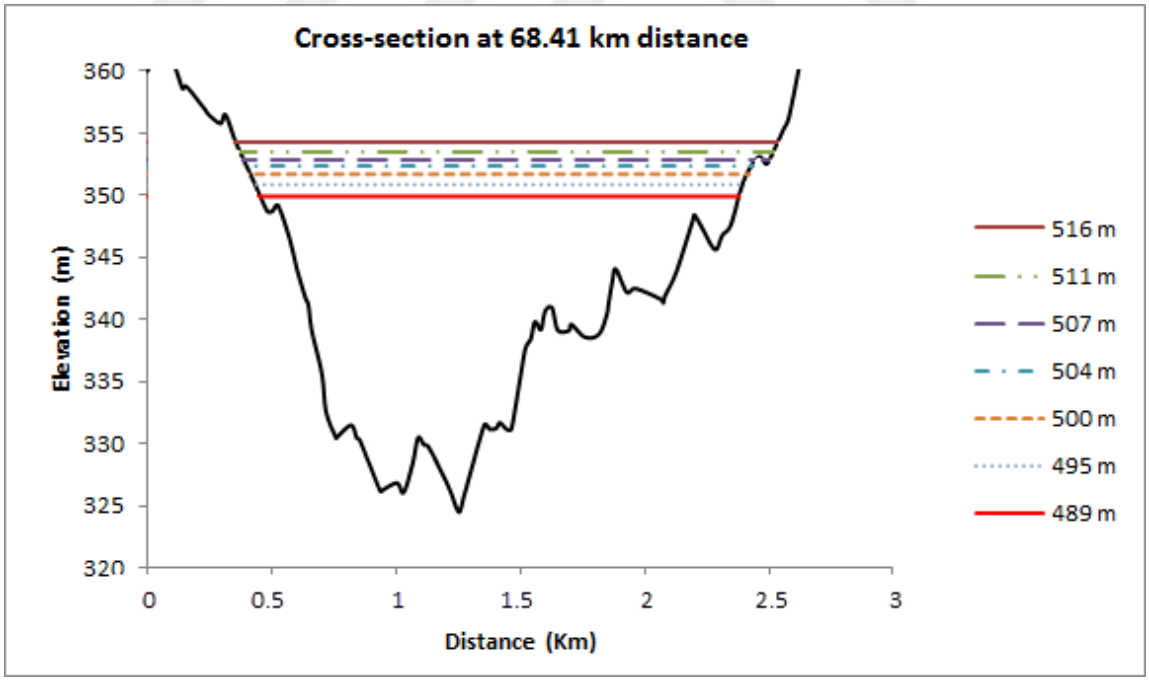

Figure B-22. Cross section number 22

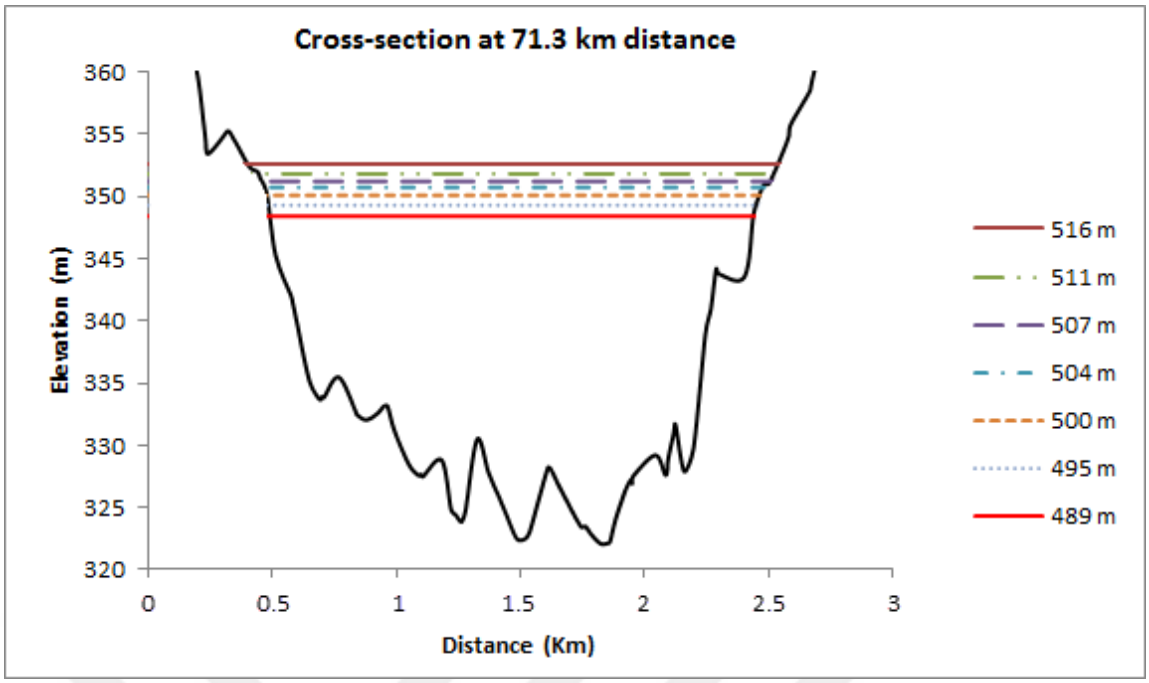

Figure B-23. Cross section number 23

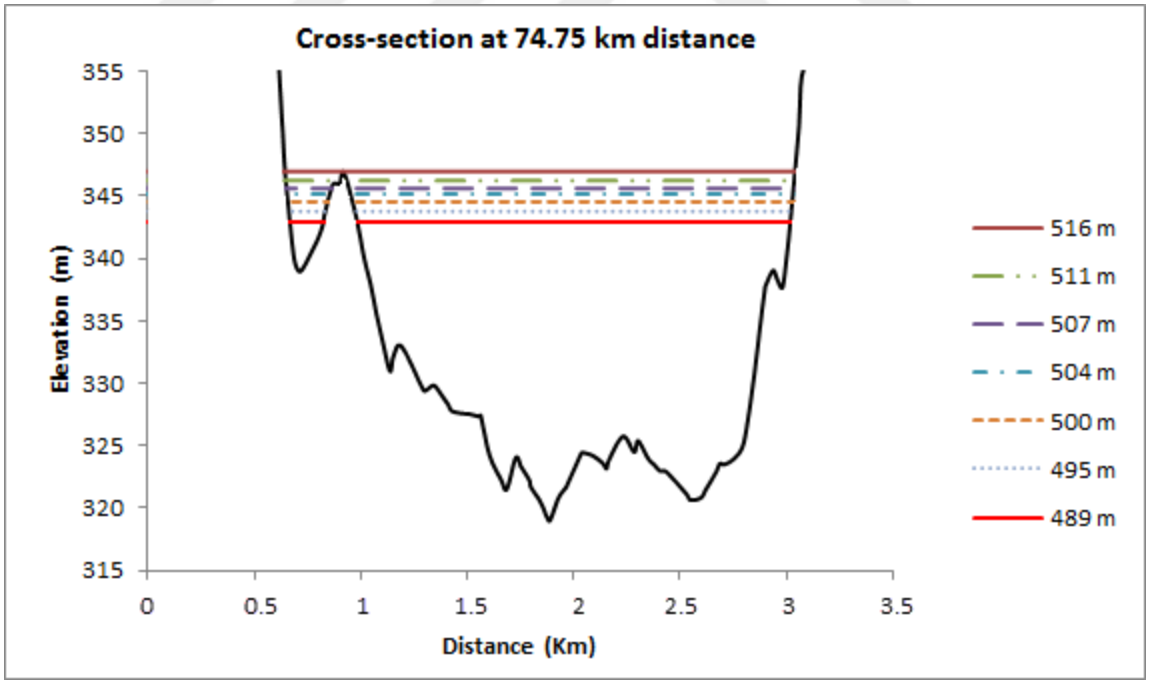

Figure B-24. Cross section number 24

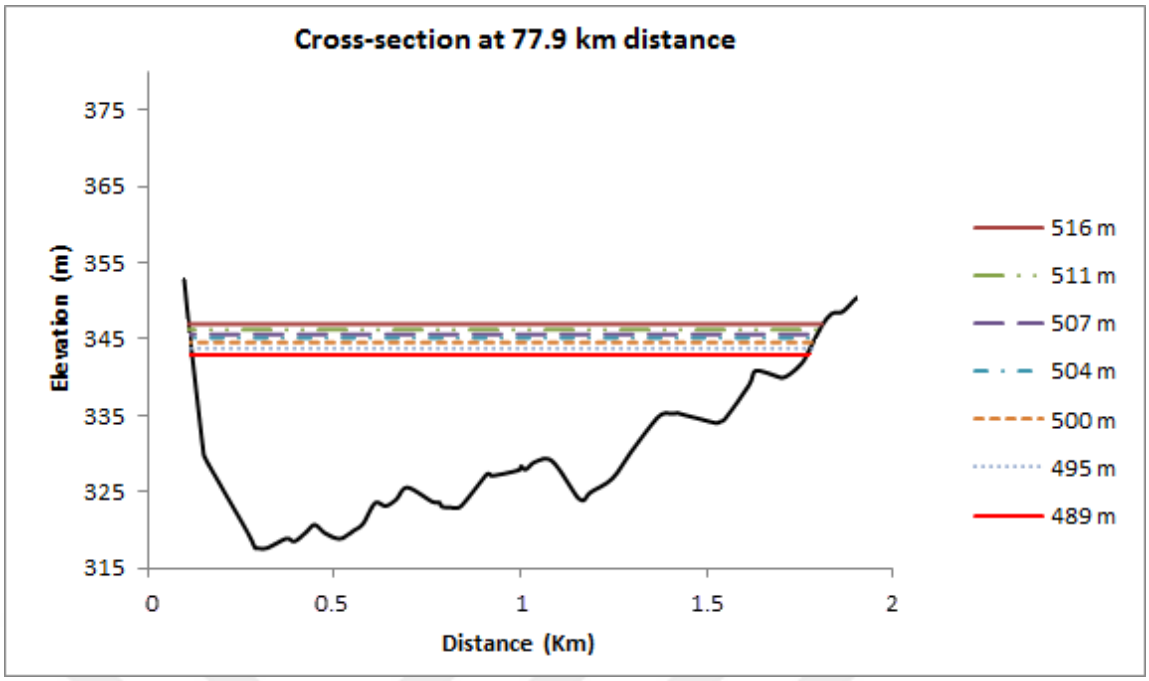

Figure B-25. Cross section number 25

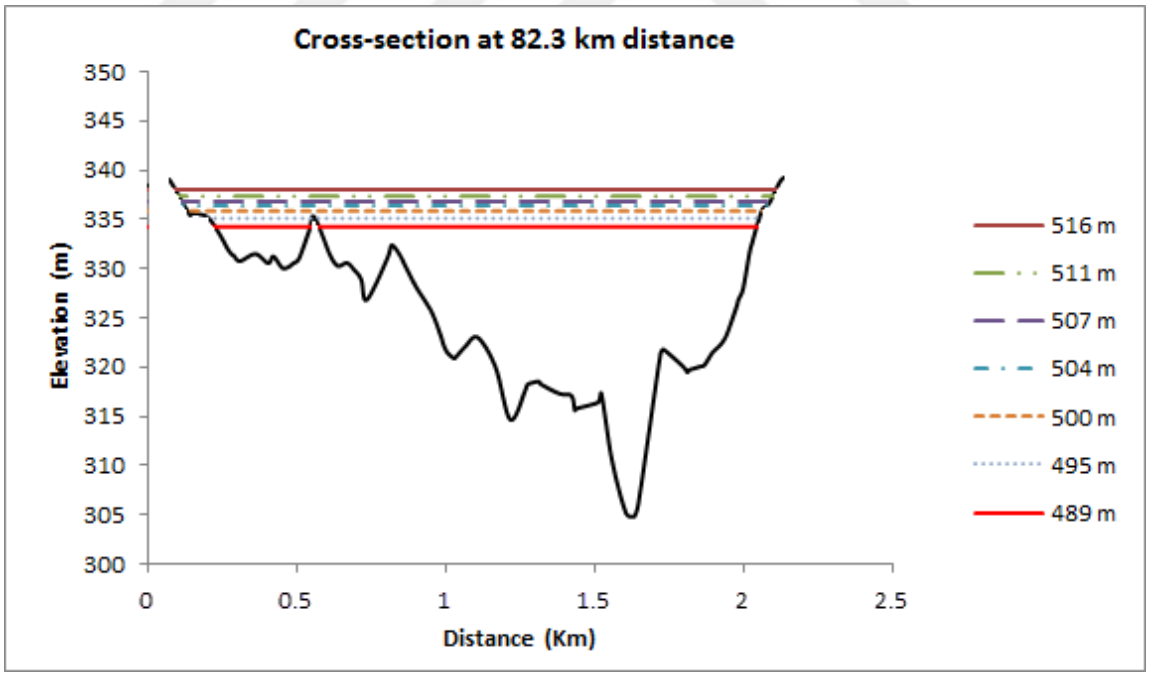

Figure B-26. Cross section number 26

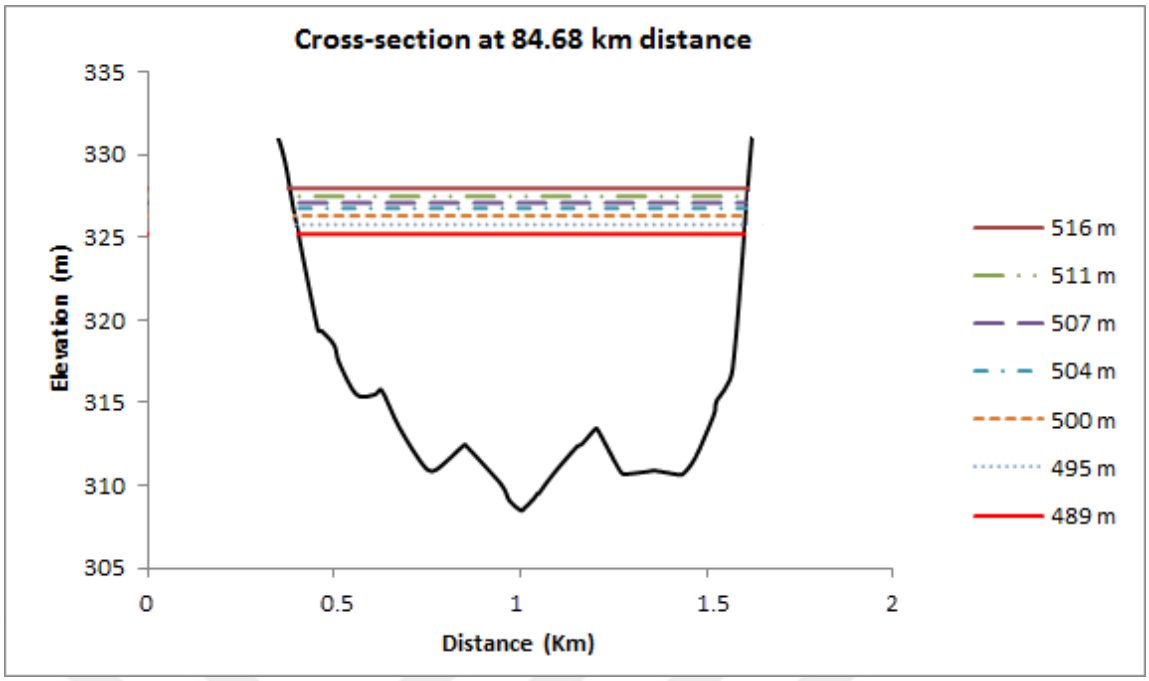

Figure B-27. Cross section number 27

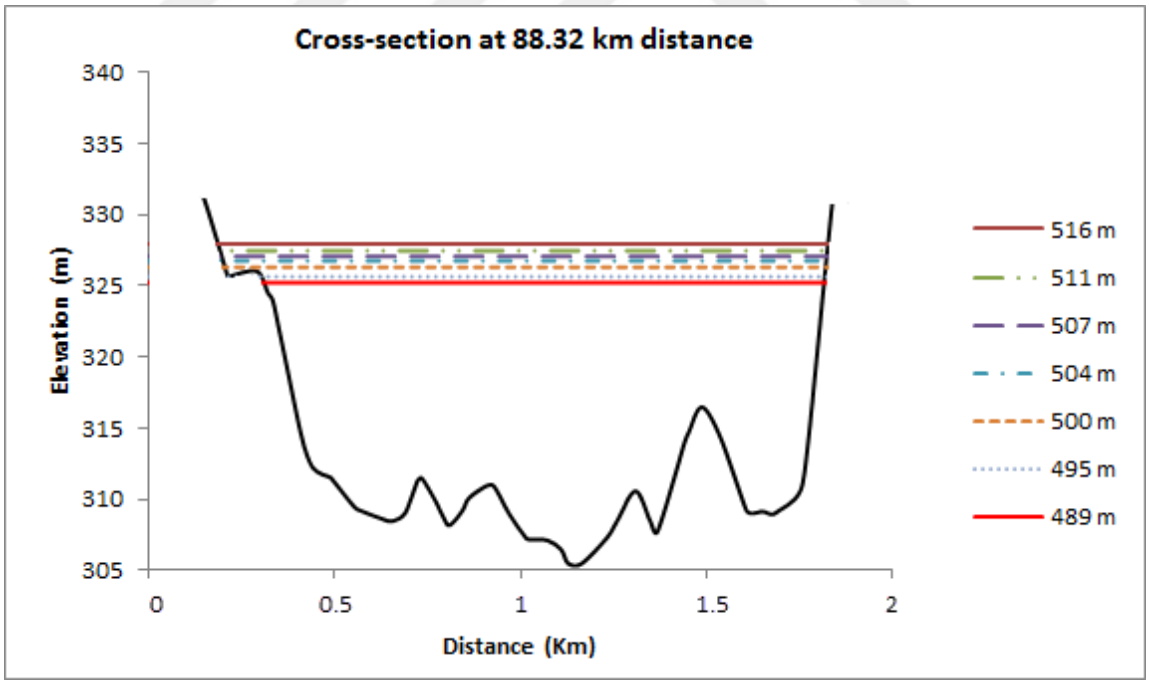

Figure B-28. Cross section number 28

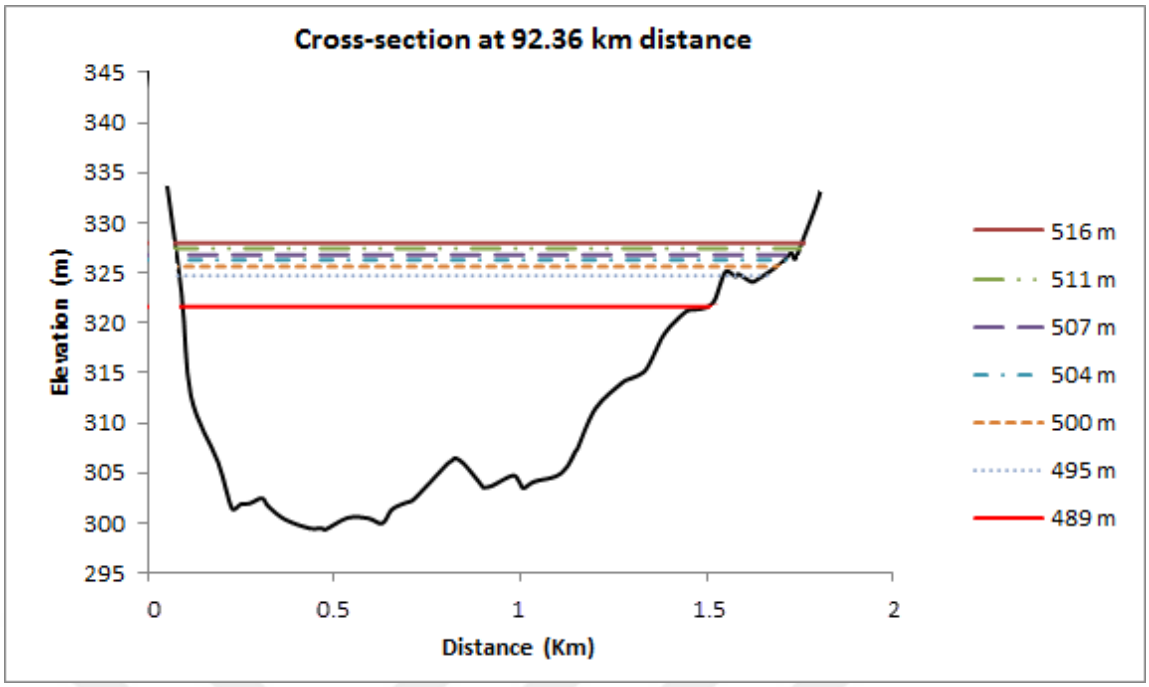

Figure B-29. Cross section number 29

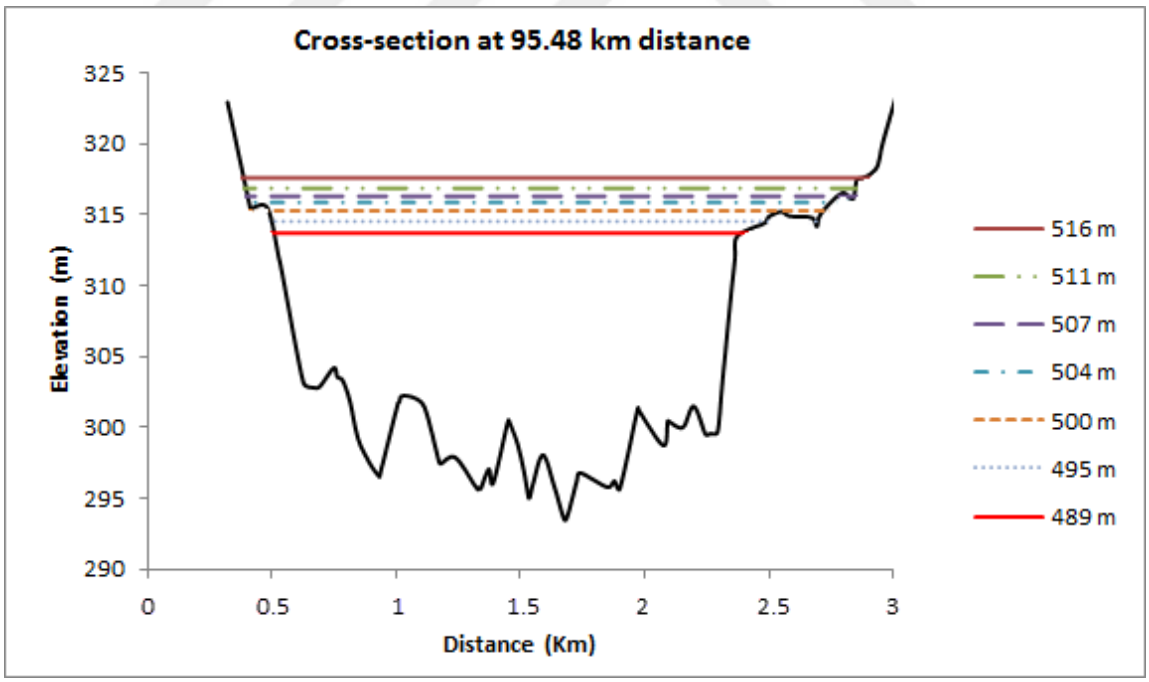

Figure B-30. Cross section number 30

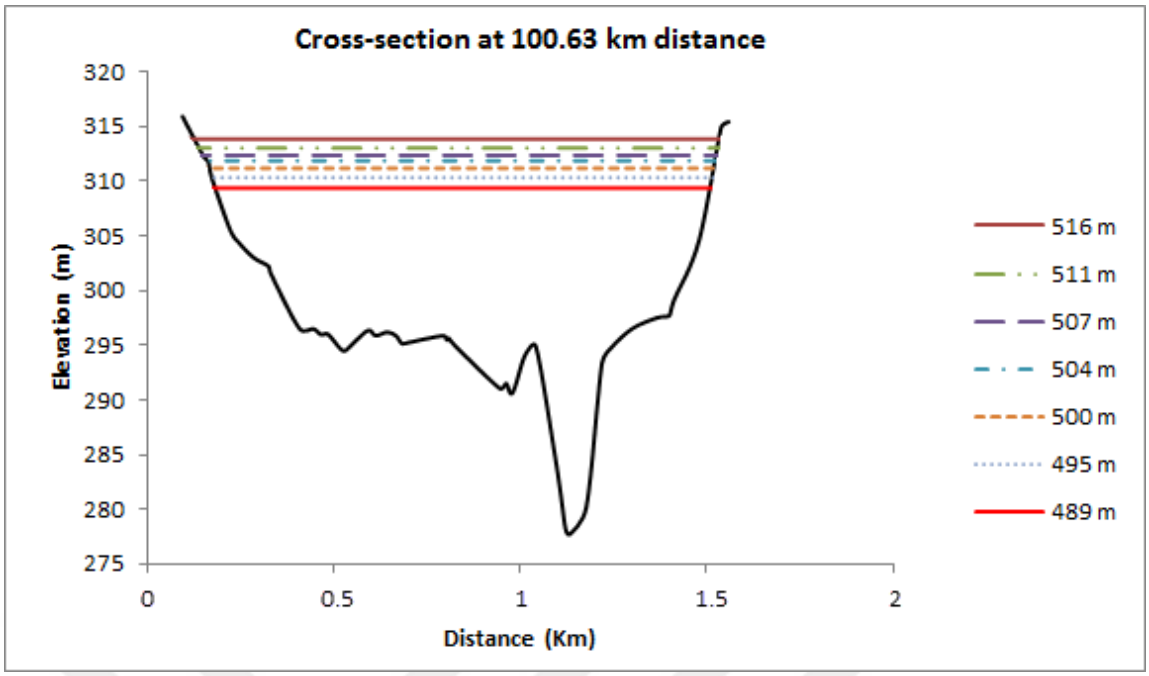

Figure B-31. Cross section number 31

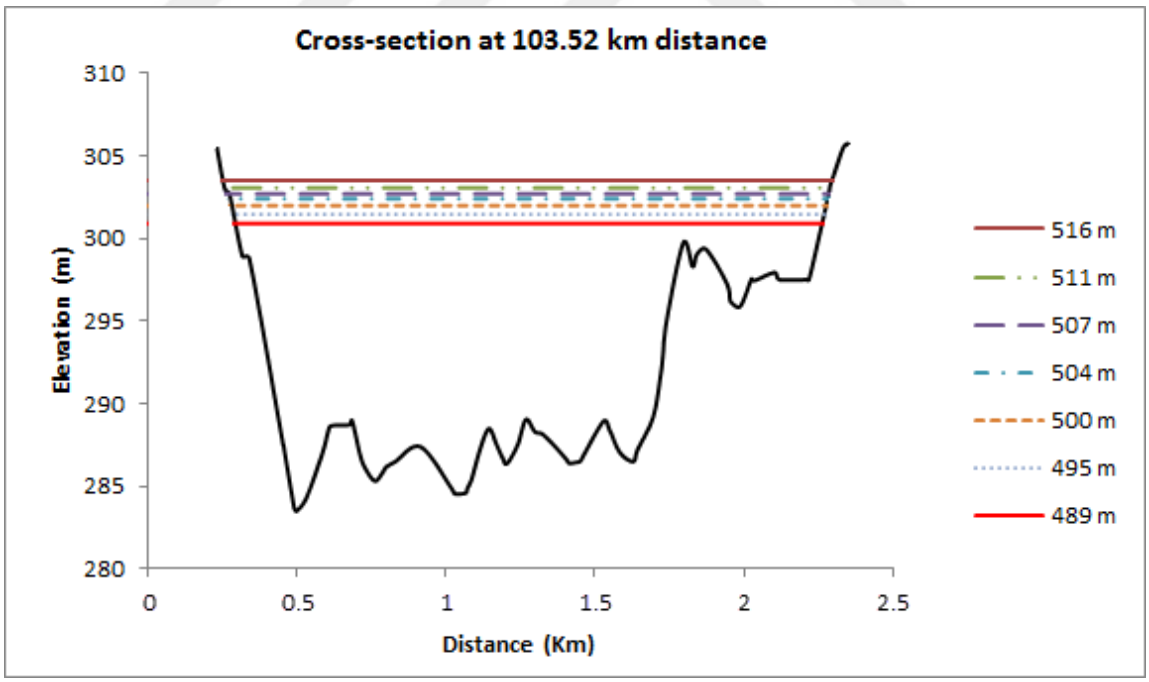

Figure B-32. Cross section number 32

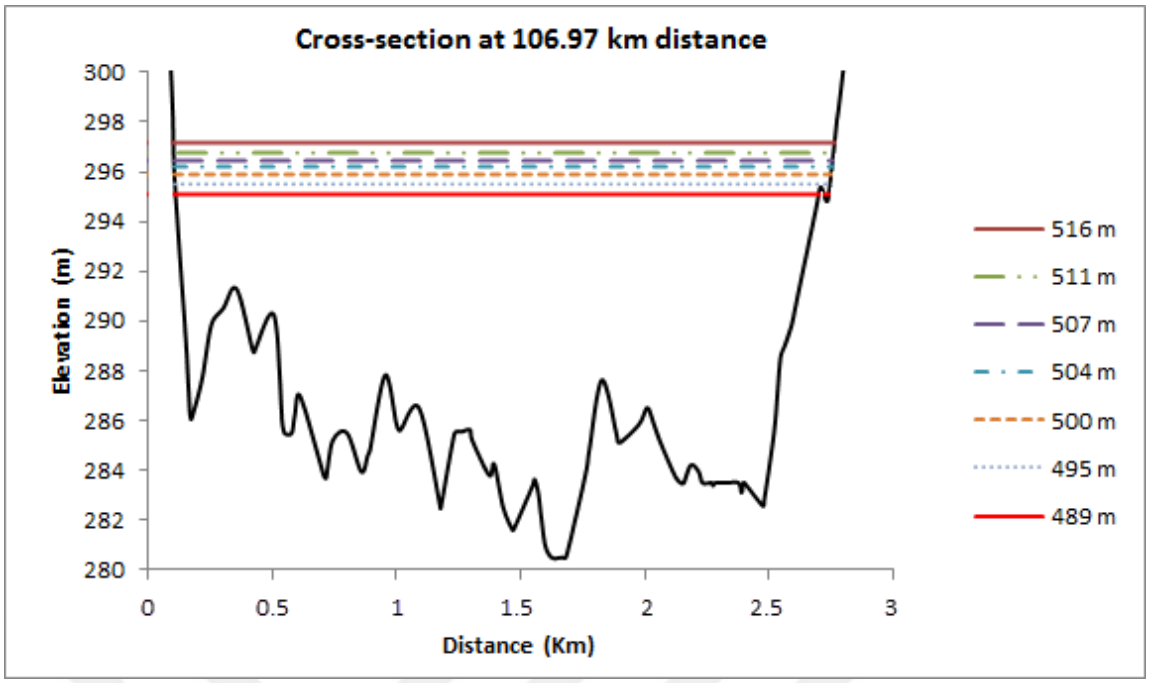

Figure B-33. Cross section number 33

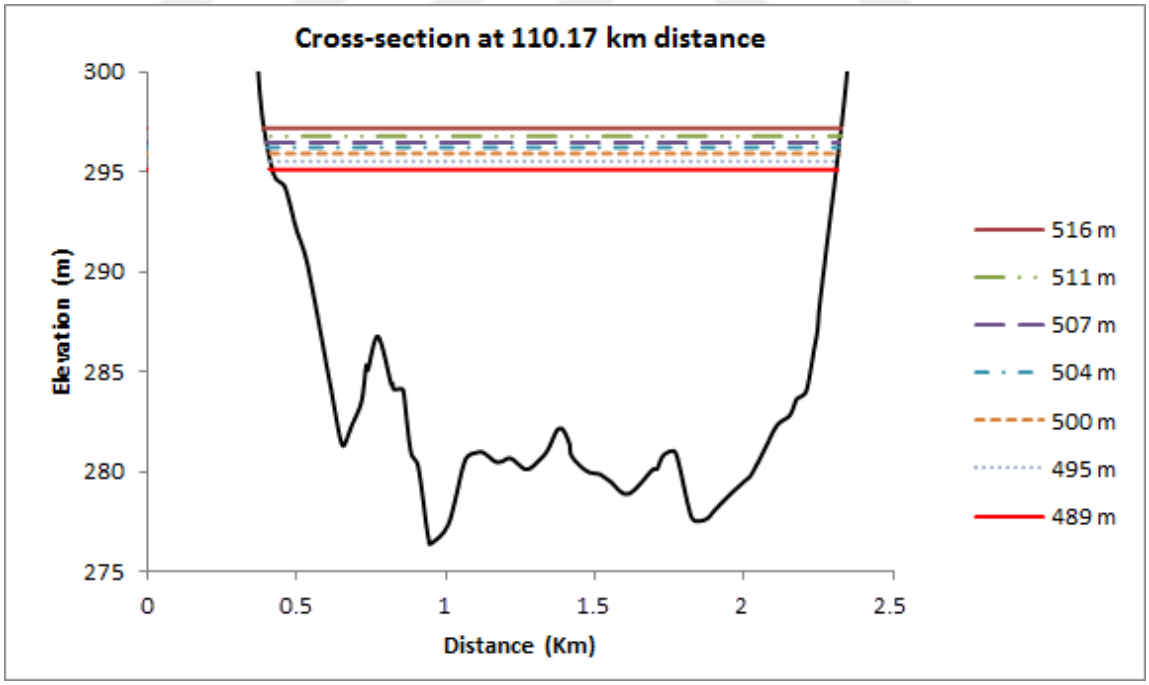

Figure B-34. Cross section number 34

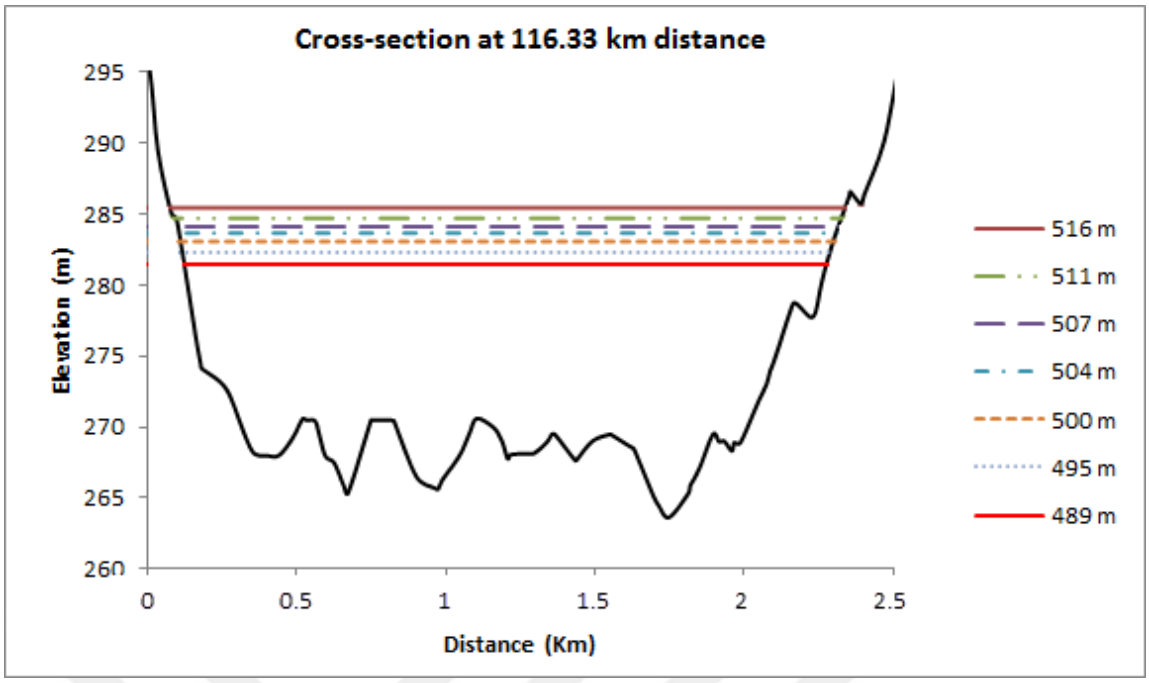

Figure B-35. Cross section number 35

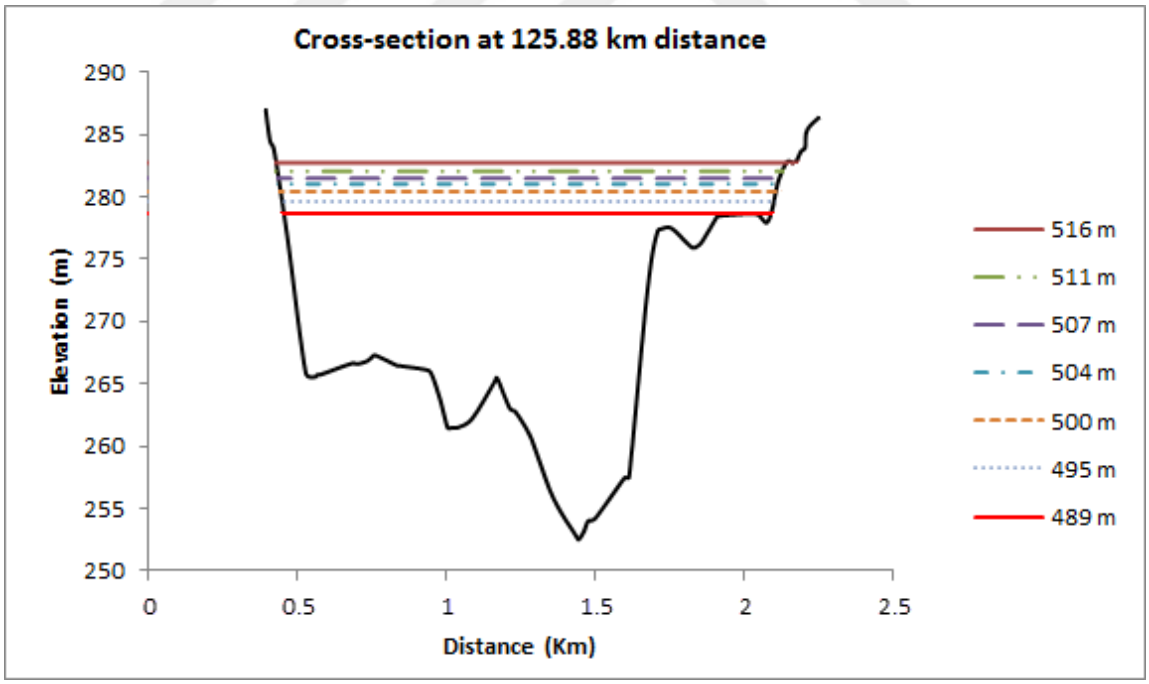

Figure B-36. Cross section number 36

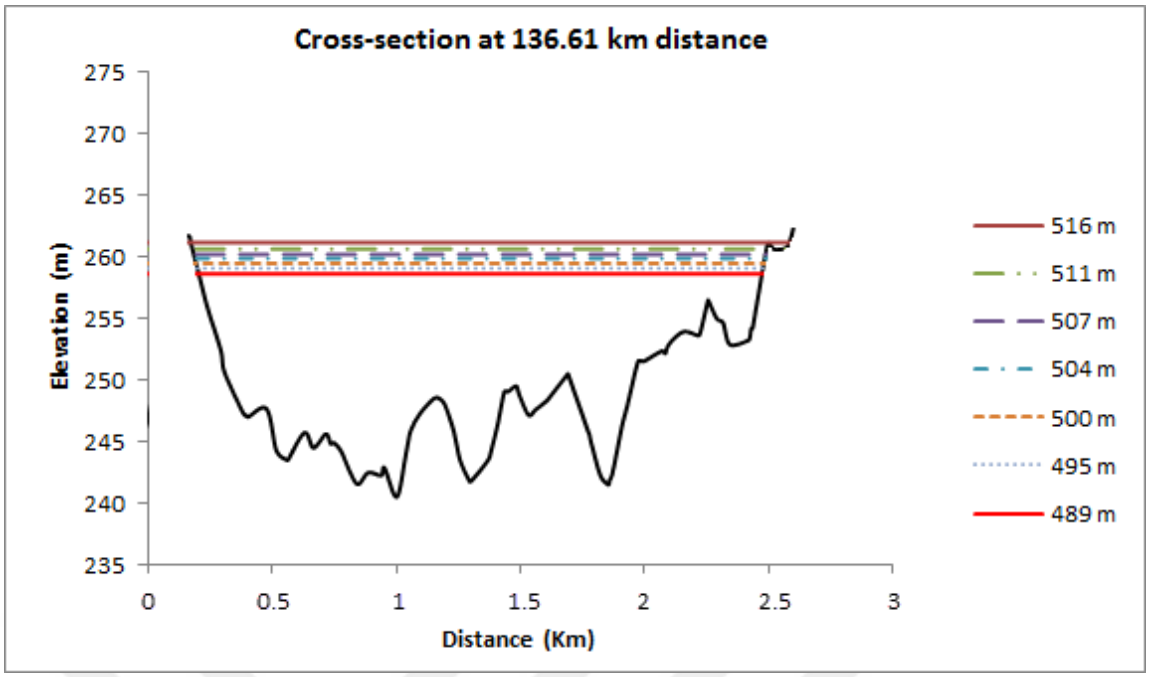

Figure B-37. Cross section number 37

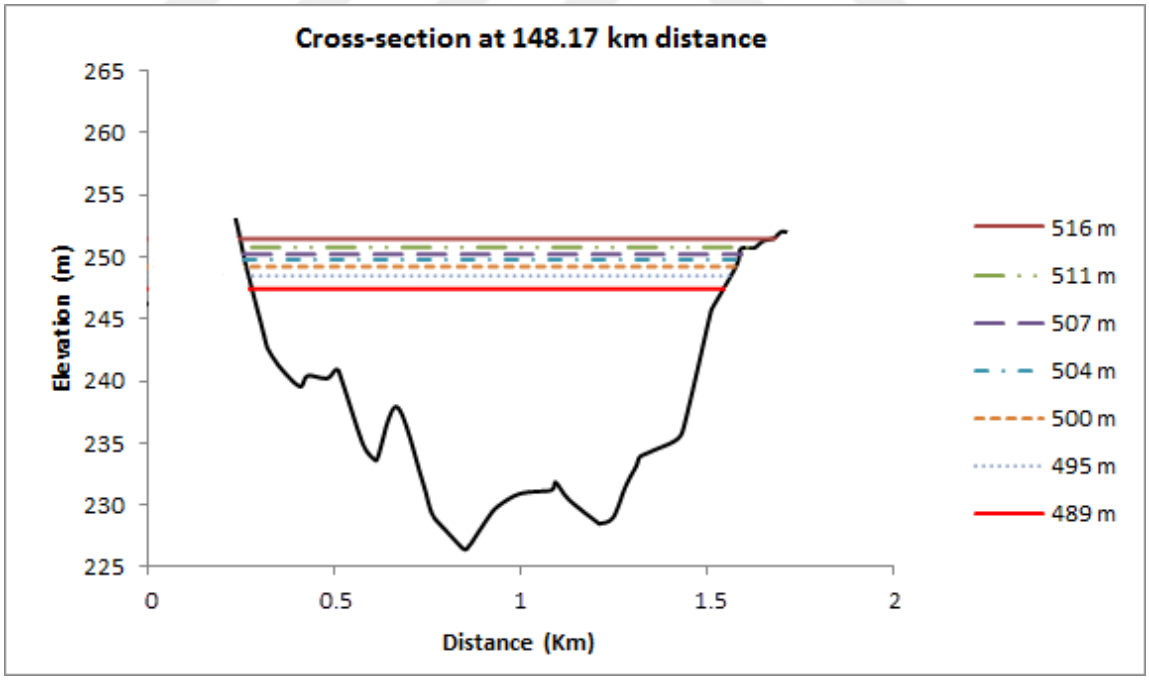

Figure B-38. Cross section number 38

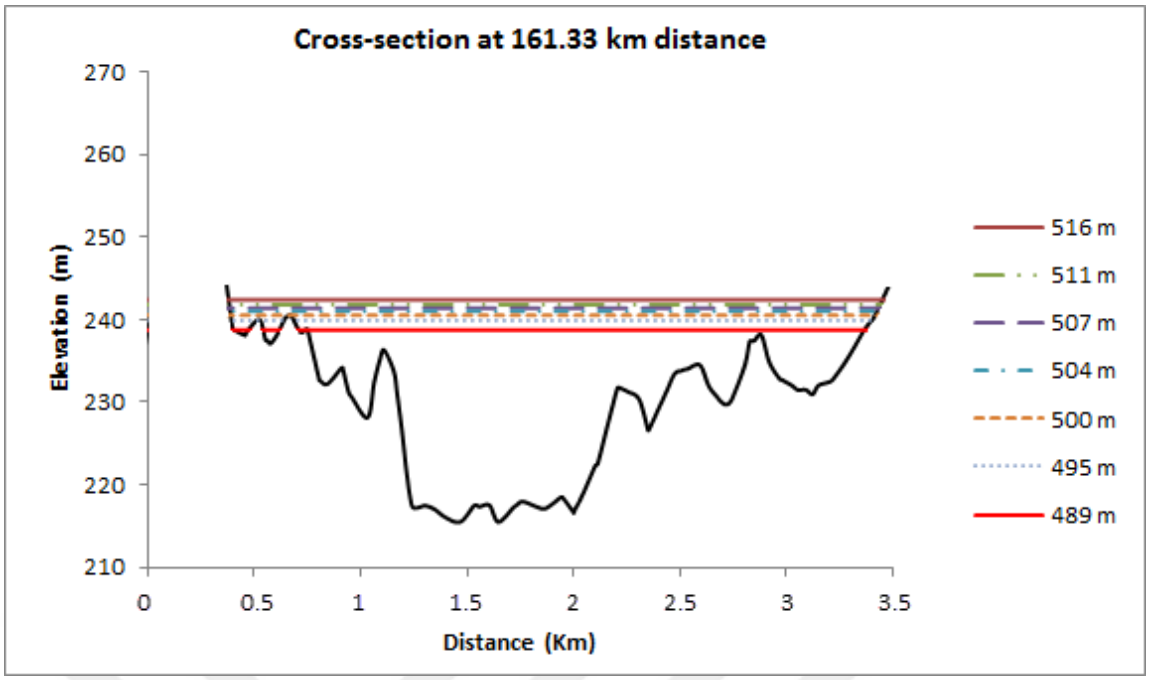

Figure B-39. Cross section number 39

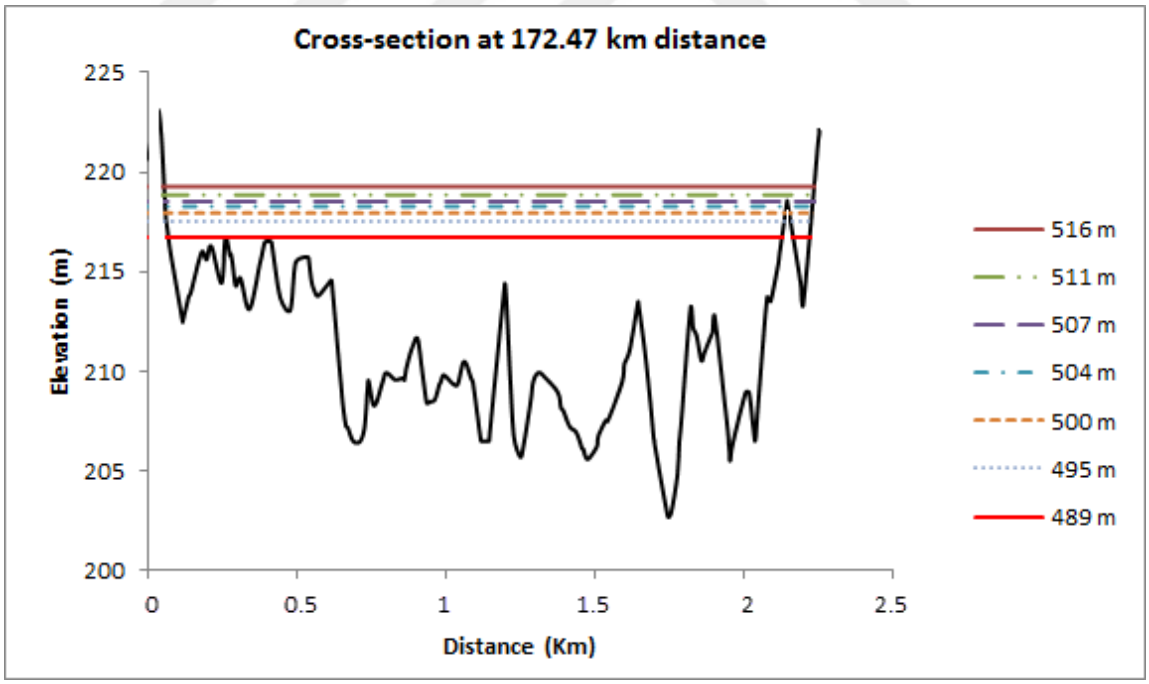

Figure B-40. Cross section number 40

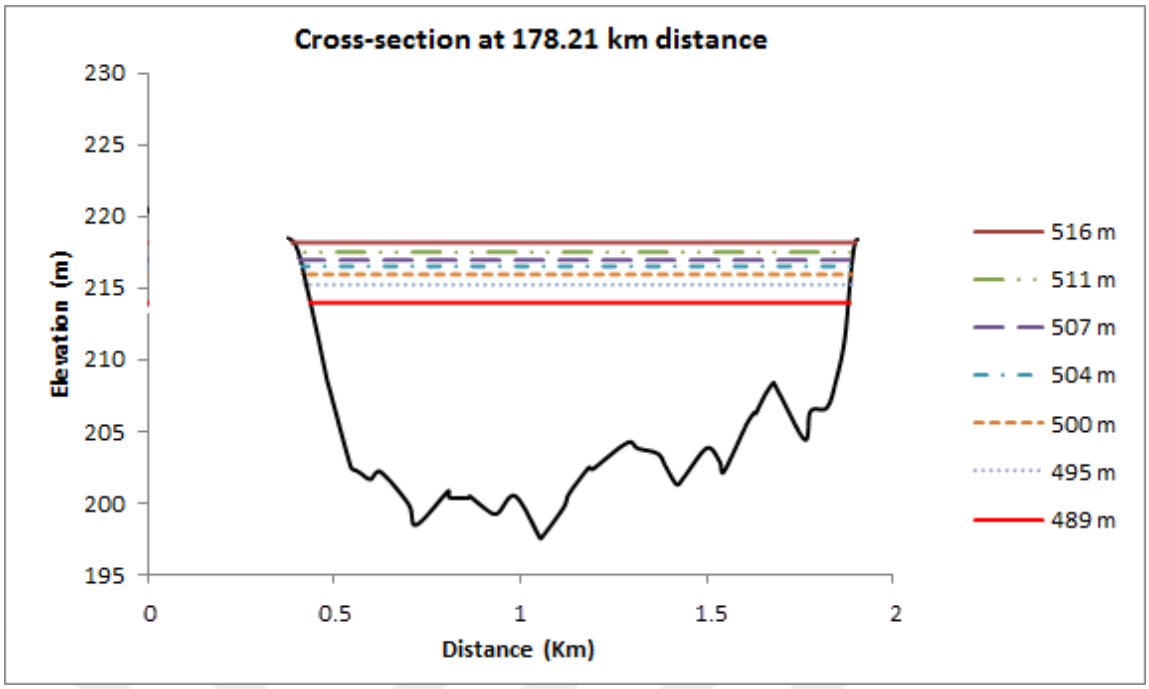

Figure B-41. Cross section number 41

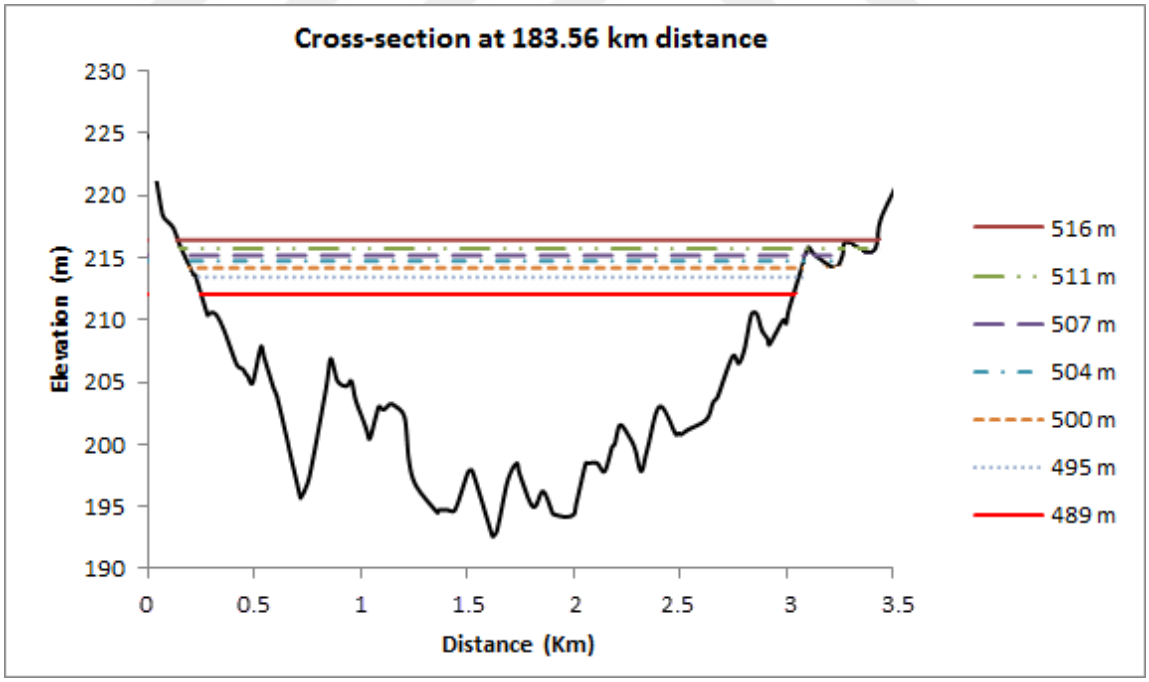

Figure B-42. Cross section number 42

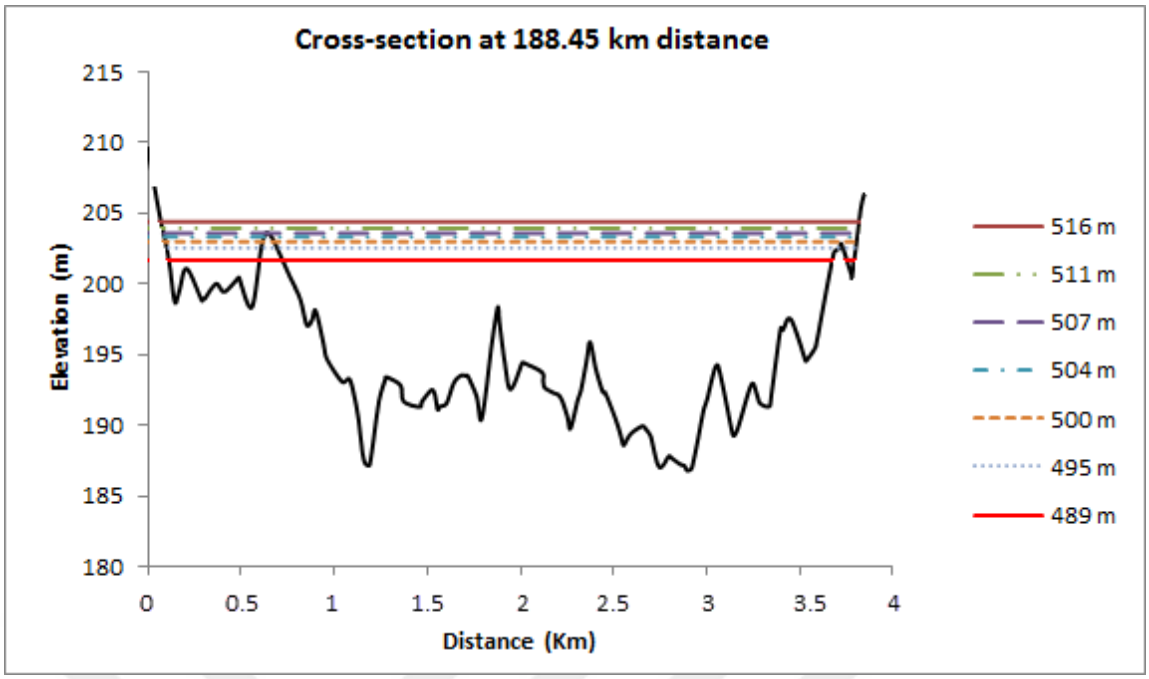

Figure B-43. Cross section number 43

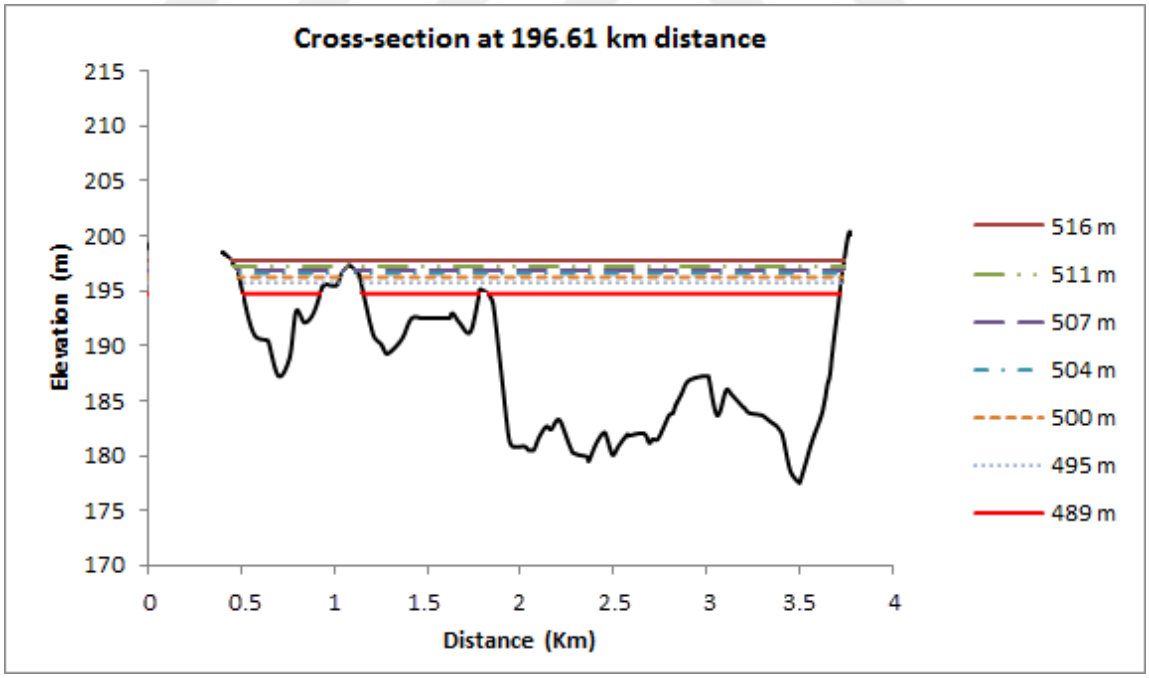

Figure B-44. Cross section number 44

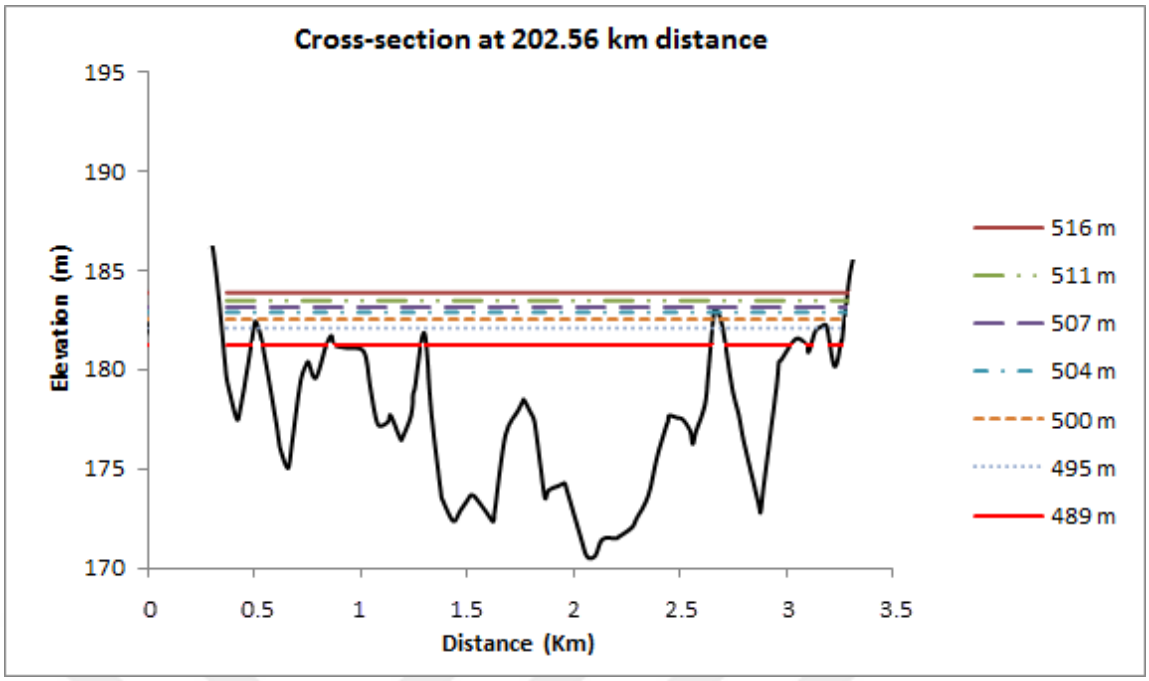

Figure B-45. Cross section number 45

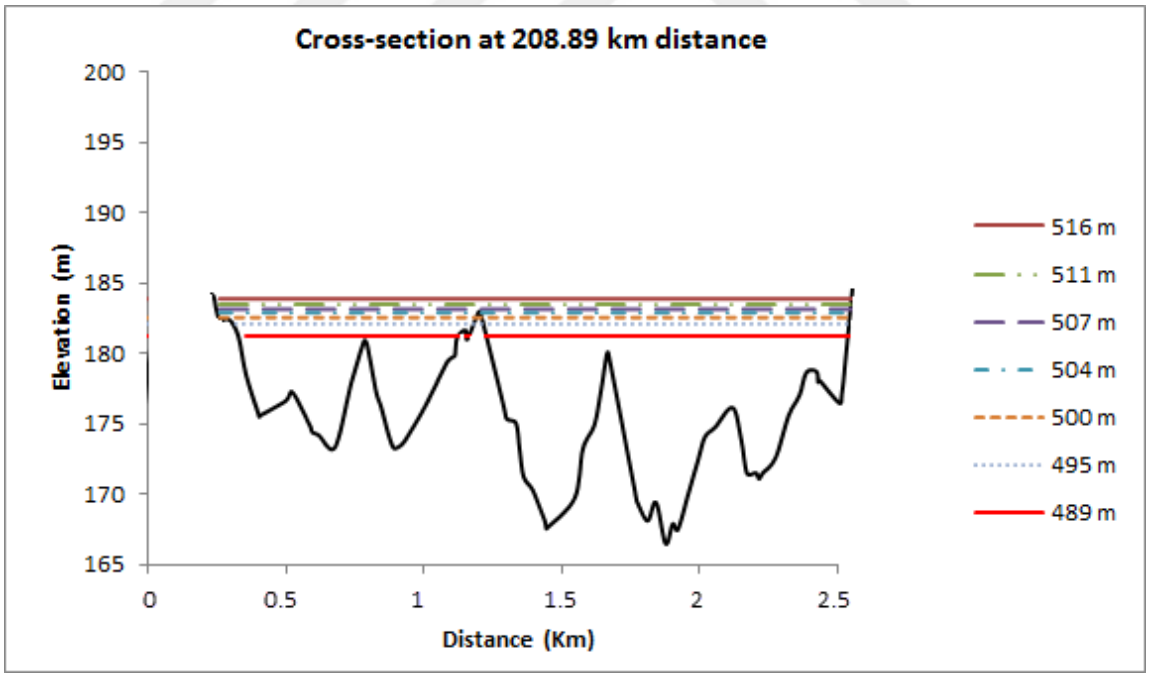

Figure B-46. Cross section number 46

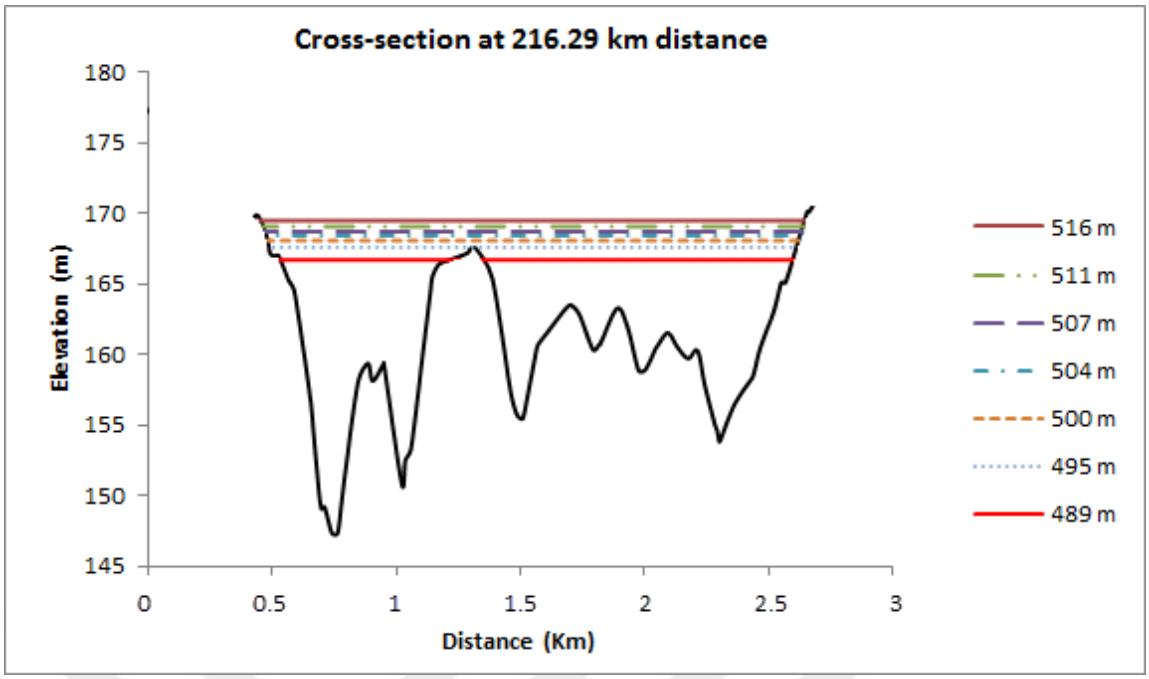

Figure B-47. Cross section number 47

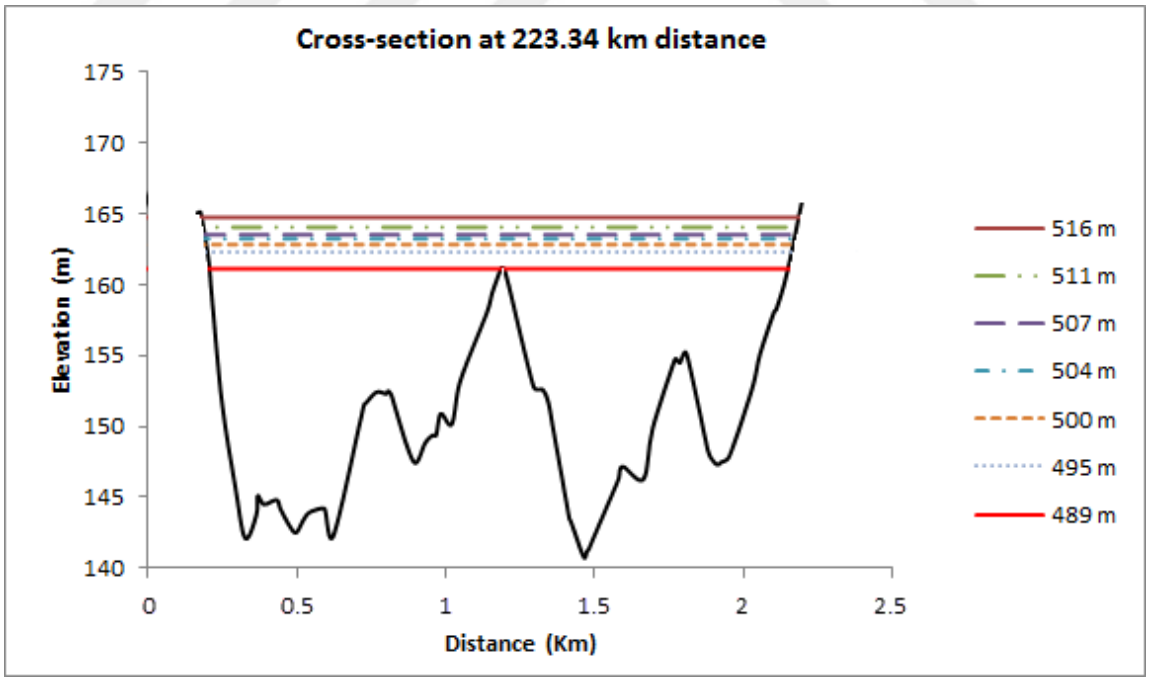

Figure B-48. Cross section number 48

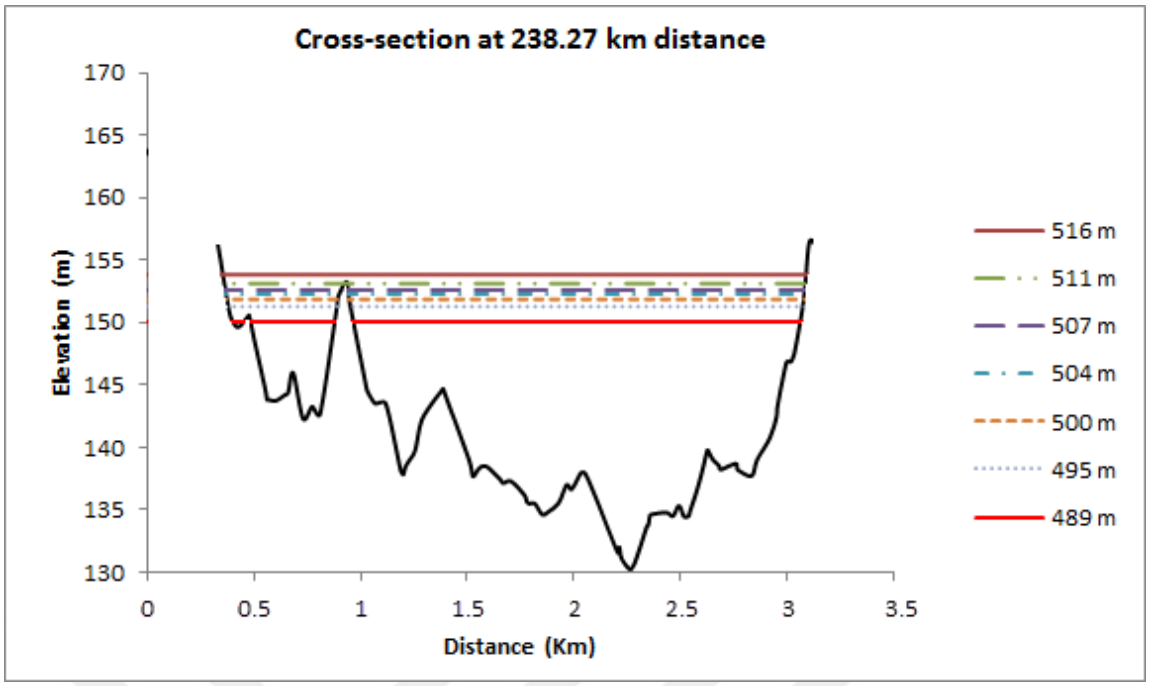

Figure B-49. Cross section number 49

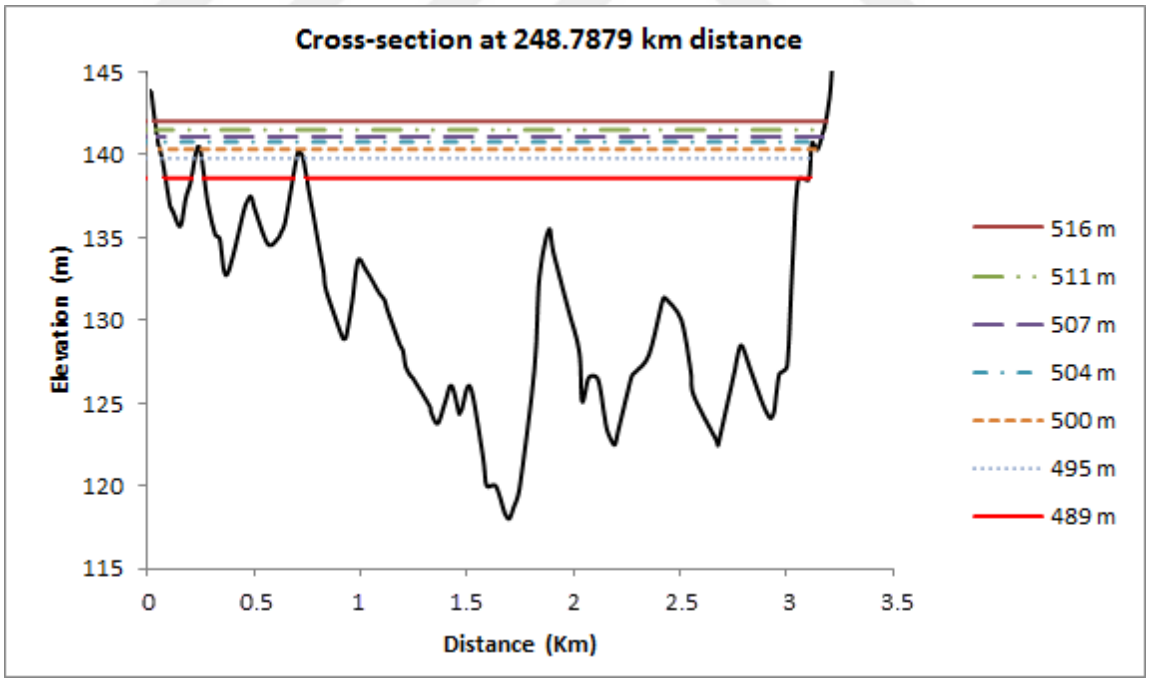

Figure B-50. Cross section number 50

Appendix C

Tables of comparison between predictor equations and three different simulated scenarios for checking validity and comprehensive at (GEP) equations

- **<u>Checking Flood Traveling Time equation (T)</u>: Units are in (hour)**

Table C-1. Checking Flood Traveling Time equation

First checking scenario		Second checking scenario		Third checking scenario	
Simulated result by (SMPDBK)	Achieved result by (GEP)	Simulated result by (SMPDBK)	Achieved result by (GEP)	Simulated result by (SMPDBK)	Achieved result by (GEP)
0.11	0.07	0.12	0.11	0.12	0.13
0.13	0.10	0.13	0.13	0.14	0.15
0.15	0.15	0.16	0.185	0.17	0.20
0.18	0.20	0.18	0.23	0.19	0.24
0.19	0.27	0.20	0.28	0.20	0.30
0.28	0.32	0.28	0.34	0.29	0.35
0.32	0.37	0.31	0.38	0.31	0.39
0.46	0.44	0.45	0.45	0.44	0.45
0.54	0.50	0.53	0.50	0.52	0.50
0.63	0.58	0.61	0.58	0.6	0.58
0.68	0.68	0.67	0.67	0.66	0.67
0.82	0.80	0.8	0.79	0.78	0.78
0.98	0.94	0.95	0.92	0.92	0.91
1.22	1.08	1.19	1.05	1.17	1.04
1.30	1.20	1.26	1.16	1.22	1.14
1.41	1.36	1.37	1.32	1.33	1.29
1.60	1.55	1.55	1.50	1.50	1.46
1.62	1.64	1.57	1.59	1.52	1.55
1.74	1.74	1.68	1.69	1.63	1.65
1.97	1.88	1.91	1.82	1.84	1.78
2.05	2.03	1.99	1.96	1.92	1.91
2.31	2.23	2.24	2.15	2.17	2.10
2.33	2.35	2.26	2.26	2.19	2.21
2.36	2.49	2.28	2.40	2.21	2.34
2.47	2.62	2.39	2.53	2.31	2.47
2.73	2.81	2.65	2.71	2.56	2.64

Table C-1 continued

3.15	2.92	3.03	2.82	2.92	2.74
3.18	3.08	3.06	2.97	2.95	2.90
3.32	3.26	3.18	3.14	3.06	3.06
3.35	3.40	3.21	3.28	3.09	3.19
3.38	3.64	3.25	3.51	3.12	3.41
3.55	3.777	3.42	3.64	3.30	3.54
4.22	3.94	4.07	3.80	3.92	3.70
4.47	4.09	4.31	3.94	4.18	3.84
4.52	4.39	4.35	4.23	4.22	4.12
4.59	4.86	4.39	4.68	4.26	4.56
5.80	5.39	5.62	5.20	5.47	5.07
5.85	5.99	5.68	5.77	5.52	5.63
5.91	6.68	5.74	6.44	5.58	6.29
7.52	7.28	7.26	7.02	7.02	6.86
7.60	7.59	7.33	7.32	7.09	7.15
7.67	7.88	7.40	7.61	7.17	7.42
8.40	8.15	8.01	7.87	7.75	7.69
8.85	8.61	8.42	8.31	8.16	8.12
8.94	8.94	8.50	8.63	8.24	8.43
9.03	9.29	8.50	8.97	8.32	8.77
10.70	9.72	10.32	9.38	9.99	9.17
10.81	10.12	10.42	9.78	10.09	9.55
10.92	10.98	10.53	10.62	10.19	10.37
11.03	11.59	10.63	11.21	10.29	10.96

- **<u>Checking Flood Flow Equation (Q)</u>:Units are in (M^3/s)**

Table C-2. Checking Flood Flow Equation

First checking scenario		Second checking scenario		Third checking scenario	
Simulated result by (SMPDBK)	Achieved result by (GEP)	Simulated result by (SMPDBK)	Achieved result by (GEP)	Simulated result by (SMPDBK)	Achieved result by (GEP)
310948.4	302201.1	344187	331378.9	383530.2	365533.7
305086	300363.3	339051.5	329541.2	379325.7	363695.9
304584.8	297523.8	338134	326701.7	377688.7	360856.5
304225.2	294950.4	337681.8	324128.3	377217.8	358283
292028.2	291910	328229.1	321087.8	370635.8	355242.6
289107.9	289258.5	324946.9	318436.4	366929.4	352591.2
286217.1	287364.1	321697.5	316541.9	363260.1	350696.7
274551.7	284544.4	310078.3	313722.3	352579.3	347877.1

Table C-2 continued

271806.2	282200.5	306977.6	311378.3	349053.6	345533.1
264889.7	279099.3	298306.7	308277.1	338325.4	342431.9
262240.8	275505.2	295323.8	304683.1	334942.1	338837.9
259618.5	271400.1	292370.3	300577.9	331592.5	334732.7
257022.3	267039.9	289446.6	296217.7	328276.6	330372.5
254452.1	262875.8	286552.3	292053.6	324993.9	326208.4
251907.5	259766.1	283686.7	288944	321743.9	323098.7
249388.5	255516.4	280849.8	284694.2	318526.6	318849
246894.6	250899.9	278041.3	280077.8	315341.2	314232.5
244425.6	248492.4	275260.9	277670.2	312187.9	311825
241981.4	246207.4	272508.3	275385.2	309065.9	309540
239561.6	243277.4	269783.3	272455.3	305975.4	306610.1
237166	240307.9	267085.4	269485.7	302915.5	303640.5
234794.3	236204.3	264414.6	265382.2	299886.5	299536.9
232446.4	233957.9	261770.4	263135.8	296887.7	297290.5
230121.9	231345.1	259152.8	260523	293918.7	294677.8
227820.7	229007.3	256561.2	258185.2	290979.4	292340
225542.5	225839.1	253995.6	255017	288069.8	289171.7
223287.1	224164.4	251455.6	253342.2	285189.2	287497
221054.2	221665	248941.1	250842.9	282337.1	284997.7
218843.7	218971.5	246451.7	248149.4	279513.8	282304.2
216655.2	216949	243987.2	246126.9	276718.7	280281.7
214488.7	213726	241547.3	242903.8	273951.5	277058.6
212343.8	211974.8	239131.8	241152.7	271212	275307.5
210220.3	209950.9	236740.5	239128.7	268499.8	273283.5
208118.1	208125.3	234373.1	237303.1	265814.8	271457.9
206037	204764.8	232029.4	233942.7	263156.7	268097.5
203976.6	199959.6	229709.1	229137.5	260525.1	263292.3
201936.8	195132.3	227412	224310.1	257919.9	258464.9
199917.5	190619.2	225137.9	219797.1	255340.7	253951.8
197918.3	186341	222886.5	215518.9	252787.3	249673.6
195939.1	183439.8	220657.6	212617.7	250259.4	246772.5
193979.7	182200.5	218451.1	211378.4	247756.8	245533.1
192040	181205.1	216266.5	210383	245279.3	244537.8
190119.6	180426.6	214103.9	209604.5	242826.5	243759.2
188218.4	179410.7	211962.9	208588.6	240398.2	242743.4
186336.2	178892.4	209843.2	208070.2	237994.2	242225
184472.8	178547.8	207744.8	207725.7	235614.3	241880.5
182628.1	178414.2	205667.4	207592	233258.2	241746.8
180801.8	178557.2	203610.7	207735.1	230925.6	241889.9
178993.8	179731.4	201574.6	208909.3	228616.3	243064.1
177203.9	181267.1	199558.8	210445	226330.2	244599.8

- **<u>Checking Flood Elevation Equation (FL)</u>: Units are in (m.a.s.l)**

Table C-3. Checking Flood Elevation Equation

First checking scenario		Second checking scenario		Third checking scenario	
Simulated result by (SMPDBK)	Achieved result by (GEP)	Simulated result by (SMPDBK)	Achieved result by (GEP)	Simulated result by (SMPDBK)	Achieved result by (GEP)
455.087	430.995	458.449	432.001	462.235	433.151
434.266	429.058	436.034	430.065	438.015	431.215
418.676	426.038	419.788	427.044	421.029	428.194
416.859	423.268	417.856	424.275	418.965	425.425
416.859	419.957	417.856	420.963	418.965	422.113
416.859	417.033	417.856	418.039	418.965	419.189
416.859	414.922	417.856	415.928	418.965	417.078
416.859	411.746	417.856	412.752	418.965	413.902
416.859	409.074	417.856	410.080	418.965	411.230
400.641	405.491	401.421	406.498	402.326	407.648
395.115	401.270	396.718	402.276	398.513	403.426
382.764	396.351	383.307	397.357	383.938	398.507
382.764	391.006	383.307	392.013	383.938	393.163
377.906	385.778	378.960	386.784	380.161	387.934
377.491	381.789	378.610	382.795	379.881	383.945
377.491	376.211	378.610	377.218	379.881	378.368
369.582	369.976	370.548	370.982	371.648	372.132
369.356	366.645	370.484	367.651	371.648	368.801
369.356	363.431	370.484	364.437	371.648	365.587
362.907	359.228	363.937	360.235	365.086	361.385
357.759	354.871	359.031	355.877	360.450	357.027
351.373	348.674	352.531	349.681	353.824	350.831
349.785	345.189	350.894	346.195	352.147	347.345
344.244	341.045	345.326	342.051	346.542	343.201
344.244	337.249	345.326	338.255	346.542	339.405
335.536	331.962	336.526	332.969	337.608	334.119
326.090	329.096	326.870	330.103	327.672	331.253
326.090	324.720	326.870	325.726	327.672	326.876
325.294	319.859	326.45	320.866	327.672	322.016
314.983	316.1029	316.007	317.109	317.156	318.259
310.825	309.9061	312.011	310.912	313.340	312.062
301.773	306.4204	302.507	307.426	303.236	308.576
295.738	302.2763	296.283	303.282	296.917	304.432
295.738	298.4227	296.283	299.428	296.917	300.579
282.759	291.0059	283.811	292.012	284.997	293.162
280.120	279.5224	281.193	280.528	282.330	281.678

Table C-3continued

259.302	266.606	259.951	267.612	260.826	268.762
248.933	252.7019	249.942	253.708	251.063	254.858
240.276	236.8614	241.127	237.867	242.053	239.017
217.773	223.4608	218.352	224.467	219.017	225.617
215.661	216.5475	216.651	217.553	217.767	218.703
213.884	210.1183	214.890	211.124	216.017	212.274
202.804	204.2313	203.396	205.237	204.118	206.387
196.029	194.4133	196.684	195.419	197.434	196.569
182.361	187.2482	182.974	188.254	183.645	189.404
182.361	179.6378	182.974	180.644	183.645	181.794
167.868	170.7299	168.505	171.736	169.218	172.886
162.626	162.248	163.336	163.254	164.348	164.404
151.622	144.2773	152.393	145.283	153.415	146.433
140.128	131.632	140.887	132.638	141.716	133.788